SMALL MOLECULE COMPOUNDS TARGETING DNA BINDING DOMAIN OF STAT3 FOR INHIBITION OF TUMOR GROWTH AND METASTASIS

Wei Huang

Submitted to the faculty of the University Graduate School
in partial fulfillment of the requirements
for the degree
Doctor of Philosophy
in the Department of Pharmacology and Toxicology,
Indiana University

February 2014

Accepted by the Graduate Faculty, Indiana University, in partial fulfillment of the requirements for the degree of Doctor of Philosophy.

_____
Jian-Ting Zhang, Ph.D., Chair

_____
Travis J. Jerde, Ph.D.

Doctoral Committee

January 15, 2014

_____
Karen E. Pollok, Ph.D.

_____
Ahmad R. Safa, Ph.D.

_____
Zhong-Yin Zhang, Ph.D.

ACKNOWLEDGEMENTS

I am grateful for having the opportunity to complete my Ph.D. study with the support and encouragement of my mentor, Dr. Jian-Ting Zhang. I also sincerely appreciate the guidance by other members of my dissertation committee, Dr. Ahmad R. Safa, Dr. Karen E. Pollok, Dr. Travis Jerde and Dr. Zhong-Yin Zhang. Especially, thanks to Dr. Jing-Yuan Liu and her laboratory members for their work in *in-silico* screening and analyses, thanks to Dr. Zhong-Yin Zhang and Dr. Yan-Tao He for their help in synthesizing chemical compounds, thanks to Dr. Karen E. Pollok and *In Vivo* Therapeutics Core personnel for their contribution in animal studies, thanks to Dr. David R. Jones for his work in pharmacokinetic analysis, thanks to Dr. Jing-Wu Xie and his laboratory members for their assistance on immunohistochemistry staining and thanks to Dr. George E. Sandusky for his contribution to histology analysis.

Many thanks to all the people whom I have worked with in Dr. Zhang's laboratory for their assistance and friendship. In particular, I would like to thank Dr. Zi-Zheng Dong for his patient instruction on my experiments. Thanks to all of the faculty, graduate students and staff in Department of Pharmacology and Toxicology for their help and support throughout the years of my graduate studies. I appreciate everyone present in my life in Indianapolis and I have enjoyed my journey in the United States.

Wei Huang

Small molecule compounds targeting DNA binding domain of STAT3 for inhibition of tumor growth and metastasis

Signal transducer and activator of transcription 3 (STAT3) is constitutively activated in malignant tumors, and its activation is associated with high histological grade and advanced cancer stage. STAT3 has been shown to play important roles in multiple aspects of cancer aggressiveness including proliferation, survival, self-renewal, migration, invasion, angiogenesis and immune response by regulating the expression of diverse downstream target genes. Thus, inhibiting STAT3 promises to be an attractive strategy for treatment of advanced tumors with metastatic potential. We firstly identified a STAT3 inhibitor, inS3-54, by targeting the DNA-binding site of STAT3 using an *in-silico* screening approach; however, inS3-54 was finally found not to be appropriate for further studies because of low specificity on STAT3 and poor absorption in mice. To develop an effective and specific STAT3 inhibitor, we identified 89 analogues for the structure-activity relationship analysis. By using hematopoietic progenitor cells isolated from wild-type and STAT3 conditional knockout mice, further studies showed that three analogues (A18, A26 and A69) only inhibited STAT3-dependent colony formation of hematopoietic progenitor cells, indicating a higher selectivity for STAT3 than their parental compound, inS3-54. These compounds were found to (1) inhibit STAT3-specific DNA binding activity; (2) bind to STAT3 protein; (3) suppress

proliferation of cancer cells harboring aberrant STAT3 signaling; (4) inhibit migration and invasion of cancer cells and (5) inhibit STAT3-dependent expression of downstream targets by blocking the binding of STAT3 to the promoter regions of responsive genes in cells. In addition, A18 can reduce tumor growth in a mouse xenograft model of lung cancer with little effect on body weight. Taken together, we conclude that it is feasible to inhibit STAT3 by targeting its DNA-binding domain for discovery of anticancer therapeutics.

Jian-Ting Zhang, Ph.D., Chair

TABLE OF CONTENTS

I. Introduction 1

A. Signal transducers and activators of transcription 1

B. STAT3 activation and protein structure 2

C. Regulation of STAT3 signaling and roles of aberrant STAT3 signaling in cancers 7

D. Clinical implications of STAT3 9

E. Strategies to inhibit aberrant STAT3 signaling 12

F. Specific aims of the present work 15

II. Materials and Methods 17

A. Materials 17

B. Cell lines and culture 19

C. Structure-based virtual compound screening 19

D. STAT3-dependent luciferase reporter assay 21

E. Molecular dynamics simulation and calculation of binding free energy 22

F. Electrophoretic mobility shift assay 22

G. Preparation of inS3-54-conjugated EAH-Sepharose 4B and pull down assay 24

H. Preparation of A26-conjugated CNBr-activated Sepharose 4B and pull down assay 26

I. Glutathione assay 27

J. Cytotoxicity assay 30

K. Enzyme-linked immunosorbent assay for quantification of apoptosis 30

L. Hematopoietic progenitor cell colony formation assay 33

M. Cell migration assay 33

N. Cell invasion assay 34

O. Western blot analysis 35

P. Real-time polymerase chain reaction 36

Q. Co-immunoprecipitation 39

R. Cellular fractionation 39

S. Chromatin immunoprecipitation 40

T. Determinaiton of *in vivo* study conditions 42

U. Mouse xenograft model of lung cancer 42

V. Immunohistochemistry staining 43

III. Experimental Results 45

Part I. Development of inS3-54 45

A. Identification of a STAT3 inhibitor targeting DBD of STAT3 45

B. InS3-54 selectively inhibits the DNA-binding activity of STAT3 but not that of STAT1 67

C. Binding of inS3-54 to STAT3 74

D. InS3-54 does not inhibit STAT3 dimerization 80

E. InS3-54 favorably inhibits cancer cell survival possibly by inducing apoptosis 84

F. InS3-54 inhibits cancer cell migration and invasion 89

G. InS3-54 inhibits the expression of STAT3 downstream target genes and STAT3 binding to its endogenous target sequences 99

Part II. Development of inS3-54 analogues 108

A. Analogues of inS3-54 targeting the DBD of STAT3 are developed 108

B. InS3-54 analogues selectively inhibit the DNA-binding activity of STAT3 other than that of STAT1 124

C. InS3-54 analogues bind to STAT3 129

D. InS3-54 analogues favorably inhibit cancer cell survival possibly by inducing apoptosis 134

E. Rationale for focusing on A18 in the following experiments 139

F. A18 inhibits cancer cell migration and invasion 143

G. A18 inhibits the expression of STAT3 downstream target genes and STAT3 binding to its endogenous target sequences 152

H. A18 inhibits tumor growth *in vivo* 160

IV. Discussion 167

A. Contribution of the present study 167

B. Challenges to target STAT3 168

C. Targeting of inS3-54 and its analogues to STAT3 171

D. Structure-activity relationship of inS3-54 and its analogues 175

E. Mechanism of inS3-54 and its analogues 179

V. Summary and Conclusion 182

VI. Future Plans 184

VII. References 186

Curriculum Vitae

LIST OF TABLES

Table 1. Representative STAT3 downstream targets 4

Table 2. Primers used for real-time PCR 38

Table 3. 100 top-scoring compounds obtained from virtual screening 47

Table 4. Binding free energy and energy components of inS3-54 69

Table 5. Chemical properties of inS3-54 and its analogues 111

Table 6. Summary of inS3-54 and its active analogues 119

Table 7. Observation of solubility of each compound in formulations commonly used for *in vivo* studies 140

Table 8. Toxicity and PK characteristics of inS3-54 and its analogues 142

LIST OF FIGURES

Figure 1. Schematic diagram of canonical JAK/STAT3 signaling pathway. 3

Figure 2. Schematic diagram of STAT3 structure. 6

Figure 3. Schematic diagram of GSH-Glo™ glutathione assay. 29

Figure 4. Schematic diagram of apoptosis ELISA assay. 32

Figure 5. Schematic diagram and identification of inS3-54 by structure-based virtual screening. 63

Figure 6. Effects of inS3-54 on STAT3 dependent and independent luciferase reporter activity. 65

Figure 7. Molecular dynamics simulation of inS3-54 binding to STAT3 or STAT1. 70

Figure 8. InS3-54 inhibits the DNA-binding activity of STAT3 but not that of STAT1. 72

Figure 9. Binding of inS3-54 to STAT3. 76

Figure 10. InS3-54 does not alkylate cysteine using glutathione as a substrate. 79

Figure 11. InS3-54 does not affect STAT3 dimerization. 81

Figure 12. InS3-54 favorably inhibits cancer cell proliferation. 86

Figure 13. InS3-54 induces apoptosis. 88

Figure 14. InS3-54 inhibits cancer cell migration. 92

Figure 15. InS3-54 inhibits cancer cell invasion. 95

Figure 16. Effects of inS3-54 on cell growth and apoptosis of confluent cells. 97

Figure 17. InS3-54 inhibits the expression of STAT3 downstream target

genes. 102

Figure 18. InS3-54 does not affect IL-6 induced STAT3 phosphorylation. 105

Figure 19. InS3-54 inhibits STAT3 binding to chromatin. 106

Figure 20. InS3-54 inhibits the binding of STAT3 to the promoter regions of responsive genes. 107

Figure 21. Identification of inS3-54 analogues. 120

Figure 22. Effect of inS3-54 and its active analogues on colony formation of hematopoietic progenitor cells. 123

Figure 23. InS3-54 analogues inhibits the DNA-binding activity of STAT3 but not that of STAT1. 125

Figure 24. Binding of inS3-54 analogues to STAT3. 131

Figure 25. A18 does not alkylate cysteine using glutathione as a substrate. 133

Figure 26. InS3-54 analogues inhibit cancer cell proliferation. 135

Figure 27. InS3-54 analogues induce apoptosis. 138

Figure 28. A18 inhibits cancer cell migration. 145

Figure 29. A18 inhibits cancer cell invasion. 148

Figure 30. Effects of A18 on cell growth and apoptosis of confluent cells. 150

Figure 31. A18 inhibits the expression of STAT3 downstream target genes. 154

Figure 32. A18 does not affect IL-6 induced STAT3 phosphorylation. 157

Figure 33. A18 inhibits STAT3 binding to chromatin. 158

Figure 34. A18 inhibits the binding of STAT3 to the promoter regions of responsive genes. 159

Figure 35. A18 reduces tumor growth *in vivo*. 163

Figure 36. A18 reduces lung metastases in a mouse xenograft model of lung cancer. 165

Figure 37. A18 reduces the expression of STAT3 downstream targets *in vivo*. 166

Figure 38. SAR analysis of inS3-54 analogues. 178

ABBREVIATIONS

ATP	Adenosine triphosphate
BFU-E	Erythroid hematopoietic progenitor cells
BSA	Bovine serum albumin
CCD	Coiled-coil domain
CFU-CEMM	Multi-potential hematopoietic progenitor cells
CFU-GM	Granulocyte macrophage hematopoietic progenitor cells
ChIP	Chromatin immunoprecipitation
Co-IP	Co-immunoprecipitation
C_t	Threshold cycle
DBD	DNA-binding domain
DNA	Deoxyribonucleic acid
DMEM	Dulbecco's modification of Eagle's medium
DMSO	Dimethyl sulfoxide
DTT	Dithiothreitol
EDC	1-ethyl-3-(3-dimethylaminopropyl) carbodiimide
EDTA	Ethylenediaminetetraacetic acid
EGF	Epidermal growth factor
EGTA	Ethylene glycol tetraacetic acid
ELISA	Enzyme-linked immunosorbent assay
EMSA	Electrophoretic mobility shift assay
FBS	Fetal bovine serum
GAPDH	Glyceraldehyde 3-phosphate dehydrogenase

GAS	γ-interferon activation sequence
GBSA analysis	Born/surface area analysis
H&E	Hematoxylin and eosin
HER2	Receptor tyrosine-protein kinase erbB-2
HGF	Hepatocyte growth factor
IAA	Iodoacetamide
IFN	Interferon
IL	Interleukin
ISRE	Interferon stimulated response element
JAK	Janus kinase
MMP	Matrix metalloproteinase
M.W.	Molecular weight
ND	Amino-terminal domain
NF-κb	Nuclear factor-κb
NOD/SCID	Nonobese diabetic/severe combined immunodeficiency
NSCLC	Non-small cell lung cancer
OD	Optical density
ODN	Oligodeoxynucleotide
PBS	Phosphate buffered saline
PCR	Polymerase chain reaction
PD	Pharmacodynamics
PDB	Protein Data Bank
PDGF	Platelet-derived growth factor

PIAS3	Protein inhibitors of activated STAT3
PK	Pharmacokinetics
PMSF	Phenylmethylsulfonyl fluoride
P.o.	Oral dosing
PTEN	Phosphatase and tensin homolog
PTP	Protein tyrosine phosphatase
PVDF	Polyvinylidene difluoride
RNA	Ribonucleic acid
SAR	Structure-activity relationship
SEM	Standard error of the mean
SD	Standard deviation
SDS-PAGE	Sodium dodecyl sulfate-polyacrylamide gel electrophoresis
SH2	Src homology 2
SHP	Src homology region 2 domain-containing phosphatase
SIE	Sis-inducible element
SOCS	Suppressor of cytokine signaling proteins
SRB	Sulforhodamine B
STAT	Signal transducer and activator of transcription
TAD	Transactivation domain
TBE buffer	Tris-borate-EDTA buffer
TE buffer	Tris-EDTA buffer
Tyr705	Tyrosine 705
VEGF	Vascular endothelial growth factor

I. Introduction

A. Signal transducers and activators of transcription

Signal transducers and activators of transcription (STATs) are a family of proteins which act as signal transducers and transcription activators in cells, including STAT1, STAT2, STAT3, STAT4, STAT5 and STAT6. STATs remain inactive in the cytoplasm under normal condition. Upon the binding of cytokines and growth factors to their receptors, STATs are phosphorylated by receptor-associated kinases, form dimers and translocate to cell nucleus to activate transcription of specific responsive genes. The discovery of STATs begins with the studies of interferon (IFN)-mediated gene expression (1). STAT1 and STAT2 are the earliest recognized STAT proteins which are required for IFN-activated gene expression (2-5). STAT1 maintains cellular homeostasis through the control of cell growth, proliferation, apoptosis and immune reactions (6). STAT1-deficient mice spontaneously developed tumors and loss of its expression is frequently detected during cancer progression, suggesting its critical role as a tumor suppressor (7). STAT2 is involved in IFN-dependent cellular antiviral response and adaptive immunity, thereby medicating host defenses against viral infections (8, 9). STAT4, which was initially observed to respond to interleukin-12 (IL-12), is involved in regulating cell proliferation, differentiation and lymphocyte function, e.g. T helper 1 cells and natural killer cells (10, 11). STAT5a and STAT5b are found to be two distinct duplicated genes which are distributed differently in a variety of tissues (12, 13). Their structures are over 90% identical but only diverse at the C-terminus. STAT5 primarily plays a crucial role in cell development (14). The last identified

STAT protein is STAT6 which is mainly expressed in bone marrow-derived cells and regulates immune response and cell development (15). Overall, STAT protein family plays diverse roles in cellular functions such as cell proliferation, differentiation, metastasis, angiogenesis and immune response.

B. STAT3 activation and protein structure

As a well-known member of STAT protein family, STAT3 was initially observed to respond to IL-6 and epidermal growth factor (EGF) (16). Numerous scientists then contributed to uncovering the complete signaling pathway (1, 17-20). As shown in **Figure 1**, the binding of IL-6 family cytokines to glycoprotein 130 receptor activates the receptor-associated Janus kinase 2 (JAK2) which then phosphorylates specific tyrosine residues of the receptor, followed by recruitment of STAT3 to the receptor via its Src homology 2 (SH2) domain. Activated JAK2 then triggers the phosphorylation of STAT3 at tyrosine 705 (Tyr705), leading to the dissociation of STAT3 from the receptor. Diverse growth factors were also observed to activate STAT3, such as EGF, hepatocyte growth factor (HGF) and platelet-derived growth factor (PDGF) (16, 21, 22). And STAT3 is also a target of non-receptor tyrosine kinases (23). Once activated, STAT3 protein forms dimers and translocates into cell nucleus where it binds to γ-interferon activation sequence (GAS) or interferon stimulated response element (ISRE) in the promoter regions of responsive genes, leading to activation of gene transcription. STAT3 target genes include regulators of crucial steps in cell proliferation, survival, differentiation and development, metastasis, angiogenesis and immune response (**Table 1**).

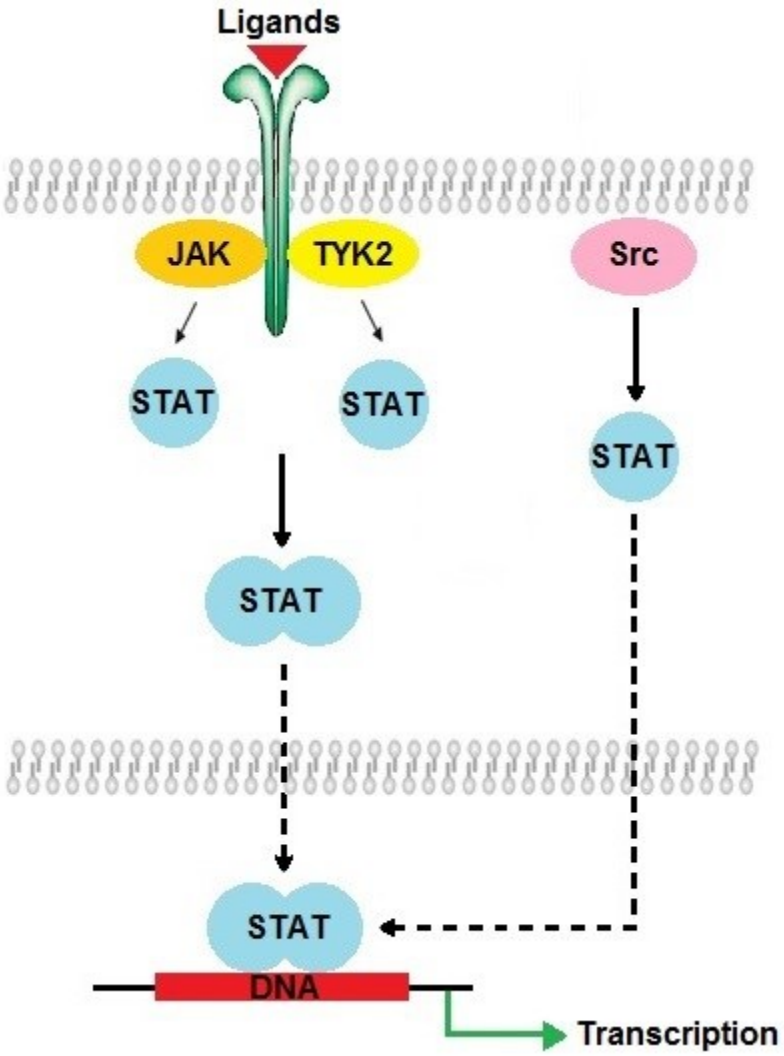

Figure 1. Schematic diagram of canonical JAK/STAT3 signaling pathway.

Upon cytokines or growth factors binding to respective receptors, JAK is activated and phosphorylates the receptor which provides a docking site for STAT3. STAT3 is then recruited to the receptor where it is phosphorylated and activated. Phosphorylated STAT3 dissociates from the cell surface and forms dimers for nucleus entry and transcription activation.

Table 1. Representative STAT3 downstream target genes

Gene	Function	Reference*
Cyclin D1	Cell cycle progression	(24)
C-myc	Cell proliferation, cell growth, apoptosis, differentiation and stem cell self-renewal	(25)
Survivin	Apoptosis suppressor	(26)
MMP-1	Breakdown of extracellular matrix	(27, 28)
MMP-2	Breakdown of extracellular matrix	(29)
MMP-7	Breakdown of extracellular matrix	(30)
MMP-9	Breakdown of extracellular matrix	(31)
MMP-10	Breakdown of extracellular matrix	(32)
Twist	Cell lineage determination and differentiation	(33)
VEGF	Vasculogenesis and angiogenesis	(34, 35)

* References represent the evidence showing the genes are transcriptionally regulated by STAT3.

The crystal structure of STAT3 protein bound to its DNA recognition site has been solved (36), providing insight into the function of STAT3. STAT3 consists of 770 amino acids in five distinct functional domains (**Figure 2**). The amino-terminal domain (ND) is responsible for stabilizing the binding of STAT3 to multiple DNA sites (37). The coiled-coil domain (CCD) mediates protein-protein interaction (36). A linker connects the DNA-binding domain (DBD) and SH2 domain which are required for DNA binding and dimerization of STAT3, respectively (38, 39). The phosphorylated tyrosine is located at the residue Tyr705. Upon phosphorylation, two STAT3 monomers are coupled via their SH2 domains, forming a dimer to bind to DNA targeting sites with a 9-base-pair consensus sequence, TTCCGGGAA (36). DBD directly binds to the specific sequence in the promoters of STAT3 target genes. The carboxy-terminal transactivation domain (TAD) where the tyrosine residue is phosphorylated contacts other components of the transcriptional machinery to activate transcription of the target genes (40).

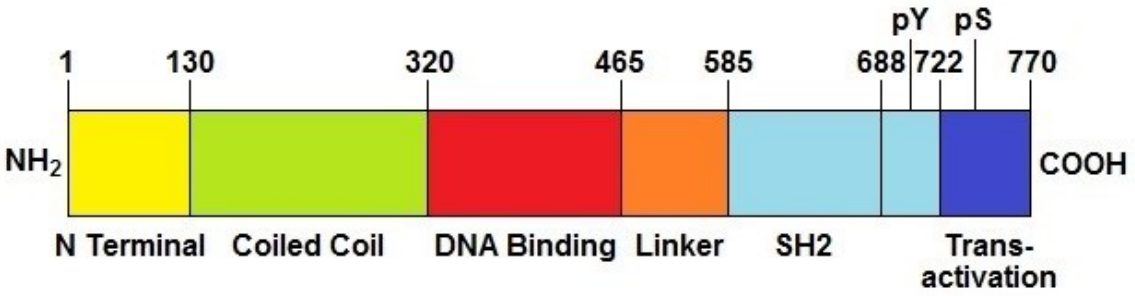

Figure 2. Schematic diagram of STAT3 structure.

N-terminal domain is involved in cooperative DNA binding. Coiled-coil domain is important for interactions with other transcriptional regulation proteins. DNA-binding domain directly contacts DNA. SH2 domain mediates formation of STAT3 dimers. The C-terminal transactivation domain is responsible for the transcriptional activation of STAT3-regulated genes.

C. Regulation of STAT3 signaling and roles of aberrant STAT3 signaling in cancers

As the activation of STAT3 is tightly regulated in cells under physiological condition, STAT3 signaling is latent and transiently activated in response to cytokines and growth factors. On the receptor level, direct ligand binding or receptor phosphorylation after ligand binding may trigger receptor endocytosis, thereby negatively regulating STAT3 signaling (41). Moreover, there are several negative regulators which act as protein tyrosine phosphatases (PTPs), e.g. Src homology region 2 domain-containing phosphatase-1 (SHP-1), SHP-2, phosphatase and tensin homolog (PTEN) and protein-tyrosine phosphatase 1D (PTP1D) (42-45). They may dephosphorylate receptors, kinases or STAT3, resulting in inactivation of STAT3 signaling. And protein inhibitors of activated STAT3 (PIAS3) can directly bind to STAT3, thereby preventing the binding of STAT3 to DNA and affecting the function of STAT3 (46). Additionally, activated STAT3 triggers transcription of diverse downstream target genes, including negative regulators which implicate in the termination of STAT3 signaling. STAT3 transcriptionally activates suppressor of cytokine signaling proteins (SOCS), leading to a negative regulation of STAT3 signaling (47). SOCS proteins may bind to JAKs or the cytokine receptors, resulting in inhibition of JAK activity or competing with STATs for binding sites on the receptors. SOCS proteins can also cause receptor degradation through ubiquitin-proteasome-mediated process.

In contrast to the strictly controlled normal cells, cancer cells usually harbor aberrant STAT3 signaling. Persistent activation of STAT3 may be derived from

constitutive activation of cytokine or growth factor receptors or aberrant activity of tyrosine kinases (48). Src oncoprotein also associates with enhanced activity of STAT3 (23, 49-51). As a result, aberrant gene transcription occurs in cancer cells and contributes to tumor cell survival and proliferation, tumor metastasis and angiogenesis as well as tumor immune evasion. As shown in **Table 1**, STAT3 regulates expression of survivin which acts as an inhibitor of apoptosis (26). STAT3-dependent overexpression of survivin inhibits apoptosis, causing resistance to chemotherapy. STAT3 is also a transcription factor of c-Myc and cyclin D1, which are proliferation-promoting genes (24, 25). Additionally, STAT3 involves in a variety of critical steps in metastasis and angiogenesis by regulating diverse genes (52-53). During tumor metastasis, individual tumor cells may break away from the original tumor and invade nearby vessels. Specifically, STAT3 activation transcriptionally induces twist which regulates the essential process in metastasis initiation with loss of cell adhesion and improved cell mobility (33). STAT3 was also shown to regulate transcription of diverse matrix metalloproteinases (MMPs) which involve in degrading different proteins that make up the surrounding extracellular matrix and thus helping cancer cells separate from adjoining tissues, e.g. MMP-1, MMP-2, MMP-7, MMP-9 and MMP-10 (27-32). Once inside the blood vessels, some cancer cells may simply die. Some cells may be recognized and destroyed by immune cells. Other cells may survive and leave the blood vessels to a new location where they begin to reproduce, resulting in a secondary tumor formed when the tumor cells locate to a suitable microenvironment. However, solid tumor cannot grow beyond a limited size without

blood supply. STAT3 also contributes to tumor angiogenesis by transcriptional regulation of vascular endothelial growth factor (VEGF) which stimulates the growth of new blood vessels (34, 35). Furthermore, activated STAT3 has been also found to affect the interplay between tumor cells and host immune system (54). To sum up, activation of STAT3 is a tightly controlled transient process in normal cells under physiological condition whereas its aberrant signaling correlates to malignant transformation and tumorigenesis.

D. Clinical implications of STAT3

Cancer is a group of disease characterized by uncontrolled cell growth in humans. As a leading cause of mortality throughout the world, lung, stomach, liver, colon and breast cancers account for the most cancer deaths each year. In particular, deaths caused by lung cancer accounted for about 27% of all cancer deaths as of 2013 (55). And about 1 in 8 women in the United States will develop invasive breast cancer during their lifetime. Common cancer therapy includes surgery followed by chemotherapy and/or radiotherapy whereas the survival rates of cancer patients remain low due to late diagnosis or poor response to treatment. Prognosis and survival rates of cancers depend on various factors, such as cancer type, disease stage and treatment. By interfering with specific molecules that induce carcinogenesis and tumor growth, targeted therapy is expected to be more effective than the conventional chemotherapy which simply works on all rapidly dividing cells. Despite hormone-blocking therapy and HER2-targeted therapy are effective to treat hormone receptor-positive cancers by interfering with the effects

of hormones on breast cancers; however, same breast cancers, which do not express estrogen receptor, progesterone receptor and HER2 (as called triple-negative), are still difficult to be treated as most therapies target one of the three receptors. Obviously, the discovery of tumor biomarkers and the subsequent development of novel antineoplastic agents will benefit thousands of cancer patients worldwide.

Persistent activation of STAT3 has been reported in most human cancers including ovarian, endometrial, cervical, breast, colon, pancreatic, lung, brain, renal, and prostate cancers, head and neck squamous cell carcinoma, glioma, melanoma, lymphomas and leukemia (56). STAT3 thus serves as a clinically useful biomarker for metastatic tumors with advanced disease stage. For instance, early-stage patients with non-small cell lung cancer (NSCLC) have higher long-term survival after surgery; however, approximately 75% of NSCLC patients are diagnosed in advanced stages (57). A meta-analysis based on 17 retrospective trials has recently revealed that high STAT3 and phospho-STAT3 expression is of prognostic significance for survival of NSCLC patients (58). STAT3 and phospho-STAT3 expression are significantly higher in NSCLC patients with poorly differentiated carcinoma, advanced disease stage and lymph node metastasis. Thus, high STAT3 or phospho-STAT3 expression is an important predictor of poor prognosis among patients with NSCLC. Moreover, Positive STAT3 expression was observed in 69.2% of breast tumors (59). And phospho-STAT3 was significantly higher in invasive carcinoma than in nonneoplastic tissue (60). Obviously, STAT3 is an important biomarker of progression in diverse cancers.

STAT3 is also an attractive therapeutic target for cancers. The mainstay of cancer treatment is surgery when the tumor is localized, followed by radiotherapy and chemotherapy. Multiple chemotherapeutic agents are used in combination to treat patients with cancers, including cyclophosphamide, methotrexate, 5-fluorouracil, doxorubicin, paclitaxel, cisplatin, *etc*. Targeted therapies are also used to fight cancers including antibodies/antagonists for hormones/receptors, signaling transduction inhibitors and angiogenesis inhibitors. By focusing on molecular and cellular targets that are specific to cancers, targeted cancer therapy may be more effective than other types of treatment, such as chemotherapy and radiotherapy, and less harmful to normal cells. Targeted agents permit the design of more rational therapeutic regimens for cancers. Inhibition of STAT3 has been shown to reduce tumor growth and metastasis in diverse studies as a common feature of many cancers is their dependence for survival on the constitutive activation of STAT3 (56, 61, 62). Given that the selection of first-line chemotherapy for cancers is complex due to the inherent biologic heterogeneity of the disease, the development of specific STAT3 inhibitors may potentially provide more options for clinical cancer therapy.

Additionally, constitutive STAT3 signaling causes resistance to chemotherapy in patients (63). As STAT3 is involved in IFN and EGF signaling, the increased level of STAT3 phosphorylation is also associated with the clinical effectiveness of targeted therapy to INF-α and EGF in cancer patients (64-67). STAT3 is thus a prognostic factor that can predict the patient's responses to related treatments. Moreover, recent studies have found that STAT3 is a

determinant of chemoresistance and is associated with tumor recurrence in a large number of solid malignancies (68). STAT3 promotes transcription of crucial regulators of cell cycle progression and anti-apoptosis. Persistent activation of STAT3 may lead to protection against cytotoxic agents in cancers. Thus, the pharmacological inhibition of STAT3 may be also a promising therapeutic strategy for the management of chemoresistance in cancers.

Overall, STAT3 has emerged as a promising drug target for cancer treatment.

E. Strategies to inhibit aberrant STAT3 signaling

A variety of STAT3 inhibitors have been previously identified (56, 61, 62). The current STAT3 inhibitors usually (1) inhibit STAT3 activation; (2) disrupt STAT3 dimerization; (3) block the binding of STAT3 to DNA.

The first proof-of-concept approach was derived from peptidic and peptidomimetic inhibitors mimicking the sequence that binds to the SH2 domain of STAT3 to disrupt its dimerization. These inhibitors consist of small peptides PpYLKTK, pYLPQTV and mimetics ISS 610 (69-71). However, the feature of peptides determines their low membrane permeability, low stability and poor bioavailability. Although ISS 610 exhibits improved activity on inhibition of STAT3 and selectivity over STAT1 and STAT5 in *in vitro* DNA-binding assays, its intracellular activity remains low as it cannot be efficiently taken up by cells. Computational approaches and assay-based screening were then used to identify a number of small molecule inhibitors targeting the SH2 domain, e.g. STA-21,

stattic, S3I-201, S3I-M2001, catechol containing compounds, FLLL32 and LLL-12 (72-81). These small molecule inhibitors appear to block the formation of STAT3 dimers and inhibit proliferation and survival of cancer cells harboring constitutive STAT3 signaling. Both peptide and non-peptide inhibitors demonstrate the feasibility of targeting the SH2 domain and dimerization of STAT3. However, most of them have limited clinical development because of their moderate activities at medium to high micromolar levels. Additionally, it has been shown recently that STAT3 involves in oncogenesis and transcriptional regulation in the absence of tyrosine phosphorylation (82-85). Thus disruption of STAT3 dimerization may be not enough to inhibit aberrant STAT3 signaling.

As the transcriptional activity of STAT3 requires physical interaction between STAT3 and the promoter regions of responsive genes, DBD is also a potential drug target. Galiellalactone, peptide aptamers, flavopiridol and a class of platinum (IV) compounds including IS3295, CPA-1, CPA-7 and platinum (V) tetrachloride were found to interfere with STAT3 binding to DNA and inhibit STAT3-dependent gene transcription, resulting in the induction of cell growth inhibition and apoptosis in human breast, lung and prostate cancer cells (86-92). Some of these inhibitors have been evaluated in animal models and they appear to reduce growth of xenograft tumors. All these findings suggest that DBD is likely druggable, however, specificity may be a difficult problem to solve. For example, a small molecule compound NSC-368262 (C48) has been recently identified as a STAT3 inhibitor that alkylates cysteine 468 at the DNA-binding interface, but mixing glutathione with C48 confirmed alkylation of the thiol group of glutathione by C48,

indicating it may alkylate every surface-exposed cysteine residues (93). On the other hand, decoy oligodeoxynucleotides (ODNs) are also a novel strategy by mimicking STAT3 specific DNA-binding sequence and competing for binding to STAT3, leading to suppression of STAT3-mediated gene transcription (94-98). Decoy ODNs usually represent preferable specificity over other modalities, however, an important issue is a suitable bioavailability profile for these biological agents. Amazingly, the first human trial of a STAT3 decoy ODN in head and neck tumors has been successfully completed (99). These findings show that STAT3 decoy ODN can be modified to enable systemic delivery and be used to inhibit tumor growth through intravenous injection.

STAT3 signaling can be also indirectly modulated by targeting the upstream components of STAT3 activation. These inhibitors include JAK inhibitors such as AG490, resveratrol, WP1066, AZD1480 and TG101209, receptor tyrosine kinase inhibitor such as tyrphostins and Src kinase inhibitor such as indirubin (100-107). Moreover, targeting upstream factors for STAT3 expression such as antisense oligonucleotides have been considered and tested (108, 109). Due to implication of other pathways, these inhibitors may be limited to specifically inhibit STAT3 signaling.

In summary, the preclinical investigation of STAT3 inhibitors provides a great foundation rationale for further development of novel anti-cancer drugs. The progress in studying these candidate inhibitors imply that STAT3 is a druggable target in human cancers. However, none of these STAT3 inhibitors has been

approved for clinical use. More studies are clearly needed for further development of clinically available agents.

F. Specific aims of the present work

It is well recognized that STAT3 is an attractive target for drug development. The major problems in successful development of STAT3 inhibitors consist of low biological activity, low membrane permeability and low specificity. An ideal STAT3 inhibitor should target STAT3 but not affect upstream components or other STAT family members. As reviewed above, the peptidic and peptidomimetic inhibitors are more easily to be designed and developed but have low membrane permeability due to the feature of peptides. Although small molecule compounds targeting SH2 domain show enhanced membrane permeability, the clinical development has been slow. No inhibitors targeting SH2 domain has entered clinical trials so far and unphosphorylated STAT3 also plays an important role in oncogenesis (82-85). Thus, inhibiting DNA binding is a promising strategy as the first clinical trial of STAT3 decoy ODN was successful (99). Although STAT3 ODN can be modified to enable systemic delivery, intravenous injection is not a user-friendly route of administration.

Based on the current progress of STAT3 inhibitors as discussed above, my study was designed to identify small molecule compounds targeting the DBD of STAT3 and to investigate the mechanism of the candidate compounds for development of effective and specific STAT3 inhibitors targeting DBD. The first aim is to identify small molecule compounds targeting the DBD of STAT3 using

structure-based virtual compound screening and STAT3-dependent luciferase activity assay as well as to verify the effects and specificity of the candidate compounds on STAT3 protein. Structure-activity relationship analysis was performed to optimize the chemical structure to achieve the optimal biological activity and specificity. The anti-tumor effects of the candidate compounds were investigated, including cell survival, apoptosis, cell migration and invasion. Finally, the *in vivo* efficacy of the most promising compound was evaluated in a mouse xenograft tumor model.

The second aim is to investigate the detailed mechanism of the candidate compounds on inhibition of aberrant STAT3 signaling. Specifically, the effects on STAT3 signaling pathway were assessed to verify the efficacy and specificity of the compounds, e.g. the activation of STAT3, the dimerization of STAT3, the binding of STAT3 to DNA and the expression of STAT3 downstream targets.

The outcome from this study would lead to a better understanding of development of STAT3 inhibitors targeting the DBD and thus help develop better antineoplastic drugs and therapeutic regimens for cancer treatment.

II. Materials and Methods

A. Materials

Cell culture mediums Dulbecco's Modification of Eagle's Medium (DMEM, Catalog No.: 10-013-CV), RPMI-1640 (Catalog No.: 10-040-CV), DMEM/Ham's F-12 50/50 Mix (Catalog No.: 11320-033) and Opti-MEM (Catalog No.: 51985-034) as well as cell culture materials including fetal bovine serum (FBS; Catalog No.: 104375), equine serum (Catalog No.: 26050), trypsin-versene mixture (Catalog No.: 17-161-E) and penicillin/streptomycin (Catalog No.: 17-602-E) were purchased from Corning cellgro (Manassas, VA), Life Technologies (Grand Island, NY) or Lonza (Walkersville, MD). Luciferase Assay System (Catalog No.: E4030), Dual-Luciferase® Reporter Assay System (Catalog No.: E1910), GSH-Glo™ Glutathione Assay System (Catalog No.: V6911), T4 polynucleotide kinase (Catalog No.: M410A) and its buffer (Catalog No.: C131B) were obtained from Promega (Madison, WI). Metafectene® transfection reagent (Catalog No.: T020-1.0) was purchased from Biontex Laboratories GmbH (Martinsried, Germany). Quick Spin Columns (Catalog No.: 1522981) and Cell Death Detection ELISA^{PLUS} Photometric Enzyme Immunoassay Kit (Catalog No.: 1774425) were purchased from Roche Diagnostics GmbH (Mannheim, Germany). BioCoat™ MatrigeI™ Invasion Chambers (Catalog No.: 354480) came from BD Biosciences (Bedford, MA). Human insulin solution (Catalog No.: I9278-5ML), human EGF (Catalog No.: E5036-200UG), protease inhibitor cocktail (Catalog No.: P8340), fibronectin lyophilized powder (Catalog No.: F2006) and His-tagged human recombinant STAT3 protein (Catalog No.: SRP5374-20UG) were obtained from Sigma-Aldrich

(St. Louis, MO). Bio-Rad Protein Assay Dye Reagent (Catalog No.: 500-0006) and iScript™ cDNA Synthesis Kit (Catalog No.: 170-8891) were purchased from Bio-Rad Laboratories (Hercules, CA). Immobilon™ Polyvinylidene Difluoride (PVDF) Transfer Membranes (Catalog No.: IPVH00010), Chromatin Immunoprecipitation Assay Kit (Catalog No.:17-295) and purified rabbit IgG (Catalog No.: PP64B) came from EMD Millipore (Billerica, MA). EAH-Sepharose™ 4B (Catalog No.: 17-0569-01), CNBr-activated Sepharose™ 4B (Catalog No.: 71-7086-00) and Amersham™ ECL Western Blotting Detection Reagent (Catalog No.: RPN2106) were obtained from GE Healthcare (Uppsala, Sweden). SuperSignal West Dura Chemiluminescent Substrate (Catalog No.: 34075) was purchased from Pierce (Rockford, IL). RNeasy® Mini Kit (Catalog No.: 74104) was obtained from Qiagen (Valencia, CA). SYBR® Green PCR Master Mix (Catalog No.: 4309155) came from Applied Biosystems (Warrington, UK). Hot Rod Chemistry® formulation screening kit 1 and 2 (Catalog No.: HRC-K1 and HRC-K2) were purchased from Pharmatek Laboratories (San Diego, CA). ImmPRESS™ reagent kit (Catalog No.: MP-7401 and MP-7405) and ImmPACT™ DAB peroxidase substrate kit (Catalog No.: SK-4105) were obtained from Vector Laboratories (Burlingame, CA).

Antibodies against STAT3 (Catalog No.: sc-482x), STAT1 (Catalog No.: sc-346x), cyclin D1 (Catalog No.: sc-246), MMP-2 (Catalog No.: sc-10736), MMP-9 (Catalog No.: sc-10737), VEGF (Catalog No.: sc-152) and twist (Catalog No.: sc-81417) were purchased from Santa Cruz (Dallas, TX). Antibodies against STAT3 (Catalog No.: 9139), phospho-STAT3 (Catalog No.: 9145), survivin (Catalog No.: 2802 and 2808), histone H2A (Catalog No.: 2578) and histone H3 (Catalog No.:

9715) were obtained from Cell Signaling Technology (Danvers, MA). Monoclonal antibodies against FLAG (Catalog No.: F3165), α-Tubulin (Catalog No.: T9026) and β-actin (Catalog No.: A5316) as well as horseradish peroxidase-conjugated secondary antibodies to mouse IgG (Catalog No.: A9309) or rabbit IgG (Catalog No.: A9169) came from Sigma-Aldrich.

All other chemicals were of molecular biology grade from Sigma-Aldrich or Fisher Scientific (Chicago, IL).

B. Cell lines and culture

Human lung cancer cell line A549, human breast cancer cell lines MDA-MB-231, MDA-MB-231-STAT3 (MDA-MB-231-STAT3 cells stably cloned with STAT3-dependent luciferase reporter were obtained from Dr. Jiayuh Lin at Ohio State University) and MDA-MB-468 and human normal lung fibroblast cell line IMR90 were cultured in DMEM, supplemented with 10% FBS and appropriate antibiotics (100 units/mL penicillin and 100 μg/mL streptomycin) in a 37°C humidified atmosphere containing 5% CO_2. Human lung cancer cell line H1299 was maintained in RPMI-1640 medium containing 10% FBS and appropriate antibiotics at 37°C with 5% CO_2. Human normal breast epithelial cell line MCF10A1 was cultured in DMEM/Ham's F-12 50/50 Mix with 10% equine serum, 10 μg/mL insulin, 25 ng/mL EGF, 500 ng/mL hydrocortisone, 100 ng/mL cholera toxin and appropriate antibiotics at 37°C with 5% CO_2.

C. Structure-based virtual compound screening

(Courtesy of Dr. Jing-Yuan Liu)

To identify the potential small molecule compounds that can directly disrupt the interaction between STAT3 and its DNA substrates, the crystal structure of STAT3β-DNA complex was retrieved from Protein Data Bank (http://www.rcsb.org/pdb; PDB code: 1BG1). The DNA in the crystal structure was removed and the protein chain was prepared for molecular docking. The coordinates of DBD and Linker domain (residues 320-550), which are directly involved in DNA binding, were applied to the calculation. The DNA-binding groove consisting of residues 329-332, 340-346, 406-412 and 465-468 was chosen as the targeting area for molecular docking. Molecular surface was computed using the software Distributed Molecular Surface. Partial charges and protons were added to the protein by DockPrep module of Chimera (110). 200,000 small molecule virtual compounds obtained from ChemDiv library (San Diego, CA) were screened using the molecular docking program DOCK 6.0 (111). The docking of each compound was scored with the DOCK GRID scoring function. The 1,000 top-scoring compounds were then analyzed and re-scored using the AMBER scoring function of DOCK 6.0 package (112).

The top-scoring compounds were also docked onto the DBD of STAT1 (PDB code: 1BF5). Compounds scored well with STAT1 were eliminated and the remaining compounds with poor scores for STAT1 were further clustered using the software Molecular Operating Environment and visually examined using Chimera ViewDock function. A total of 100 compounds were finally selected based on the combination of GRID and AMBER scores, drug likeness (Lipinski's rule of five) as

well as based on the consideration of maximizing compounds from different clusters.

D. STAT3-dependent luciferase reporter assay

MDA-MB-231-STAT3 cell line stably transfected with a high level of STAT3-dependent luciferase reporter was used to screen the potential STAT3 inhibitors as described previously (74). Cells were seeded at 5×10^4 cells per well in a 12-well plate. Next day, cells were exposed to 0.1% dimethyl sulfoxide (DMSO) vehicle control or the candidate compounds at 20 μM for 48 hours and the luciferase activity was then measured by Luciferase Assay System according to the manufacturer's instructions. In brief, growth medium was removed from cultured cells after treatment followed by washing with 1× phosphate buffered saline (PBS; 8 g/L NaCl, 0.2 g/L KCl, 1.44 g/L Na_2HPO_4, 0.24 g/L KH_2PO_4, pH 7.4) three times. Cells were dispensed in 200 μL of 1× cell culture lysis reagent provided by the kit and then lysed by three freeze-thaw cycles (incubation in dry ice-ethanol bath for 2 minutes followed by incubation at 37°C for 10 minutes). Cell suspensions were subjected to centrifugation at 13,000 rpm for 2 minutes. Then 5 μL of supernatant was mixed with 25 μL of luciferase assay reagent for measurement of the luminescence by using Berthold Detection Systems Sirius Luminometer (Titertek-Berthold, Germany) and the luciferase activity levels were finally normalized to total protein content measured using Bio-Rad Protein Assay Dye Reagent.

To verify the specificity of STAT3-dependent luciferase reporter, a luciferase reporter driven by p27 promoter containing no STAT3-binding site was used as a negative control (113). H1299 cells were transiently transfected with a p27 promoter-driven Firefly reporter plasmid and a transfection control Renilla reporter plasmid using Metafectene® transfection reagent according to the manufacturer's suggestions followed by reseeding in a 24-well plate with 5×10^4 cells per well. After 24 hours, the transfected cells were exposed to the candidate compounds for 48 hours. The p27 promoter-driven Firefly reporter activity was determined by using Dual-Luciferase® Reporter Assay System and then normalized to the co-transfected Renilla, following the manufacturer's instructions.

E. Molecular dynamics simulation and calculation of binding free energy

(Courtesy of Dr. Jing-Yuan Liu)

To verify the preference of candidate compounds on STAT3 over STAT1, the binding free energy of inS3-54 to STAT3 or STAT1 was computed by 3-ns molecular dynamics simulation followed by Born/surface area (GBSA) energy analysis. Briefly, a total of 20 snapshots were collected from the production trajectory for MM-GBSA free energy calculations using the formula $\Delta G_{bind} = G_{complex} - G_{STAT} - G_{inS3\text{-}54}$, where $G = G_{solute} + G_{solvent}$.

F. Electrophoretic mobility shift assay

As the compounds were designed to target the DBD of STAT3, electrophoretic mobility shift assay (EMSA) was used to determine the inhibitory

effects of compounds on DNA-binding activity of STAT3 and STAT1. For preparation of cell lysates, 4×10^6 H1299 cells were plated in a 150-mm tissue culture dish for 24 hours, followed by transient transfection with FLAG-tagged constitutively dimerizable STAT3c or STAT1 expression construct using Metafectene® transfection reagent according to the supplier's instructions. 48 hours after transfection, cells were harvested and re-suspended in hypertonic buffer (20 mM HEPES·KOH, pH 7.9, 1.5 mM $MgCl_2$, 420 mM KCl, 0.2 mM EDTA, 0.5 mM DTT, 1 mM PMSF, 1 mM $NaVO_3$, 20 mM NaF, 20% glycerol, 0.01 mM NaP_2O_7) as well as centrifuged at 13,000 g for 10 minutes at 4°C after three freeze-thaw cycles (dry ice-ethanol bath for 2 minutes and 37°C for 10 minutes). The supernatant was collected, aliquoted and stored at -70°C. For preparation of [^{32}P]-labeled sis-inducible element (SIE) probe, 40 ng of unlabeled SIE probe (5'-AGCTTCATTTCCCGTAAATCCCTA-3') was incubated at 37°C for 45 minutes with 50 µCi γ-^{32}P-adenosine triphosphate (ATP) and 10 units of T4 polynucleotide kinase in 10 µL kinase reaction buffer. Radiolabeled probe was then purified by Quick Spin Column to remove free nucleotides. The purified probe was then qualified by using Beckman Coulter LS 6500 Multi-purpose Scintillation Counter (Beckman Coulter, Brea, CA), diluted to $5x10^4$ cpm/µL and stored at -70°C. For EMSA, 20 µg of cell lysate was pre-incubated with indicated compounds for 30 minutes at room temperature in the binding buffer (10 mM HEPES·KOH, pH 7.9, 0.1 µg/µL poly(dI·dC), 50 mM KCl, 10% glycerol, 0.05 µg/µL BSA, 1 mM DTT and 0.2 mM PMSF) before adding 5×10^4 cpm [^{32}P]-labeled SIE probe. For supershift and competition, 4 µL specific antibody against STAT3 or STAT1 or 100-fold

excess non-radioactive SIE probe was added to the reaction mixture and incubated for 30 minutes before adding the radiolabeled probe. All mixture reactions were incubated for 20 minutes at room temperature and then separated on 6% native polyacrylamide gel in 0.25× TBE buffer (22.5 mM Tris·boric acid, pH 8.3, 0.5 mM EDTA). Radiolabeled bands were finally visualized by autoradiography.

G. Preparation of inS3-54-conjugated EAH-Sepharose 4B and pull down assay

EAH-Sepharose 4B containing 7-11 μmol conjugated amino group in 1 mL of drained gel was used to conjugate inS3-54 containing carboxyl group through the carbodiimide coupling method according to manufacturer's instructions. For the coupling reaction, 200 μL EAH-Sepharose 4B gels were washed on a sintered glass filter with 16 mL of distilled water adjusted to pH 4.5 with HCl, followed by 16 mL of 0.5 M NaCl. (±) 2 mg inS3-54 or irrelevant compound (C5) dissolved in 240 μL of 50% (v/v) dimethylformamide solution was mixed with drained EAH-Sepharose 4B. 1-ethyl-3-(3-dimethylaminopropyl) carbodiimide (EDC) was added to EAH-Sepharose 4B solution as a catalyst for the coupling reaction at a final concentration of 0.1 M. The reaction mixtures were rotated for 24 hours at 4°C. After the coupling reaction had finished, the gels were washed with 16 mL of 50% (v/v) dimethylformamide to remove free compounds and the remaining active groups were blocked in a further carbodiimide reaction with 1 M acetic acid under catalysis of 0.1 M EDC. The gels were then washed alternatively with 0.5 M NaCl

in 0.1 M Tris·HCl (pH 8.3) and 0.5 M NaCl in 0.1 M sodium acetate/acetic acid buffer (pH 4.0) for at least three cycles. The gels were further washed with double distilled water and stored at 4°C in binding buffer (10 mM MES/NaOH, pH 6.5, 150 mM NaCl, 2 mM $MgCl_2$, 2 mM $CaCl_2$, 5 mM KCl, 0.5% NP-40) used for the following pull-down assay. The coupling efficacy was verified by monitoring whether the transparent beads turn color after coupled with the orange (inS3-54) or yellow (C5) compounds.

For pull-down assay, inS3-54-conjugated beads and two kinds of control beads (vehicle control and irrelevant compound C5) equilibrated with binding buffer were blocked with 10% non-fat milk in binding buffer containing 2 mM PMSF and 1:1000 diluted protease inhibitor cocktail followed by incubation with 120 μg total lysate of H1299 cells harboring FLAG-STAT3c in the same buffer at 37°C for 1 hour. The unbound proteins were removed by washing with the binding buffer seven times and the proteins bound to inS3-54-conjugated beads were directly separated by 10% sodium dodecyl sulfate-polyacrylamide gel electrophoresis (SDS-PAGE) followed by either gel silver staining or immunoblotting with respective antibodies. The bound proteins were also eluted from the beads by excess free inS3-54 followed by SDS-PAGE and Western blot analysis. For competition analysis, cell lysates were pre-incubated with DMSO vehicle, 10 μM inS3-54 or C5 at 37°C for 1 hour prior to incubation with inS3-54-conjugated beads. To investigate the potential direct interaction between inS3-54 and STAT3, 1 μg of commercial human recombinant STAT3 protein with His-tag was also applied to pull down assay following the same procedure.

H. Preparation of A26-conjugated CNBr-activated Sepharose 4B and pull down assay

CNBr-activated Sepharose 4B was used for coupling the compound A26 containing imino group by the cyanogen bromide method according to the manufacturer's instructions. For the coupling reaction, 1 g lyophilized CNBr-activated Sepharose 4B was dissolved in 3.5 mL of 1 mM HCl and washed with 200 mL of 1 mM HCl on a sintered glass filter. (±) 10 μmoles of A26 or inactive compound (PHP) was dissolved in 5 mL of coupling buffer (0.1 M $NaHCO_3$, pH 8.3, 0.5 M NaCl) and mixed with the prepared CNBr-activated Sepharose 4B in a stoppered vessel, followed by rotation overnight at 4°C. After the coupling reaction, the excess compounds were washed with at least 25 mL of coupling buffer. Any remaining active groups were further blocked with 0.1 M Tris·HCl, pH 8.0 overnight at 4°C. Finally, the gels were washed with at least three cycles of alternating pH with 0.1 M sodium acetate/acetic acid, pH 4.0 containing 0.5 M NaCl and 0.1 M Tris·HCl, pH 8.0 containing 0.5 M NaCl and stored at 4°C in 0.1 M Tris·HCl, pH 8.0 containing 0.5 M NaCl. Since A26 is yellow and PHP is pale yellow in color, the conjugation of A26 or PHP to CNBr-activated Sepharose 4B can be verified by monitoring the change in color of the beads.

For pull-down assay, A26-conjugated and two kinds of control beads (DMSO vehicle control and irrelevant compound PHP) equilibrated with washing buffer (20 mM Tris-HCl, pH 8.0, 75 mM KCl, 1 mM EDTA, 15% glycerol, 0.5% NP-40) were blocked with 10% non-fat milk in the binding buffer (20 mM Tris-HCl, pH 8.0, 150 mM KCl, 1 mM EDTA, 15% glycerol, 0.5% NP-40, 0.2 mM PMSF and

1:1000 diluted protease inhibitor cocktail) followed by incubation with 120 μg total lysate of H1299 cells transfected with FLAG-STAT3 in the same buffer both at 37°C for 1 hour. The unbound proteins were removed by washing seven times with the washing buffer and the bound proteins were subjected to SDS-PAGE followed by analysis of FLAG-STAT3c using Western blot analysis. For competition analysis, cell lysates were pre-incubated with DMSO vehicle, 10 μM inS3-54 analogues or PHP at 37°C for 1 hour prior to incubation with A26-conjugated beads.

I. Glutathione assay

Glutathione served as a substrate to determine whether inS3-54 or its analogue A18 might act as an alkylating agent to surface-exposed cysteine as described previously (93). It is assumed that an agent that alkylates cysteine residues may also alkylate glutathione via its thiol group. To determine whether or not glutathione was alkylated by the compounds, A549 or MDA-MB-231 cells were exposed to DMSO vehicle or indicated compounds for 48 hours. Following treatment, the glutathione level was measured using GSH-Glo™ Glutathione Assay Kit which provides a luminescence-based assay for the detection and quantification of glutathione. Briefly, 5×10^3 cells were harvested and dispensed in 50 μL of GSH-Glo™ reagent containing luciferin-NT substrate and glutathione S-transferase diluted in GSH-Glo™ reaction buffer, followed by incubation at room temperature for 30 minutes. As shown in **Figure 3**, luciferin is generated from the luminogenic luciferin-NT substrate, catalyzed by glutathione S-transferase in the presence of glutathione. Then, reaction mixtures were further incubated for 15

minutes with 100 µL/well of luciferin detection reagent which simultaneously stops the previous reaction and initiate a luminescent signal. Finally, the luminescence produced was read by Berthold Detection Systems Sirius Luminometer. The luminescent signal produced is directly proportional to the amount of glutathione in cells. The relative level of glutathione was compared with that of DMSO vehicle control which did not receive drug treatment. Iodoacetamide (IAA), which binds covalently to the thiol group of cysteine, was used as a positive control.

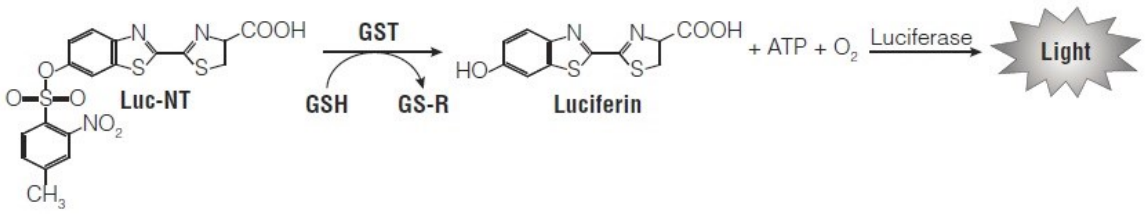

Figure 3. Schematic diagram of GSH-Glo™ glutathione assay.

The assay is based on the conversion of a luciferin derivative into luciferin in the presence of glutathione, catalyzed by glutathione S-transferase. The signal generated in a coupled reaction with firefly luciferase is proportional to the amount of glutathione present in the sample. GSH: glutathione; GST; glutathione S-transferase; GS-R: glutathione derivative. The figure is adapted from GSH-GloTM Glutathione Assay Technical Manual provided by the manufacturer.

J. Cytotoxicity assay

Cytotoxicity of indicated compounds to cancer cells was determined using sulforhodamine B (SRB) colorimetric assay as previously described (114, 115). 1×10^3 cells/well were plated in a 96-well plate overnight. Cells were then treated with indicated compounds for 72 hours. After treatment, the culture medium was removed and the cells were fixed and stained by addition of 0.4% (w/v) SRB in 1% acetic acid solution followed by incubation at room temperature for 20 minutes. The plate was washed four times with 1% acetic acid to remove the unbound SRB and air-dried overnight at room temperature. The bound SRB was then solubilized in 100 µL of 10 mM unbuffered Tris·base. Optical density (OD) was determined at 570 nm using BioTek Synergy H1 Hybrid Microplate Reader (BioTek, Winooski, VT). Cell viability was determined as compared with vehicle control (0.1% DMSO) and calculated using the following formula: survival (%) = $OD_{Treatment}/OD_{DMSO} \times 100\%$. The cell survival curve was plotted by the survival fractions on y-axis against the logarithmic concentrations on x-axis. IC_{50} of indicated compounds for each cell line was finally computed using the GraphPad Prism software (GraphPad Software, La Jolla, CA).

K. Enzyme-linked immunosorbent assay for quantification of apoptosis

To investigate the potential contribution of indicated compounds to apoptosis, Cell Death Detection ELISA^{PLUS} Photometric Enzyme Immunoassay was used for the quantitative determination of cytoplasmic histone-associated DNA fragments after induced cell death as we previously described (115). Briefly,

exponentially growing A549 or MDA-MB-231 cells were seeded in a 12-well plate at 7.5×10^4 cells/well. 24 hours after plating, cells were exposed to various compounds under indicated conditions. Growth medium was removed from cultured cells after treatment followed by washing with 1× PBS one time. 1×10^4 cells were then collected and resuspended in 200 µL of lysis buffer provided by the kit, followed by incubation at room temperature for 30 minutes. Cell lysates were centrifuged at 200 g for 10 minutes. As shown in **Figure 4**, 20 µL of supernatant for each sample was placed into a streptavidin-coated microplate, followed by adding a mixture of biotin-conjugated anti-histone antibody and horseradish peroxidase-conjugated anti-DNA antibody as well as incubating at room temperature for 2 hours. During the incubation interval, nucleosomes were captured via their histone components by the biotin-conjugated anti-histone antibody, while binding to the streptavidin-coated microplate. Simultaneously, the DNA fragments of nucleosomes were detected by anti-DNA antibody. After removal of unbound antibodies by a washing step, the amount of nucleosomes was quantified by the peroxidase retained in the immunocomplex with ABTS as a substrate. The relative level of DNA fragmentation was compared with that of DMSO vehicle control that did not receive drug treatment.

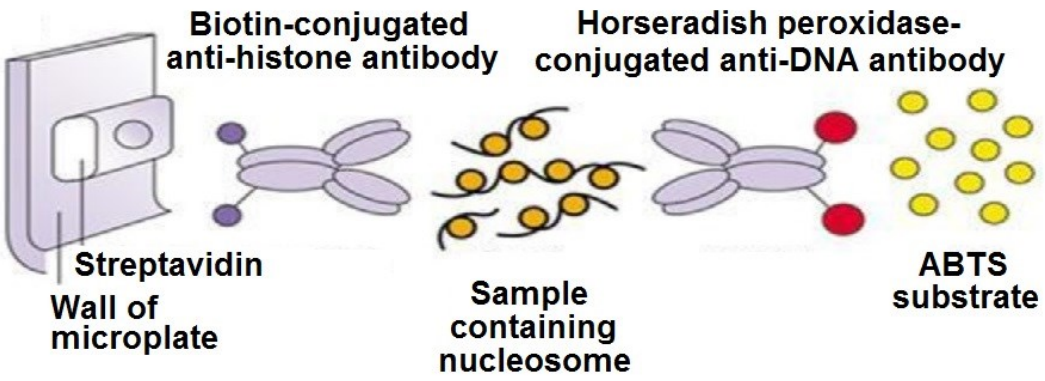

Figure 4. Schematic diagram of apoptosis ELISA assay.

The assay is used for the quantitative *in vitro* determination of cytoplasmic histone-associated DNA fragments after induced cell death. The figure is adapted from Cell Death Detection ELISA^{PLUS} Photometric Enzyme Immunoassay Kit Instructions provided by the manufacturer.

L. Hematopoietic progenitor cell colony formation assay

(Courtesy of Dr. Hal Broxmeyer)

Hematopoietic progenitor cell colony formation assay was performed as previously described (116, 117). A STAT3 allele in which exons 18–20 were flanked by loxP sequences was generated. Removal of exons 18–20, which encode the SH2 domain of STAT3, was expected to eliminate the function of the protein. A mouse strain (C57BL/6) for tissue-specific gene deletion where Cre expression is driven by a TIE2 gene promoter/enhancer cassette was used to generate the unique strain of mice with tissue-specific deletion of STAT3 during hematopoiesis. The TIE2 gene promoter triggered Cre expression in bone marrow and endothelial cells. In two steps of breeding STAT3-loxP with Tie2-Cre, the mice that are homozygous for STAT3-loxP and Tie2-Cre^{+} were obtained as the conditional STAT3 knock-out mice. 5×10^4/mL $STAT3^{+/+}$ and $STAT3^{-/-}$ mouse bone marrow cells were then isolated and stimulated *in vitro* with 1 unit/mL recombinant human erythropoietin, 50 ng/mL recombinant mouse stem cell factor, 5% (v/v) pokeweed mitogen mouse spleen cell conditioned medium and 0.1 mM hemin in the presence of DMSO vehicle control or indicated compounds. Colonies were scored 7 days after incubation at 5% CO_2 and lowered (5%) O_2.

M. Cell migration assay

Wound filling assay was used to determine the inhibitory effect of indicated compounds on cell migration as described previously (118). Briefly, 1×10^5 cells/well A549 or MDA-MB-231 cells were seeded in a 6-well plate. 24 hours after

plating, cells reached 90%~100% confluence as a monolayer. 200-μL pipette tip was used to scratch the monolayer across the center of each well. After scratching, cells were gently washed one time with fresh medium to remove the detached cells and then incubated with or without the treatment of indicated compounds. The wound filling process over a 24-hour period was monitored and photographed at different time intervals (0, 6, 12 and 24 hours following treatment) with a magnification of 40× using Zeiss Axiovert 25 Microscopic Camera System (Carl Zeiss, Göttingen, Germany) as well as quantified by measuring the remaining gap between two migrating edges in Photoshop software. The migration rate on various time intervals was calculated using the following formula: migration rate (%) = (mean distance between both edges at 0 hr - mean distance between both edges at T hrs)/ mean distance between both edges at 0 hr × 100%.

N. Cell invasion assay

To determine the inhibitory effect of indicated compounds on cell invasion, cell invasion assay was carried out using BioCoat™ Matrigel™ Invasion Chambers following the manufacturer's instructions. The package was firstly removed from -20°C storage and pre-coated with 250 μL of 30 μg/μL fibronectin per well overnight at 4°C. Matrigel inserts were then pre-warmed in serum-free medium at 37°C for 1 hour. 1.25×10^5 cells per well were plated in the upper compartments of 24-well Matrigel invasion chambers with serum-free medium in the absence or presence of indicated compounds. Medium containing 10% FBS in the lower chambers serves as a chemo-attractant. The Matrigel™ matrix provides a true barrier to non-

invasive cells while presenting an appropriate protein structure for invading cells to penetrate before passing through the 8-μm pores on the chamber membrane. After incubation at 37°C for 6 or 24 hours, the non-invading cells attached on the upper surface of the membrane were gently removed with a cotton swab. Cells invading to the undersurface of the membrane were stained with a fixative/staining solution (0.1% crystal violet, 1% formalin, 20% ethanol), photographed and counted for invasive cell number in 10 randomly selected fields for each treatment using Zeiss Axiovert 25 Microscopic Camera System. The invasion rates of indicated compounds were quantified by invasive cell numbers compared to DMSO control.

O. Western blot analysis

Western blot analysis was used to determine the protein expression level. 1×10^6 MDA-MB-231 or A549 cells were seeded in 100-mm tissue culture dishes and exposed to various treatments under appropriate conditions. After treatment, cells were harvested and suspended in lysis buffer containing 50 mM Tris·HCl, pH 7.4, 150 mM NaCl, 0.5% NP-40, 20 mM EDTA, 50 mM NaF, 1 mM Na_3VO_4, 2 mM PMSF and 1 mM DTT followed by incubation on ice for 10 minutes. The cell lysates were sonicated briefly (3 cycles of 7 seconds with 40% amplitude) and centrifuged at 13,000 rpm for 20 minutes at 4°C. The soluble supernatants were collected and their protein concentrations were measured using Bio-Rad Protein Assay Dye Reagent.

Equivalent amount of cell lysate protein (40~60 μg) was separated on 10%~15% SDS-PAGE and transferred onto a PVDF membrane. The blot was then blocked with 5% non-fat milk in PBS containing 0.1% Tween-20 at room temperature for 1 hour and probed with the desired primary antibody to specific protein (diluted according to the manufacturer's instructions) at room temperature for 2 hours or at 4°C overnight. Subsequently, the blot was incubated with appropriate horseradish peroxidase-conjugated secondary antibody and the immunoreactive protein bands were visualized using Amersham™ ECL Western Blotting Detection Reagent or SuperSignal West Dura Chemiluminescent Substrate and captured by X-ray film or FluoChem™ HD2 Imaging System (ProteinSimple, Santa Clara, CA). The relative protein levels were determined by the density of Western blot bands as measured by Image J software (National Institutes of Health) and normalized against the internal control β-actin.

P. Real-time polymerase chain reaction

Real-time polymerase chain reaction (PCR) was used to determine the mRNA expression level in tumor cells following treatment. Total RNAs were isolated from cultured cells using RNeasy® Mini Kit according to the manufacturer's instructions. 4 μg of total RNAs were reverse-transcribed using iScript™ cDNA Synthesis Kit. Primers used for real-time PCR were shown in **Table 2**. Real-time PCR was performed with SYBR® Green PCR Master Mix on ABI Prism® 7500 Real-time PCR System (Applied Biosystems). The threshold cycle (C_t) is defined as the PCR cycle number at which the reporter fluorescence achieves the

threshold reflecting a statistically significant point above the calculated baseline. The C_t of indicated gene was determined and normalized against that of the internal control glyceraldehyde 3-phosphate dehydrogenase (GAPDH).

Table 2. Primers used for real-time PCR

Genes	Primers
STAT3	Forward: 5'-GGCCCCTCGTCATCAAGA Reverse: 5'-TTTGACCAGCAACCTGACTTTAGT
CyclinD1	Forward: 5'-CTTCCTCTCCAAAATGCCAG Reverse: 5'-AGAGATGGAAGGGGGAAAGA
Survivin	Forward: 5'-TGCCTGGCAGCCCTTTC Reverse: 5'-CCTCCAAGAAGGGCCAGTTC
MMP-9	Forward: 5'-TGACAGCGACAAGAAGTG Reverse: 5'-CAGTGAAGCGGTACATAGG
VEGF	Forward: 5'-TACCTCCACCATGCCAAGTG Reverse: 5'-GATGATTCTGCCCTCCTCCTT
Twist	Forward: 5'-CGGGAGTCCGCAGTCTTA Reverse: 5'-TGAATCTTGCTCAGCTTGTC
GAPDH	Forward: 5'-AAGGACTCATGACCACAGTCCAT Reverse: 5'-CCATCACGCCACAGTTTCC

Q. Co-immunoprecipitation

(Courtesy of Dr. Fang Wang)

Co-immunoprecipitation (co-IP) was used to investigate the dimerization between HA- and FLAG-tagged STAT3 following indicated treatment. 500 μg of fresh cell lysate for each treatment were mixed with 1:100 diluted normal mouse IgG in 500 μL of ice-cold lysis buffer used for cell lysate preparation and incubated for 1 hour at 4°C. The suspensions were pre-cleared with 150 μL of protein G-PLUS agarose beads for 1 hour at 4°C. After brief centrifugation at 500 g for 2 minutes, the supernatants were transferred into new microcentrifuge tubes and precipitated with 1:500 diluted monoclonal mouse anti-HA antibody for 3 hours, followed with incubation with 50 μL of protein G-PLUS agarose beads overnight at 4°C. Next day, the supernatants were discarded after centrifugation. The beads were washed five times with 1 mL of lysis buffer, followed by SDS-PAGE and Western blot analysis.

R. Cellular fractionation

To determine the STAT3 level in difference cellular fractions following treatment, cytosol, soluble nuclear and chromatin-bound proteins were isolated followed by SDS-PAGE and Western blot analysis. In brief, after A549 or MDA-MB-231 cell were exposed to 0.1% DMSO vehicle or inS3-54/A18 for 72 hours, cells were harvested, suspended in cytosol extraction buffer (10 mM HEPES·KOH, pH 7.9, 10 mM KCl, 1.5 mM $MgCl_2$, 0.34 M sucrose, 10% glycerol, 1% Triton X-100, 1 mM DTT, 10 μM leupeptin, 1:1000 diluted protease inhibitor cocktail) and

subjected to centrifugation at 4,200 g for 5 minutes to pellet nuclei. The supernatants were used as cytosolic fraction after cleaned by a further centrifugation step. The pellets were resuspended in soluble nuclear protein extraction buffer (3 mM EDTA, 0.2 mM EGTA, 1 mM DTT, 10 μM leupeptin, 1:1000 diluted protease inhibitor cocktail) and incubated on ice for 30 minutes, followed centrifugation at 5,000 g for 5 minutes. The successive supernatants were used as soluble nuclear protein fraction. The insoluble pellets were further resuspended in chromatin-bound protein extraction buffer (50 mM Tris·HCl, pH 7.4, 150 mM NaCl, 0.5% NP-40, 5 mM EDTA, 50 mM NaF, 1 mM Na_3VO_4, 1% SDS, 1 mM DTT, 10 μM leupeptin, 1:1000 diluted protease inhibitor cocktail) and sonicated to release proteins from chromatin. Difference cellular fractions were finally subjected to SDS-PAGE and Western blot analysis.

S. Chromatin immunoprecipitation

Chromatin immunoprecipitation (ChIP) was used to determine the changes in binding of STAT3 to the promoter of responsive genes in the absence or presence of indicated compounds. After treatment, H1299 cells were treated with formaldehyde at a final concentration of 1% for 10 minutes to crosslink protein and DNA, followed by harvest and incubation in SDS lysis buffer (50 mM Tris, pH 8.1, 1% SDS, 10 mM EDTA, 1 mM PMSF, 1:1000 diluted protease inhibitor cocktail) on ice for 10 minutes. Cell lysates were sonicated to shear DNA to lengths between 200 and 1000 basepairs and centrifuged at 13,000 rpm for 10 minutes at 4°C. Solubilized chromatin was diluted with ChIP dilution buffer (16.7 mM Tris·HCl, pH

8.1, 167 mM NaCl, 0.01% SDS, 1.1% Triton X-100, 1.2 mM EDTA, mM PMSF, 1:1000 diluted protease inhibitor cocktail), precleared with protein A agarose/salmon sperm DNA for 30 minutes at 4°C with agitation to reduce nonspecific background and incubated with specific STAT3 antibody overnight at 4°C with rotation. The antibody/protein complex was then collected by incubating with protein A agarose/salmon sperm DNA for one hour at 4°C and washed for 5 minutes with low salt immune complex washing buffer (20 mM Tris·HCl, pH 8.1, 150 mM NaCl, 0.1% SDS, 1% Triton X-100, 2 mM EDTA), high salt immune complex washing buffer (20 mM Tris·HCl, pH 8.1, 500 mM NaCl, 0.1% SDS, 1% Triton X-100, 2 mM EDTA), LiCl immune complex washing buffer (10 mM Tris·HCl, pH 8.1, 250 mM LiCl, 1% NP-40, 1% deoxycholic acid (sodium salt), 1 mM EDTA) and TE buffer (10 mM Tris·HCl, pH 8.0, 1 mM EDTA). DNA/protein complex was released from antibody with elution buffer (1% SDS, 0.1 M $NaHCO_3$) and the crosslink was reversed using 5M NaCl by heating overnight at 65°C. Proteins were digested with proteinase K for one hour at 45°C. DNA was recovered by phenol/chloroform extraction and cold ethanol precipitation and subjected to PCR with primers specific for cyclin D1 or twist promoter, followed by separation on 2.5% agarose gel. The sequences of the PCR primers are shown as follows: cyclin D1 sense primer, 5'-AACTTGCACAGGGGTTGTGT-3'; cyclin D1 antisense primer 5'-GAGACCACGAGAAGGGGTGACTG-3'; twist sense primer, 5'-AGTCTCCTCCGACCGCTTCCTG-3'; twist antisense primer 5'-CTCCGTGCAGGCGGAAAGTTTGG-3'. No-antibody and IgG immunoprecipitation was performed as the negative controls accordingly. A portion

of the cell lysate was kept to quantitate the amount of DNA present in samples as the input control.

T. Determination of *in vivo* study conditions

(Pharmacokinetic analyses were performed by Dr. David R. Jones.)

To determine the optimal conditions used for animal studies, the solubility of inS3-54 and its analogues was firstly tested in the commonly-used and commercially available formulation. To determine how long the compounds remain in solution, indicated compounds were dissolved in various formulations and the solubility was observed immediately and 24 hours after allowing to stand at room temperature (see **Table 6** for summary of formulations and results).

A pilot toxicity test was performed to determine the tolerance of various compounds in mice. Male and female BALB/c or nonobese diabetic/severe combined immunodeficiency (NOD/SCID) mice were administrated with increasing dosages of indicated compounds by intraperitoneal injection (i.p.) or oral dosing (p.o.) with 3 mice per group. Behavior, activity, body weight and death of animals were observed and recorded after treatment. To further investigate the pharmacokinetic (PK) characteristics of compounds and determine the optimal dosing regimens in animal studies, blood sample were also collected in 0, 2, 4, 8, 16 and 24 hours after drug administration and analyzed for determination of PK parameters.

U. Mouse xenograft model of lung cancer

(Courtesy of Dr. Karen E. Pollok and *In Vivo* Therapeutics Core)

In vivo efficacy of A18 was investigated in a mouse xenograft model of lung cancer. 5×10^6 A549 cells were injected subcutaneously in the flanks of 12 NOD/SCID mice. When the tumor volume reached about 50.0 mm^3, the mice were randomized to one vehicle control group and one A18 group (200 mg/Kg/2 days) with 6 mice per group. Drug administration was delivered by oral dosing once every other day for 4 weeks. Behavior and activity of animals were observed and recorded every two days. Tumor volume and body weight were measured twice per week. On the 35^{th} day after implant, mice were euthanized and the tumor tissues were harvested and weighed. Necropsy was also performed to determine the changes in heart, lungs, kidneys, liver and spleen. Differences between both groups were analyzed with Student's t-test. Statistical significance was considered at $p<0.05$. Due to variation in animals, data outliers were rejected by Dixon's Q test at 95% confidence.

V. Immunohistochemistry staining

(Assisted by Histology Core Facilities and Dr. George E. Sandusky)

Slides containing paraffin-embedded tissue sections were prepared by Histology Core Facilities, followed by hematoxylin and eosin (H&E) staining. Slides were then read by an experienced pathologist.

Unstained slides were used to determine the levels of STAT3 and its downstream targets in tumor tissues following drug administration. In brief, slides were deparaffinized and rehydrated by incubation in xylene overnight followed by

incubation in xylene for 30 minutes, in 100% ethanol for 2 minutes two times, in 95% ethanol for 2 minutes two times and in 75% ethanol for 2 minutes one time. Slides were washed in PBST (1×PBS, 0.1% (v/v) Tween-20) for 5 minutes. Endogenous peroxidase activity was blocked by 0.3% hydrogen peroxide, followed by washing five times in PBST for 5 minutes each. For antigen retrieval, slides were boiled in target retrieval buffer (10 mM citrate acid, 0.05% (v/v) Tween-20, pH 6.0) at 95-100°C for 30 minutes and allowed to cool at room temperature for 5 minutes, followed by washing with PBST for 5 minutes. Nonspecific binding of immunoglobulin was minimized by preincubation in 10% FBS in PBST for 30 minutes at room temperature. Slides were incubated with primary antibodies against STAT3, survivin and VEGF at 4°C overnight according to the manufacturer's instructions. Antigen-antibody complexes were detected using biotinylated anti-rabbit or anti-goat secondary antibodies followed by streptavidin-horseradish-peroxidase substrate. Slides were counterstained with hematoxylin for 2 minutes followed by dehydration in 0.25% ammonium hydroxide for 5 minutes, 75% ethanol for 2 minutes one time, 95% ethanol for 2 minutes two times, 100% ethanol for 2 minutes two times and xylene for 10 minutes two times. Coverslips were finally mounted using Cytoseal^{TM} 60 and slides were captured under microscopy.

III. Experimental Results

Part I. Development of inS3-54

A. Identification of a STAT3 inhibitor targeting the DBD of STAT3.

Disrupting STAT3-DNA interaction with small molecule compounds is an emerging therapeutic approach. To identify small molecule compounds that can disrupt STAT3-DNA interaction, the crystal structure of STAT3β homodimer bound to DNA (PDB code: 1BG1) obtained from Protein Data Bank was used for structure-based virtual screening in collaboration with Dr. Jing-Yuan Liu (**Figure 5A**). The DNA-binding groove consisting of residues 329~332, 340~346, 406~412 and 465~468 was chosen as the targeting area for docking. ChemDiv chemical database offered approximately 200,000 virtual compounds for molecular docking over the DBD of STAT3. Top-scoring compounds that contain phosphate groups mimicking phosphates in DNA were eliminated due to their potential poor membrane permeability in cells. As STAT1 and STAT3 share extensive sequence homology but play opposite roles in tumorigenesis, an ideal STAT3 inhibitor should be able to distinguish STAT1 and STAT3 (119). Therefore, the remaining 1,000 top-scoring compounds were also docked onto the DBD of STAT1 (PDB code: 1BF5) to rule out the compounds that may bind to STAT1. Subsequently, 100 potentially specific candidates were selected for *in vitro* screening (**Table 3**).

Of the 100 compounds, 57 available compounds obtained from ChemDiv Inc. were further tested for their effects on the transcriptional activity of STAT3 in a breast cancer cell line MDA-MB-231 stably transfected with a STAT3-dependent luciferase reporter. One of the compounds, #54, showed a remarkable inhibitory

effect in a time- and dose-dependent manner (**Figure 6A-B**; IC_{50}: 13.8 μM). Furthermore, the compound was found to exhibit no effect on the reporter driven by a p27 promoter lacking STAT3-binding site (**Figure 6C**). Thus, the inhibition on STAT3-dependent luciferase reporter is unlikely due to non-specific effects on the expression or activity of the luciferase reporter gene. This compound, 4-[(3E)-3-[(4-nitrophenyl)-methylidene]-2-oxo-5-phenylpyrrol-1-yl] benzoic acid, was named inS3-54 (**Figure 5C**). A further search of PubChem compound database with high throughput screening data on STAT3 inhibitors revealed no identical structure for STAT3 inhibition.

Table 3. 100 top-scoring compounds obtained from virtual screening

No.	Structure	Formula	M.W. (g/mol)
1	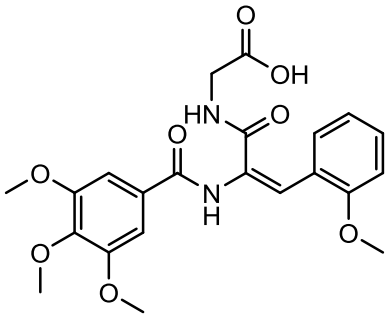	$C_{22}H_{24}N_2O_8$	444.43
2	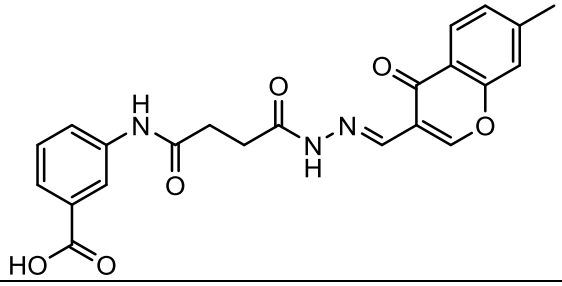	$C_{22}H_{19}N_3O_6$	421.40
3	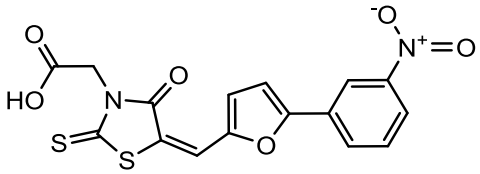	$C_{16}H_{10}N_2O_6S_2$	390.39
4	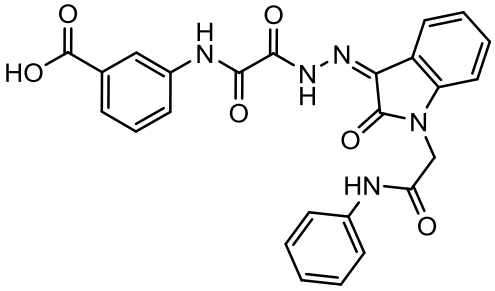	$C_{25}H_{19}N_5O_6$	485.45
5	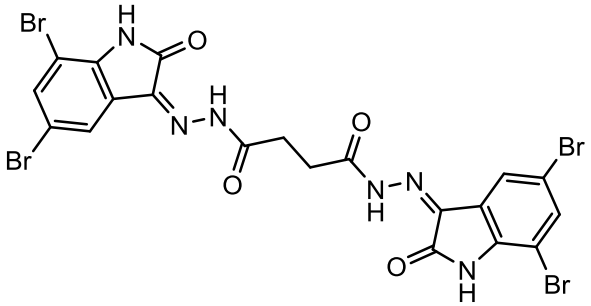	$C_{20}H_{12}Br_4N_6O_4$	719.96

6	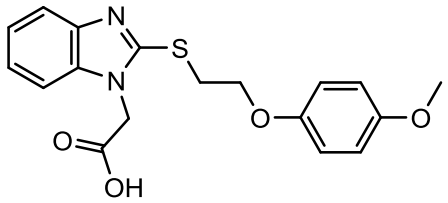	$C_{18}H_{18}N_2O_4S$	358.41
7	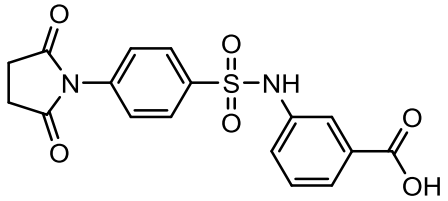	$C_{17}H_{14}N_2O_6S$	374.37
8	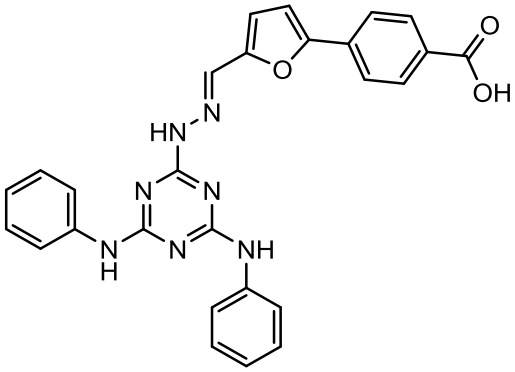	$C_{27}H_{21}N_7O_3$	491.50
9	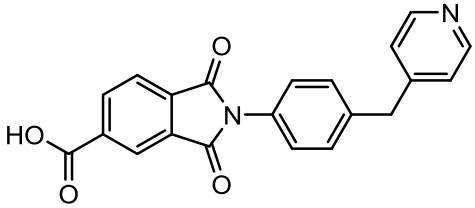	$C_{21}H_{14}N_2O_4$	358.35
10	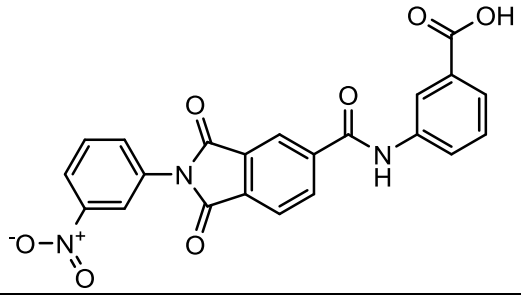	$C_{22}H_{13}N_3O_7$	431.35
11	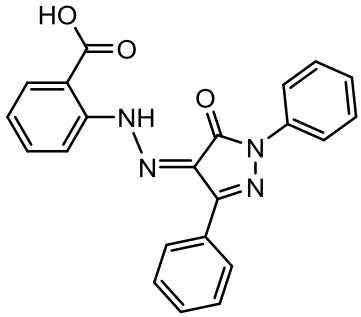	$C_{22}H_{16}N_4O_3$	384.39

12	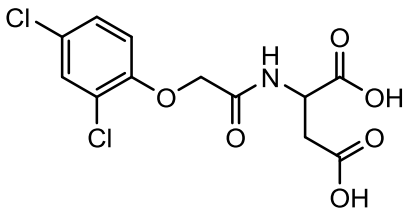	$C_{12}H_{11}Cl_2NO_6$	336.12
13	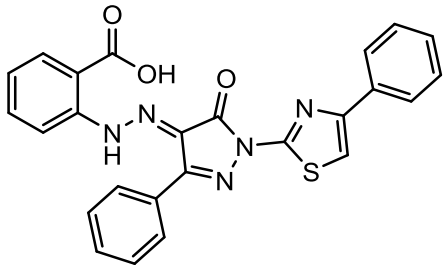	$C_{25}H_{17}N_5O_3S$	467.50
14	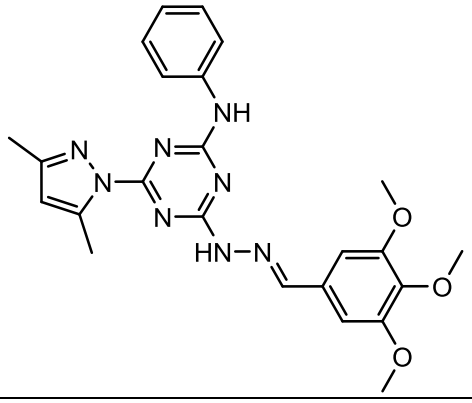	$C_{24}H_{26}N_8O_3$	474.52
15	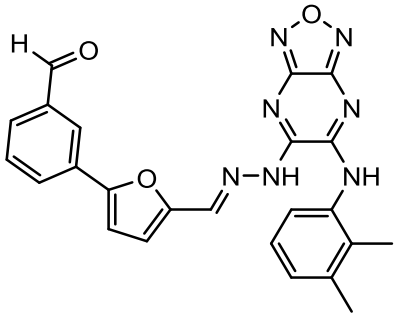	$C_{24}H_{19}N_7O_4$	469.45
16	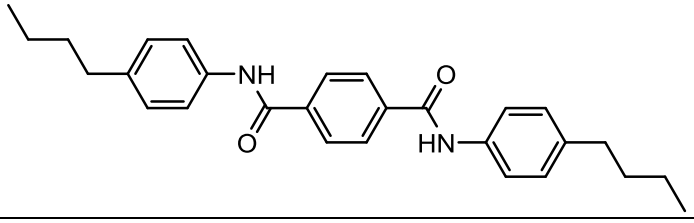	$C_{28}H_{32}N_2O_2$	428.57

17	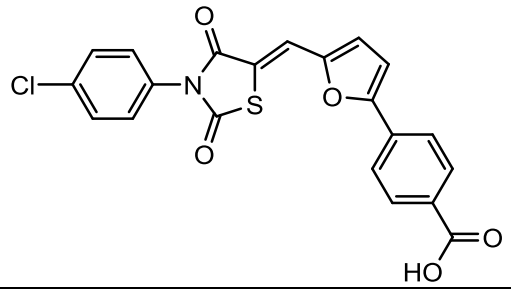	$C_{21}H_{12}ClNO_5S$	425.84
18	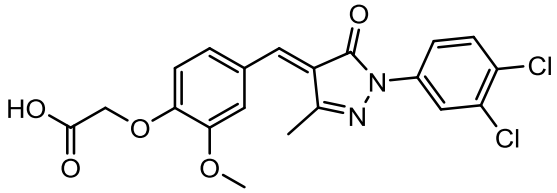	$C_{20}H_{16}Cl_2N_2O_5$	435.26
19	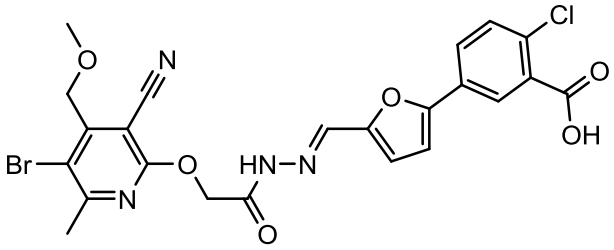	$C_{23}H_{18}BrClN_4O_6$	561.77
20	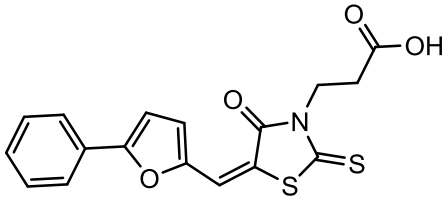	$C_{17}H_{13}NO_4S_2$	359.42
21	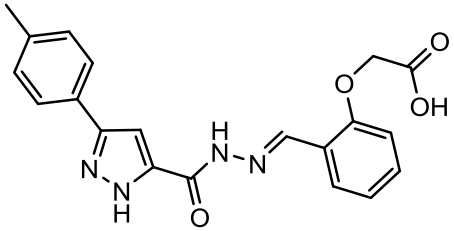	$C_{20}H_{18}N_4O_4$	378.38
22	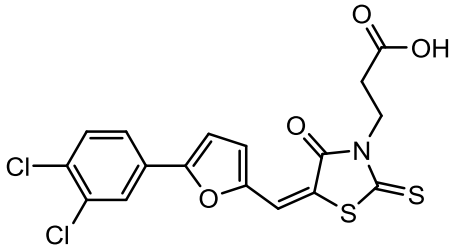	$C_{17}H_{11}Cl_2NO_4S_2$	428.31
23	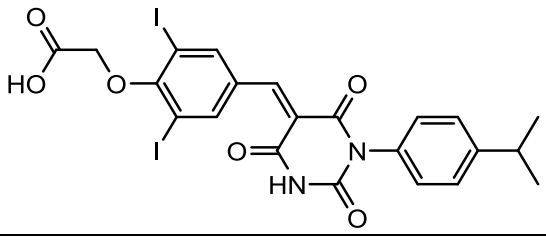	$C_{22}H_{18}I_2N_2O_6$	660.20

24	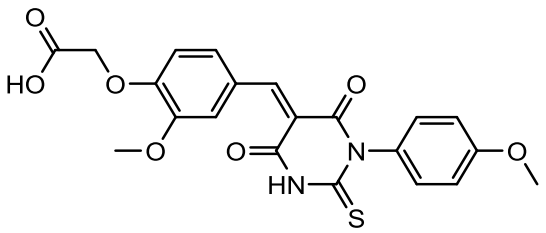	$C_{21}H_{18}N_2O_7S$	442.44
25	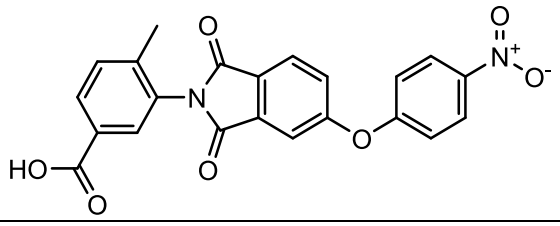	$C_{22}H_{14}N_2O_7$	418.36
26	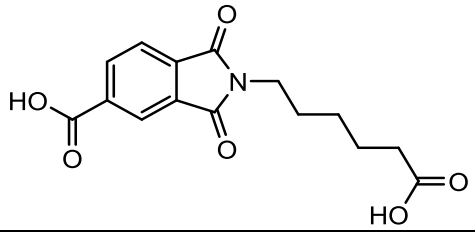	$C_{15}H_{15}NO_6$	305.28
27	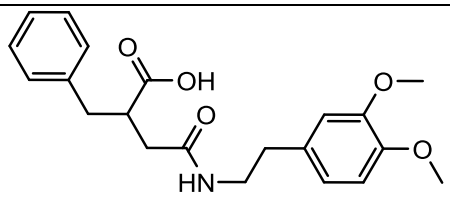	$C_{21}H_{25}NO_5$	371.43
28	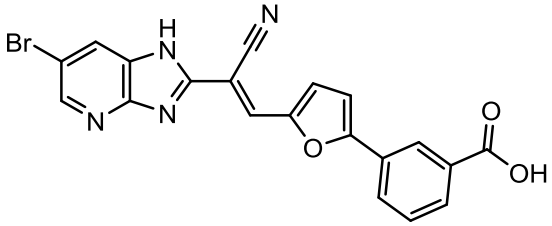	$C_{20}H_{11}BrN_4O_3$	435.23
29	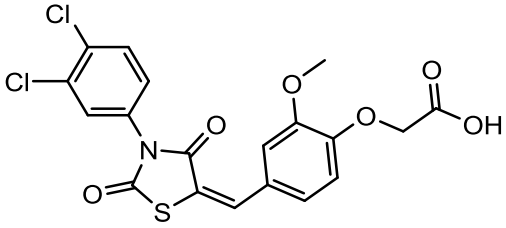	$C_{19}H_{13}Cl_2NO_6S$	454.28
30	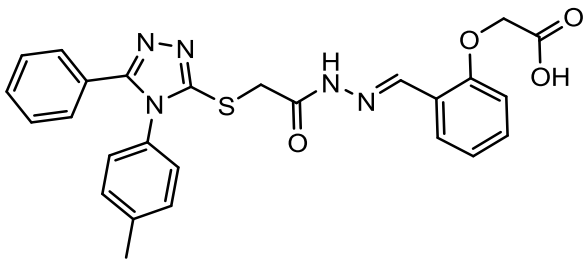	$C_{26}H_{23}N_5O_4S$	501.56

31	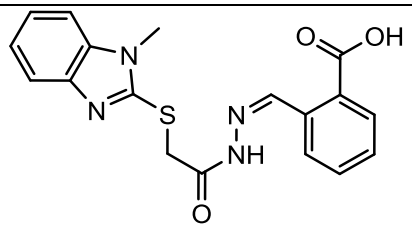	$C_{18}H_{16}N_4O_3S$	368.41
32	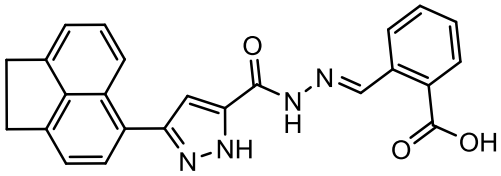	$C_{24}H_{18}N_4O_3$	410.42
33	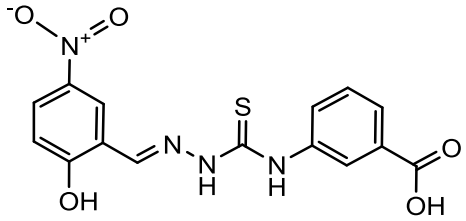	$C_{15}H_{12}N_4O_5S$	360.34
34	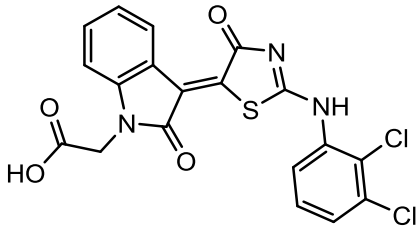	$C_{19}H_{11}Cl_2N_3O_4S$	448.28
35	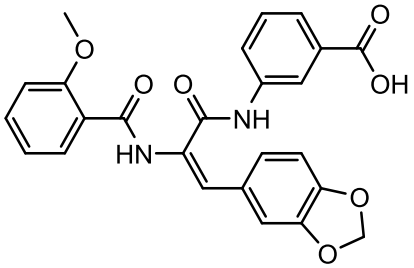	$C_{22}H_{20}N_2O_7$	460.44
36	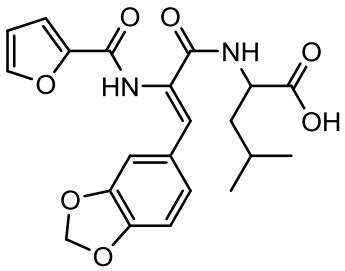	$C_{21}H_{22}N_2O_7$	414.41
37	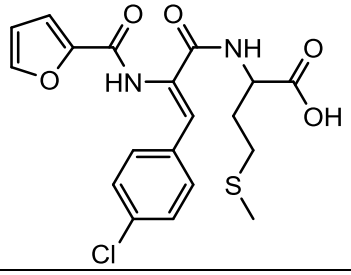	$C_{19}H_{19}ClN_2O_5S$	422.88

38	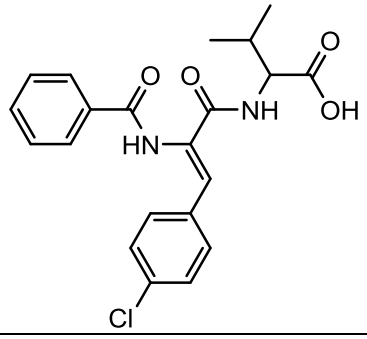	$C_{21}H_{21}ClN_2O_4$	400.86
39	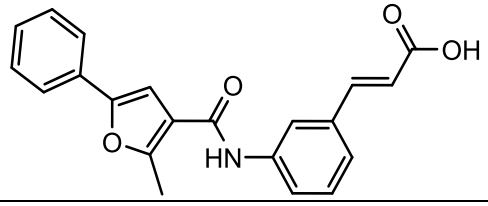	$C_{21}H_{17}NO_4$	347.36
40	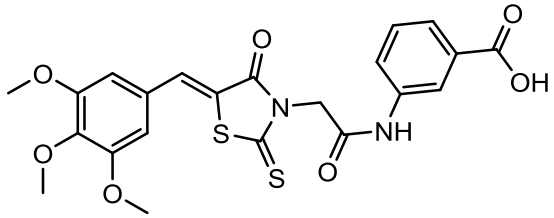	$C_{22}H_{20}N_2O_7S_2$	488.53
41	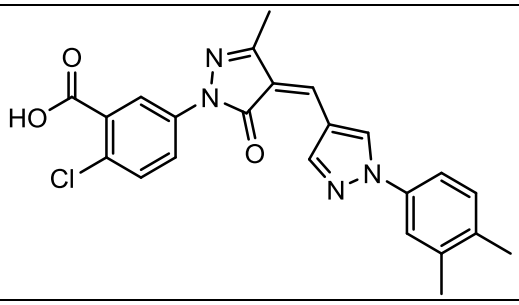	$C_{23}H_{19}ClN_4O_3$	424.87
42	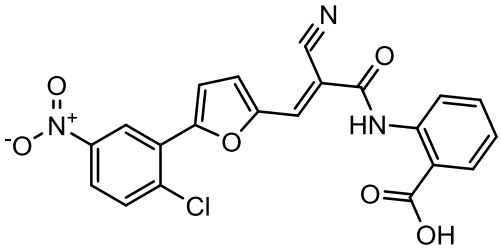	$C_{21}H_{12}ClN_3O_6$	437.79
43	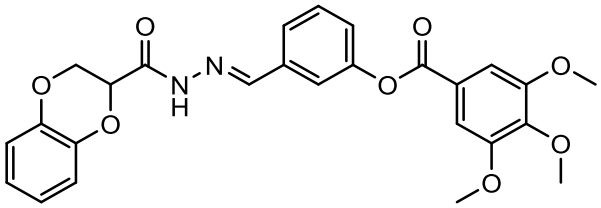	$C_{26}H_{24}N_2O_8$	492.48

44	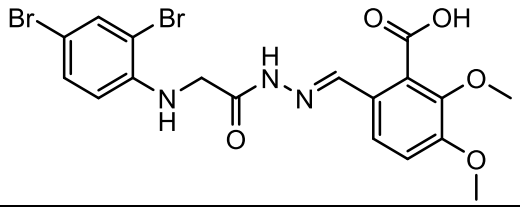	$C_{18}H_{17}Br_2N_3O_5$	515.15
45	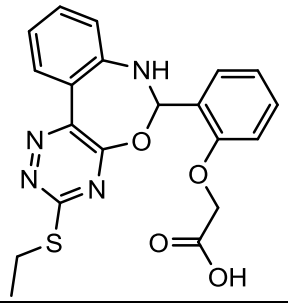	$C_{20}H_{18}N_4O_4S$	410.45
46	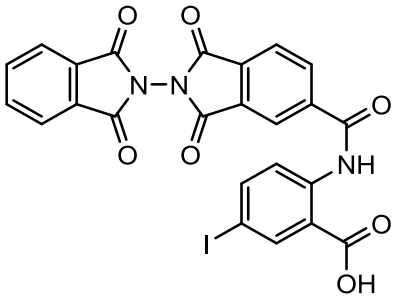	$C_{24}H_{12}IN_3O_7$	581.27
47	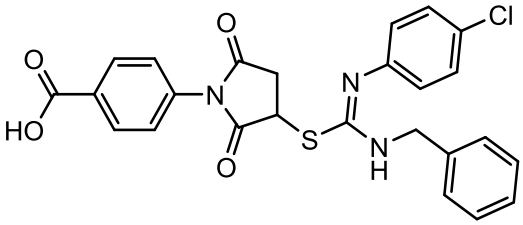	$C_{25}H_{20}ClN_3O_4S$	493.96
48	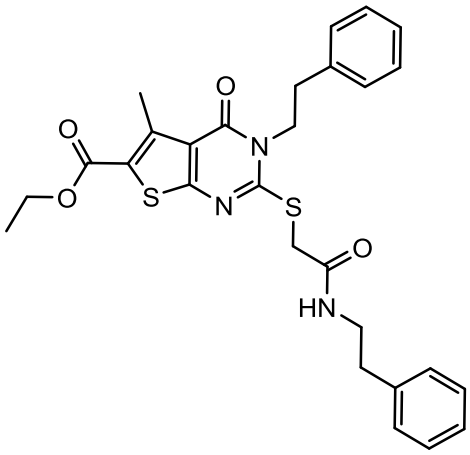	$C_{28}H_{29}N_3O_4S_2$	545.68
49	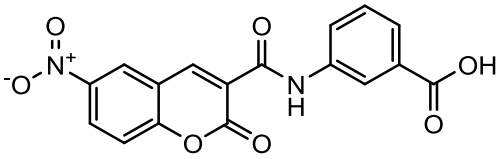	$C_{17}H_{10}N_2O_7$	354.27

50	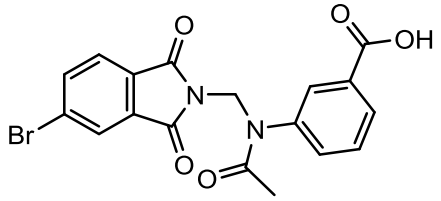	$C_{18}H_{13}BrN_2O_5$	417.21
51	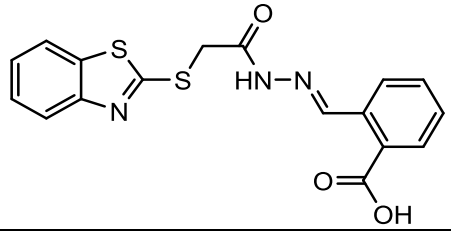	$C_{17}H_{13}N_3O_3S_2$	317.43
52	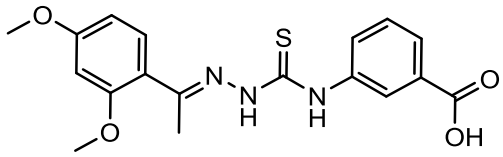	$C_{18}H_{19}N_3O_4S$	373.43
53	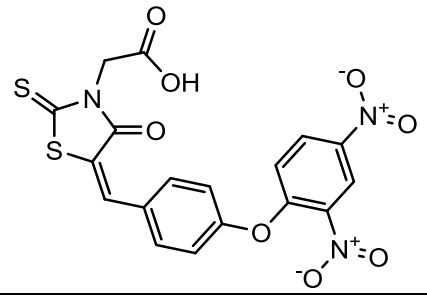	$C_{18}H_{11}N_3O_8S_2$	461.43
54	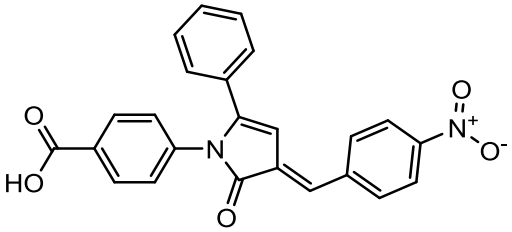	$C_{24}H_{16}N_2O_5$	412.39
55	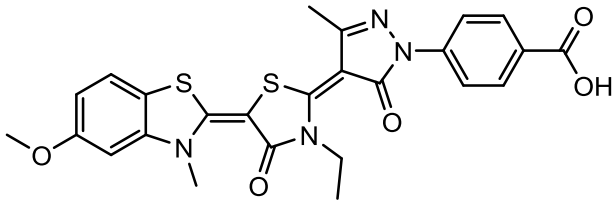	$C_{25}H_{22}N_4O_5S_2$	522.60
56	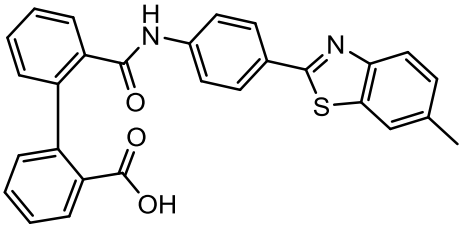	$C_{28}H_{20}N_2O_3S$	464.54

57	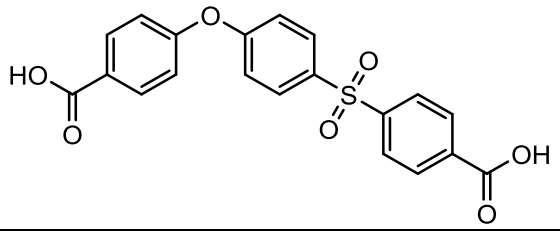	$C_{20}H_{14}O_7S$	398.39
58	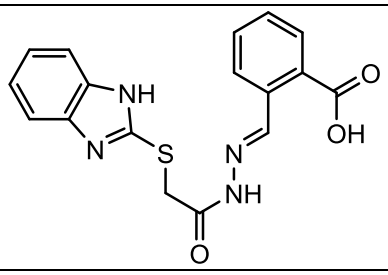	$C_{17}H_{14}N_4O_3S$	354.38
59	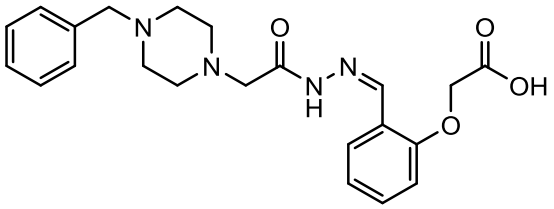	$C_{22}H_{26}N_4O_4$	410.47
60	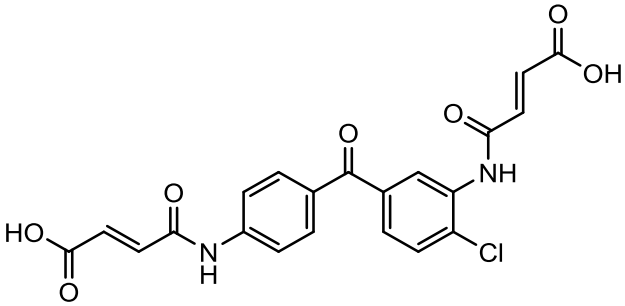	$C_{21}H_{15}ClN_2O_7$	442.81
61	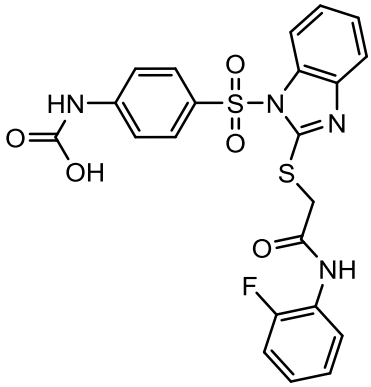	$C_{22}H_{17}FN_4O_5S_2$	500.52
62	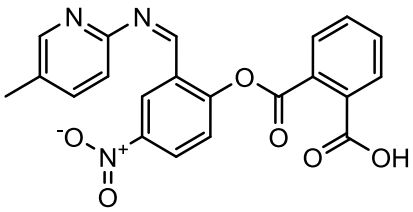	$C_{21}H_{15}N_3O_6$	405.36

63	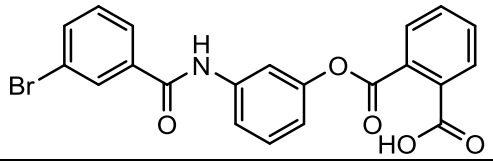	$C_{21}H_{14}BrNO_5$	440.24
64	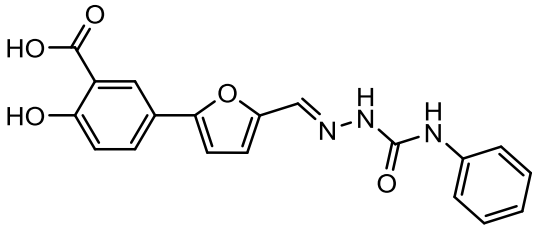	$C_{19}H_{15}N_3O_5$	365.34
65	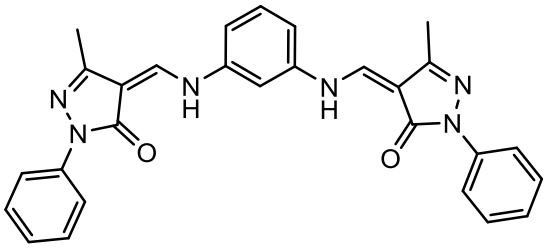	$C_{28}H_{24}N_6O_2$	476.53
66	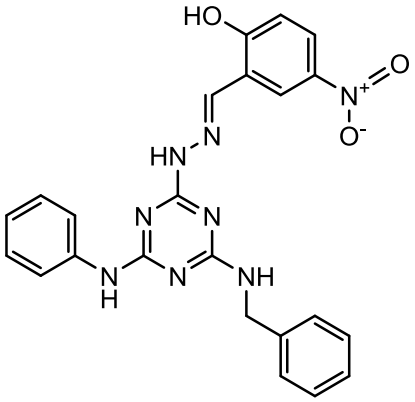	$C_{23}H_{20}N_8O_3$	456.46
67	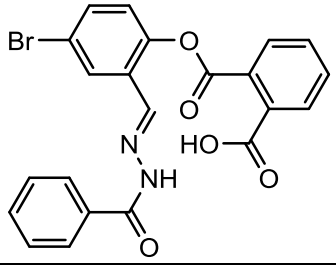	$C_{22}H_{15}BrN_2O_5$	467.27
68	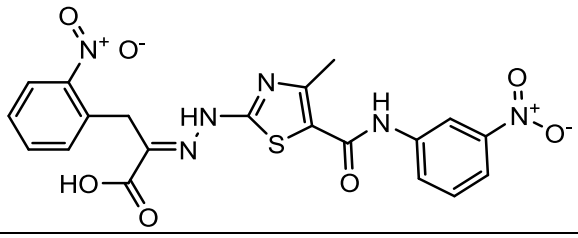	$C_{20}H_{16}N_6O_7S$	484.44

69	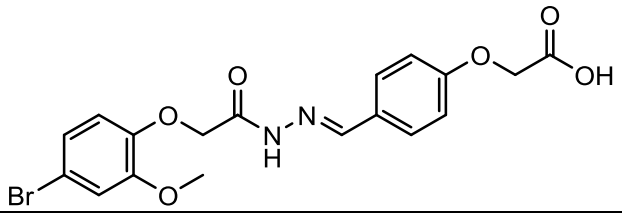	$C_{18}H_{17}BrN_2O_6$	437.24
70	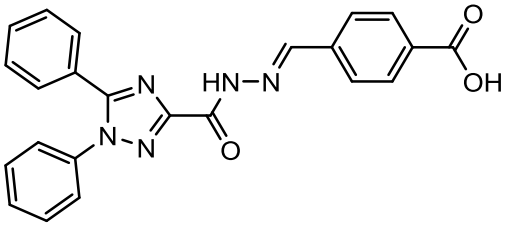	$C_{23}H_{17}N_5O_3$	411.41
71	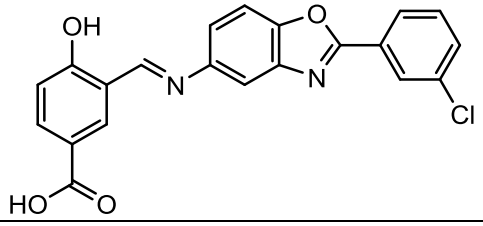	$C_{21}H_{13}ClN_2O_4$	392.79
72	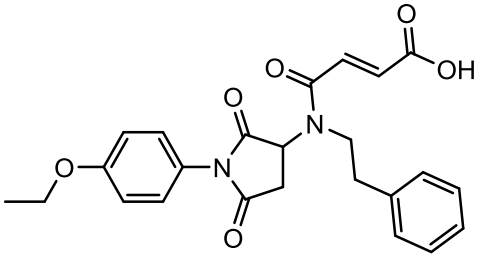	$C_{24}H_{24}N_2O_6$	436.46
73	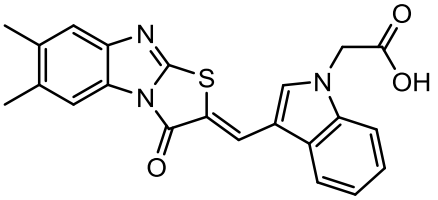	$C_{22}H_{17}N_3O_3S$	403.45
74	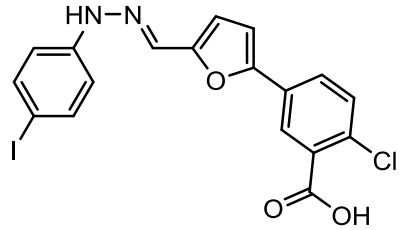	$C_{18}H_{12}ClIN_2O_3$	466.66
75	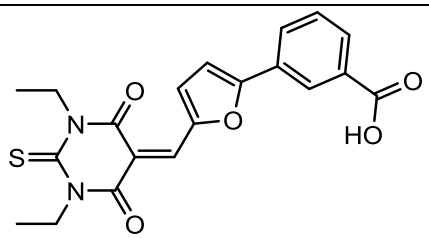	$C_{20}H_{18}N_2O_5S$	398.43

76	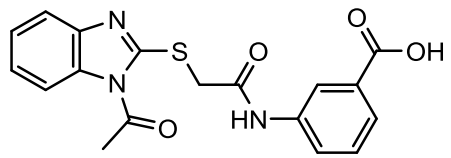	$C_{18}H_{15}N_3O_4S$	369.39
77	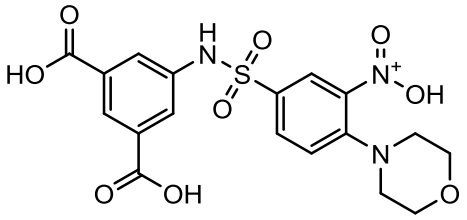	$C_{18}H_{17}N_3O_9S$	451.41
78	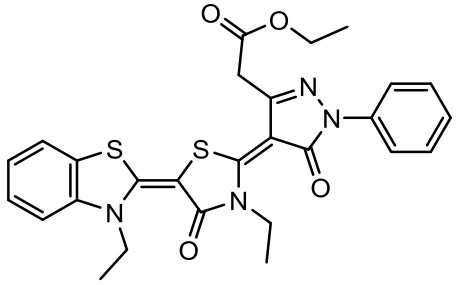	$C_{27}H_{26}N_4O_4S_2$	534.65
79	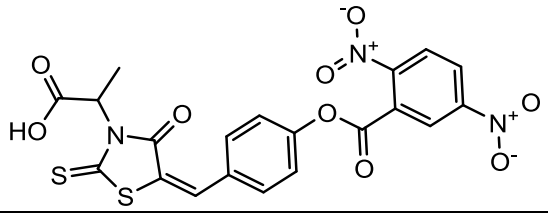	$C_{19}H_{11}N_3O_9S_2$	489.44
80	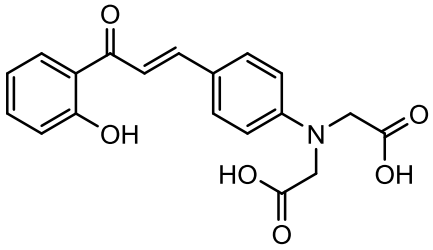	$C_{19}H_{17}NO_6$	355.34
81	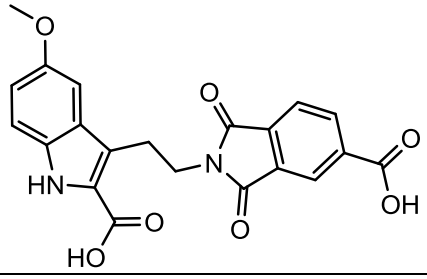	$C_{21}H_{16}N_2O_7$	408.36

82	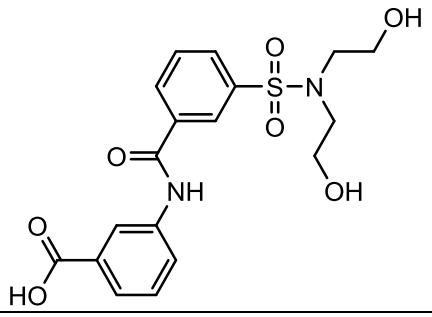	$C_{18}H_{20}N_2O_7S$	408.43
83	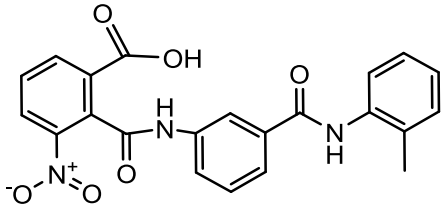	$C_{22}H_{17}N_3O_6$	419.39
84	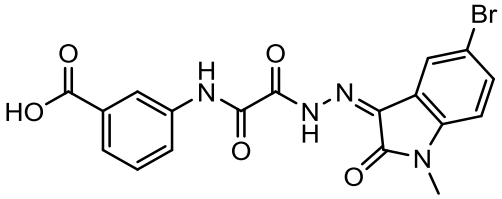	$C_{18}H_{13}BrN_4O_5$	445.22
85	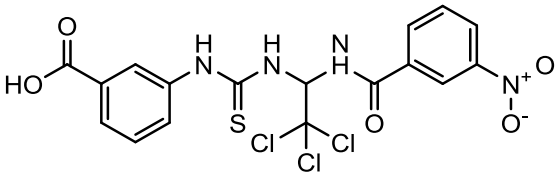	$C_{17}H_{13}Cl_3N_4O_5S$	491.73
86	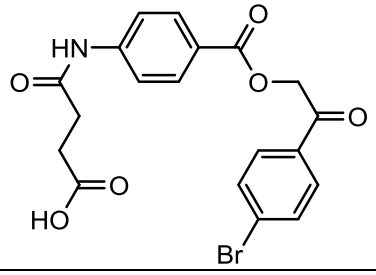	$C_{19}H_{16}BrNO_6$	434.24
87	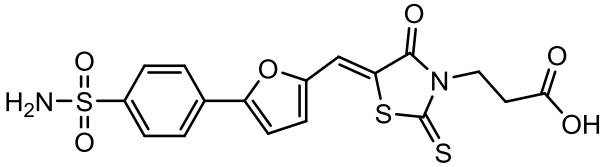	$C_{17}H_{14}N_2O_6S_3$	438.50
88	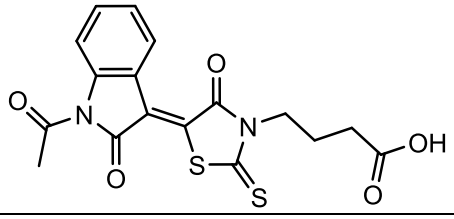	$C_{17}H_{14}N_2O_5S_2$	390.43

89	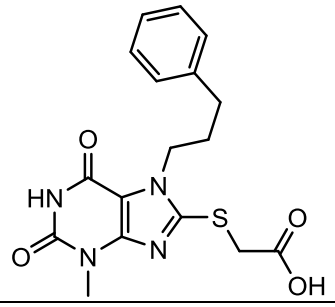	$C_{17}H_{18}N_4O_4S$	374.41
90	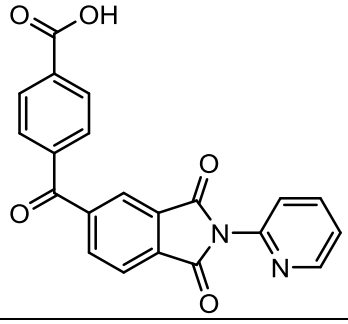	$C_{21}H_{12}N_2O_5$	372.33
91	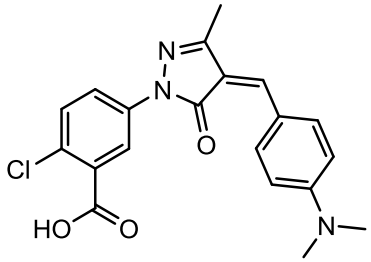	$C_{20}H_{18}ClN_3O_3$	383.83
92	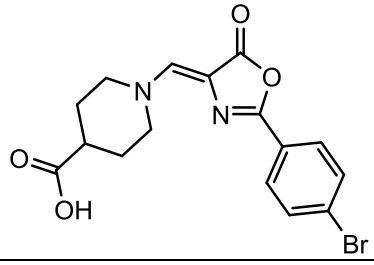	$C_{16}H_{15}BrN_2O_4$	379.21
93	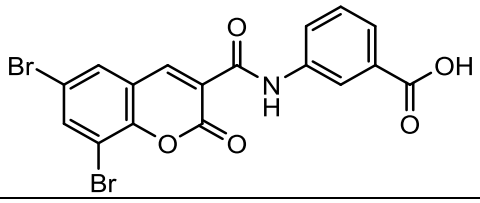	$C_{17}H_9Br_2NO_5$	467.07
94	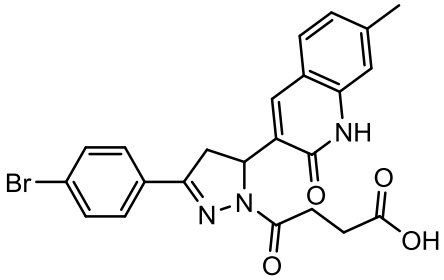	$C_{23}H_{20}BrN_3O_4$	482.33

95	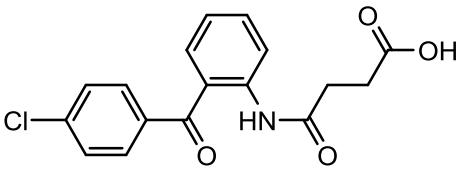	$C_{17}H_{14}ClNO_4$	331.75
96	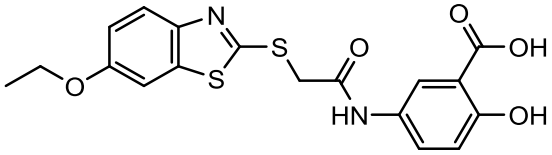	$C_{18}H_{16}N_2O_5S_2$	404.46
97	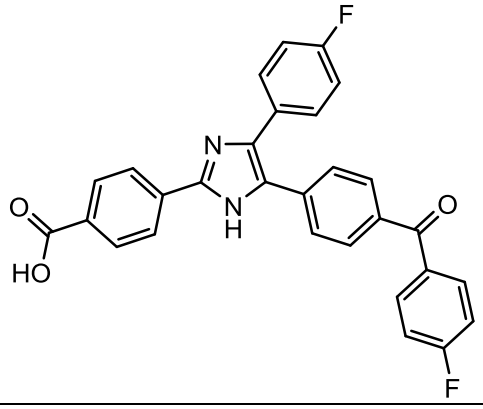	$C_{29}H_{18}F_2N_2O_3$	480.46
98	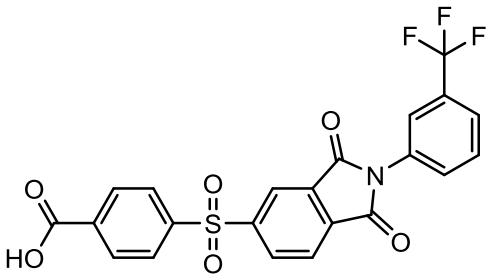	$C_{22}H_{12}F_3NO_6S$	475.39
99	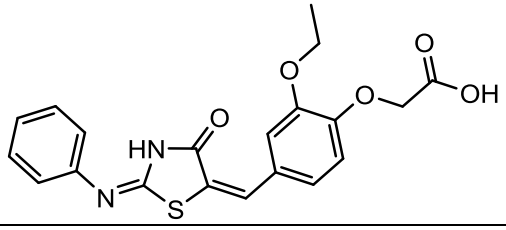	$C_{20}H_{18}N_2O_5S$	398.43
100	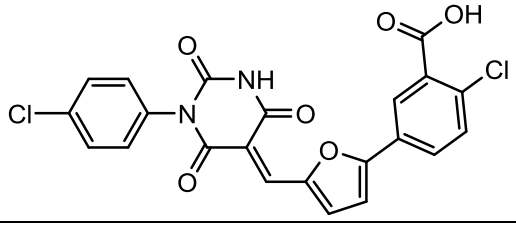	$C_{22}H_{12}Cl_2N_2O_6$	471.25

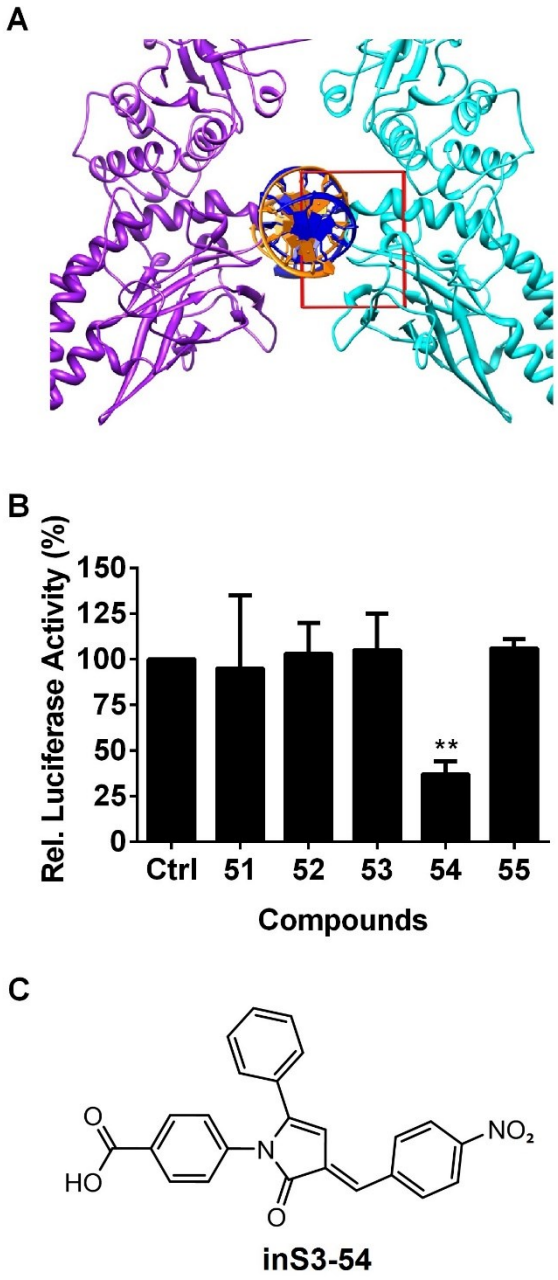

Figure 5. Schematic diagram and identification of inS3-54 by structure-based virtual screening.

(A) The crystal structure of dimeric STAT3β bound to DNA fragment (PDB code: 1BG1) was used to identify small molecule compounds that can disrupt STAT3-DNA interaction by structure-based virtual screening. The red box indicates the targeting site of one of the STAT3 subunits for molecular docking. (B) Breast

cancer cells MDA-MB-231 stably transfected with STAT3-dependent luciferase reporter were exposed to 20 μM of compounds for 48 hours followed by measurement of luciferase activity. The compound, #54, showed a remarkable inhibitory effect on STAT3-dependent luciferase reporter. (C) Chemical structure of the compound, #54 (named inS3-54). (N=3; ** $p<0.01$, by Student's t-test as compared with DMSO vehicle control)

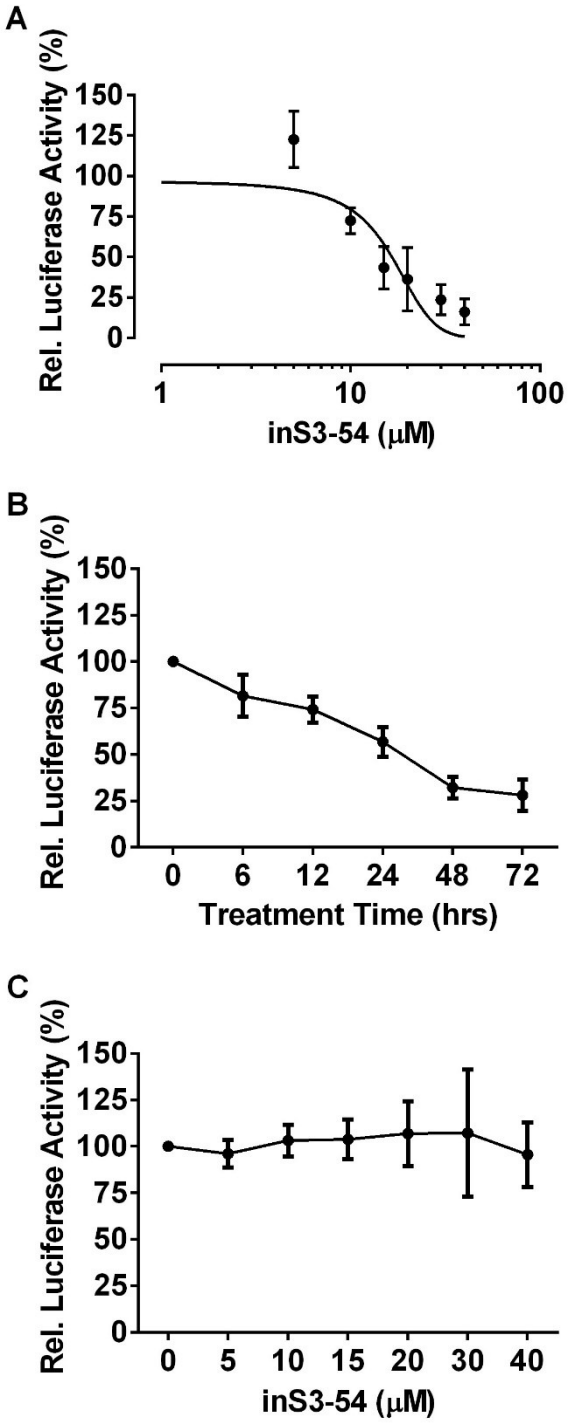

Figure 6. Effects of inS3-54 on STAT3 dependent and independent luciferase reporter activity.

(A-B) MDA-MB-231-STAT3 cells harboring a STAT3-dependent luciferase reporter construct were treated with increasing concentrations of inS3-54 for 72

hours (A) or with 20 μM inS3-54 for indicated time intervals (B), followed by luciferase reporter assay. InS3-54 suppressed STAT3-dependent luciferase reporter in a dose- and time-dependent manner. (C) H1299 cells were transiently transfected with a luciferase reporter construct driven by a p27 promoter lacking STAT3-binding sequence. 24 hours after transfection, cells were exposed to increasing concentrations of inS3-54 for 48 hours, followed by measurement of luciferase reporter activity. InS3-54 had little effect on STAT3-independent luciferase reporter.

B. InS3-54 selectively inhibits the DNA-binding activity of STAT3 but not that of STAT1.

To determine the selectivity of inS3-54 on STAT subtypes, molecular dynamics simulation and generalized GBSA analysis were performed to determine the binding free energy of inS3-54 docked in the DBD of these proteins in collaboration with Dr. Jing-Yuan Liu as described previously (120). **Table 4** shows that both STAT molecules have favorable electrostatic (ΔE_{ele}) and van der Waals (ΔE_{vdw}) interaction energy although the energy is more favorable to STAT3 than to STAT1. The energy contribution from solvation (ΔG_{solv}) reverses these favorable energy for both STAT molecules. However, the reversal effect from solvation is less for STAT3 than for STAT1. Consequently, the total binding free energy (ΔG_{bind}) is much more favorable for STAT3 (-28.4 kcal/mol) than for STAT1 (-17.1 kcal/mol). Considering the omitted entropy term, which is always unfavorable, inS3-54 may not bind to STAT1 at all or have a very low affinity. Examination of the average simulated structure of inS3-54-bound STAT1 or STAT3 agrees with the calculated ΔG_{bind}. As shown in **Figure 7A**, the residues Met331, Val343, Met420, Ile467 and Met470 make a great contribution to the binding of STAT3 to inS3-54 via hydrophobic interaction. The amino groups of Lys340 and Asn466 stabilize the carboxyl group of inS3-54 by favorable electrostatic interaction. However, the orientation of inS3-54 docked in STAT1 is distinct from that in STAT3 (**Figure 7B-C**). The binding mode in STAT1 likely results in an unfavorable total binding free energy. InS3-54 will clash with the residues Pro326 and Thr327 of STAT1 if forcing

the compound to adopt the same orientation in STAT1 as in STAT3. Based on these analyses, inS3-54 may not bind to STAT1 efficiently.

EMSA was then used to verify the above findings and to determine the inhibitory effect of inS3-54 on the DNA-binding activity of STAT3 and STAT1 using [^{32}P]-labeled double strand DNA probe and whole cell lysate extracted from H1299 cells transiently transfected with constitutively dimerizable FLAG-STAT3 (FLAG-STAT3c) or STAT1. By substituting cysteine residues for specific amino acids within the C-terminal loop in the SH2 domain of the STAT3 molecule, FLAG-STAT3c spontaneously forms homo-dimers via formation of intermolecular disulfide bond, leading to binding to STAT3 responsive element, as described previously (121). As shown in **Figure 8**, the specific binding of STAT3 or STAT1 to DNA probe was verified by super-shift and competition analyses. InS3-54 inhibited the DNA-binding activity of STAT3 in a dose-dependent manner whereas the binding activity of STAT1 was not affected by inS3-54 up to 300 μM.

To sum up, inS3-54 selectively blocks the DNA-binding activity of STAT3, without affecting STAT1.

Table 4. Binding free energy and energy components of inS3-54 in STAT1 and STAT3

	ΔE_{solute} (kcal/mol)		ΔG_{solv} (kcal/mol)		ΔE_{tot_ele} (kcal/mol)	ΔG_{bind} (kcal/mol)
	ΔE_{ele}	ΔE_{vdw}	ΔG_{es}	ΔG_{nes}		
STAT1	- 139.6±3.4	- 23.1±1.0	149.6±2.4	- 4.0±0.1	10.1±0.4	- 17.1±1.0
STAT3	- 144.3±4.4	- 27.5±0.9	148.0±2.8	- 4.6±0.1	3.6±0.8	- 28.4±0.9

Data are presented as mean±SEM.

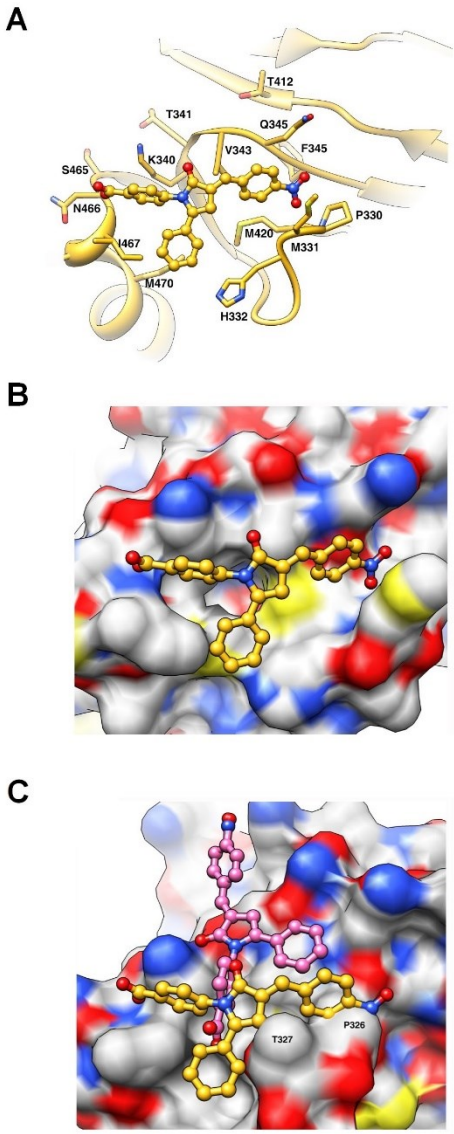

Figure 7. Molecular dynamics simulation of inS3-54 binding to STAT3 or STAT1.

(A) Average complex structure of inS3-54 in the DBD of STAT3 from molecular dynamics simulation. InS3-54 binds to the residues Met331, Val343, Met420, Ile467 and Met470 via hydrophobic interaction and the residues Lys340 and Asn466 via electrostatic interaction. InS3-54 is shown in ball-and-stick representation. (B-C) Molecular surface of STAT3 (B) and STAT1 (C) bound to inS3-54 from molecular dynamics simulation with orientation shown in gold for

STAT3 and pink for STAT1. The molecular surface is colored by atom types with gray for carbon, blue for nitrogen, red for oxygen and yellow for sulfur.

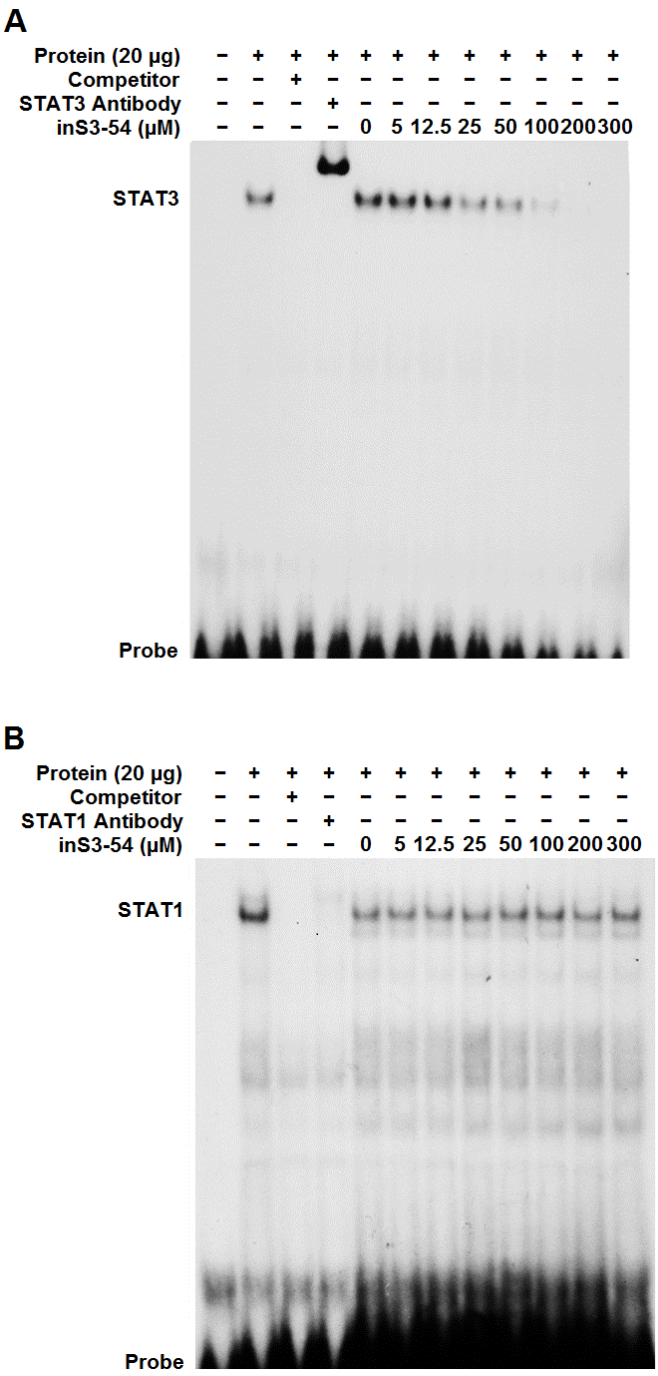

Figure 8. InS3-54 inhibits the DNA-binding activity of STAT3 but not that of STAT1.

The DNA-binding activity of STAT3 (A) and STAT1 (B) was assessed by EMSA following inS3-54 treatment. The whole cell lysates extracted from H1299 cells

transiently transfected with constitutively dimerizable FLAG-STAT3 or STAT1 were pre-incubated with increasing concentrations of inS3-54 for 30 minutes prior to addition of [^{32}P]-labeled double strand DNA probe that contains a STAT3 DNA-binding site for 20 minutes at room temperature. The reaction mixtures were then resolved on 6% non-denaturing polyacrylamide gel and detected by autoradiography. InS3-54 inhibited the binding of STAT3 to radiolabeled probe but not that of STAT1.

C. Binding of inS3-54 to STAT3.

To further verify that inS3-54 can indeed bind to STAT3, inS3-54 containing a carboxyl group was conjugated to EAH-Sepharose 4B, followed by pull down assay with lysate of H1299 cells transfected with FLAG-STAT3c (**Figure 9A**). **Figure 9B-D** shows that inS3-54-conjugated beads successfully pulled down STAT3 whereas the vehicle control beads or the irrelevant compound (C5)-conjugated beads did not. However, multiple bands were detected by gel silver staining, suggesting that other proteins may interact with inS3-54. Furthermore, pretreatment of the cell lysate with excess free inS3-54 abrogated the interaction between STAT3 and inS3-54-conjugated beads (**Figure 9E**). Importantly, the commercially purified STAT3 protein was also pulled down by inS3-54-conjugated beads (**Figure 9F**). Thus, inS3-54 can bind to STAT3 directly although the result of silver staining suggests that potential off-targets of inS3-54 may exist.

Recently, alkylation of cysteine 468 that is located in the DNA-binding domain of STAT3 has been found to define a novel site for therapeutic development (93). However, the alkylating agent reported can also interact with other surface-exposed cysteine residues by alkylating the thiol group of cysteine, indicating low specificity on STAT3. Although the molecular dynamics simulation shows that inS3-54 interacts with STAT3 via hydrophobic and electrostatic interaction, considering the similar property of their chemical structures, we tested whether or not inS3-54 might act as an alkylating agent by using glutathione as a substrate. After A549 and MDA-MB-231 cells were exposed to 20 μM inS3-54 for 48 hours, a luminescence-based glutathione assay showed that inS3-54 did not

affect the level of glutathione in cells (**Figure 10**). In contrast, the positive control IAA, which binds covalently with the thiol group of cysteine, significantly reduced the level of glutathione (**Figure 10**). Thus, inS3-54 likely does not alkylate STAT3 via alkylation of the thiol group of cysteine residues and the interaction between inS3-54 and STAT3 is not due to alkylation of cysteine residues on STAT3 under which condition the compound has inhibitory effect on STAT3 signaling.

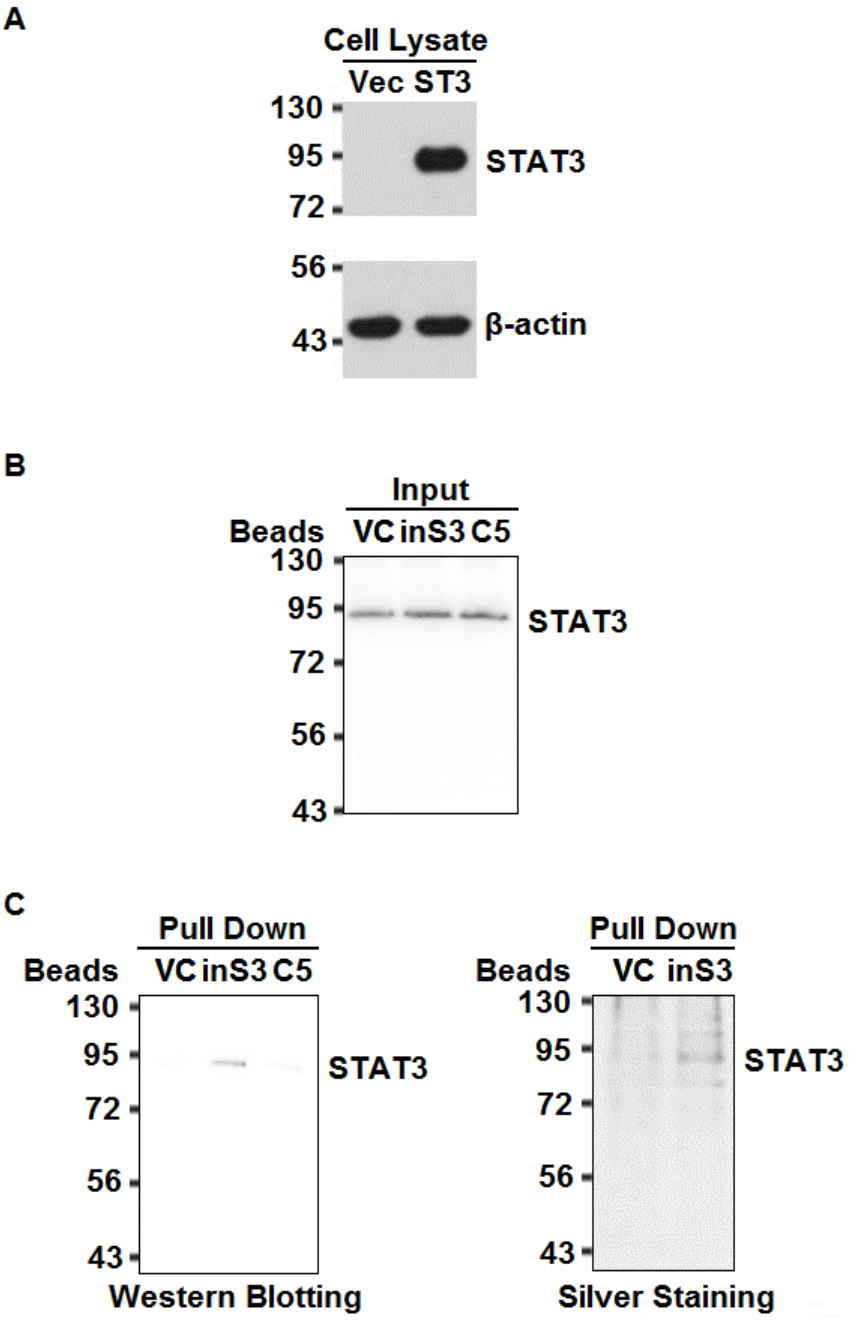

Figure 9. (Continued)

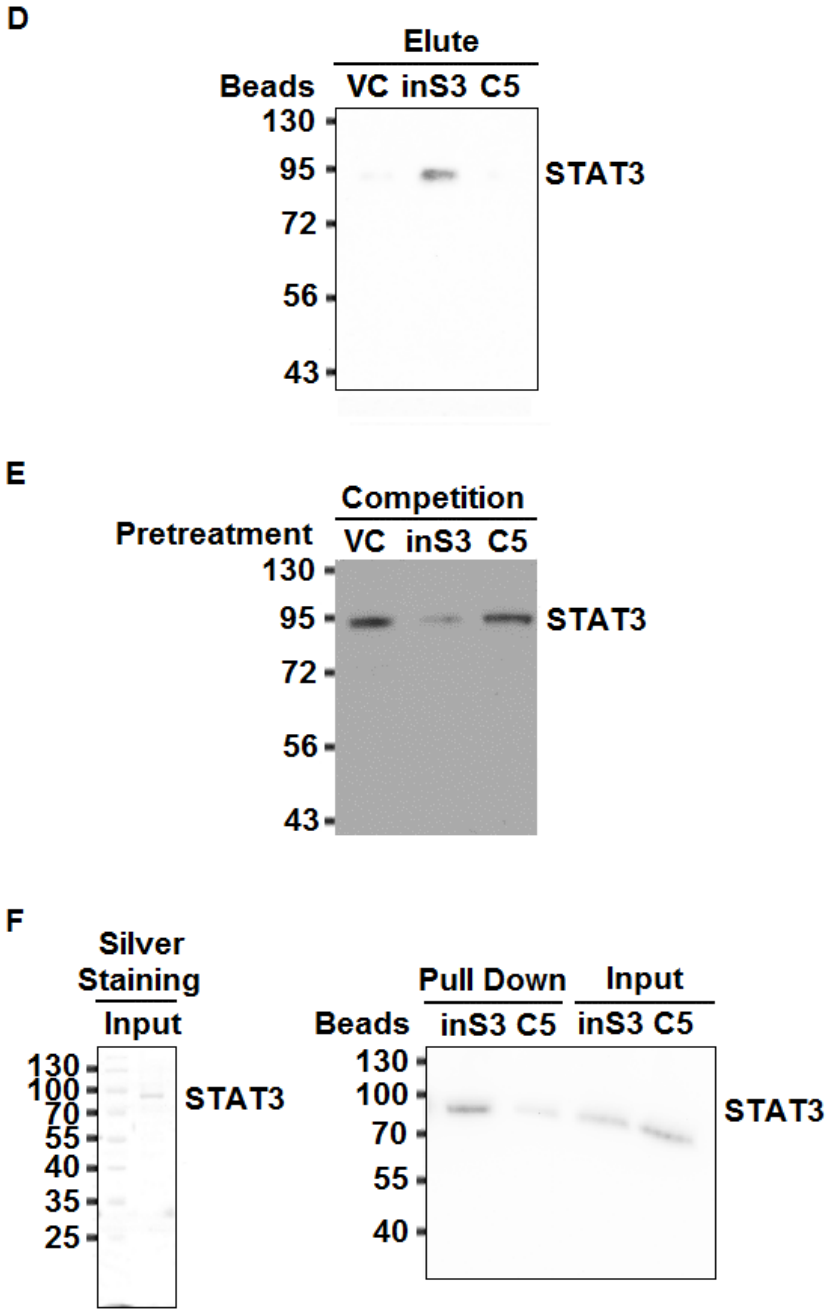

Figure 9. Binding of inS3-54 to STAT3.

(A) H1299 cells were transiently transfected by vector control (Vec) or constitutively dimerizable FLAG-STAT3c (ST3), followed by SDS-PAGE and Western blot analysis. (B-C) Total lysates obtained from FLAG-STAT3c-transfected H1299 cells were incubated with EAH-Sepharose 4B-conjugated with

vehicle control (VC), inS3-54 (inS3) or irrelevant compound (C5). Proteins bound to beads were subjected to SDS-PAGE followed by Western blot analysis probed with specific anti-FLAG antibody or gel silver staining. Unbound flow-through samples were used as the input control. (D) Proteins bound to beads were eluted from beads with excess free inS3-54. (E) Binding of STAT3 to inS3-54-conjugated EAH-Sepharose 4B beads was competed by pretreatment of excess free DMSO vehicle control (VC), inS3-54 (inS3) or irrelevant compound (C5). (F) Purified STAT3 protein with His-tag was subjected to pull down assay following the same procedure. InS3-54 can directly bind to STAT3.

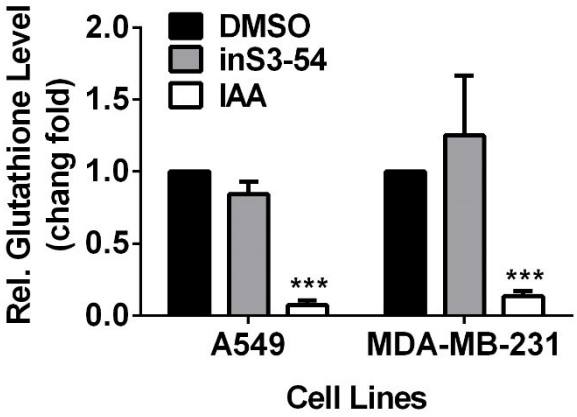

Figure 10. InS3-54 does not alkylate cysteine using glutathione as a substrate.

After A549 and MDA-MB-231 cells were exposed to DMSO (0.1%) or 20 μM inS3-54 for 48 hours or 15 mM IAA for 30 minutes, the level of glutathione was assessed by GSH-Glo^{TM} glutathione assay following the manufacturer's instructions. InS3-54 had no significant effect on the glutathione level in both cell lines under which condition the compound has inhibitory effect on STAT3 signaling. IAA was used as a positive control. (N=3; *** p<0.001, by Student's t-test as compared with DMSO vehicle control)

D. InS3-54 does not inhibit STAT3 dimerization.

The SH2 domain of STAT3 has previously been shown to be susceptible for binding with inhibitors. To rule out the possibility that inS3-54 has off-target effect on the SH2 domain without targeting the DBD of STAT3, STAT3 dimerization was investigated by transiently transfecting FLAG-STAT3c into H1299 cells followed by the treatment with 0.1% DMSO vehicle control, 20 μM inS3-54 or a previously reported STAT3 inhibitor S3I-201 that binds to the SH2 domain (74). **Figure 11A** shows that STAT3c spontaneously formed both dimeric and monomeric forms of STAT3 after transiently transfected to H1299 cells. Treatment with inS3-54 did not affect the production of dimeric STAT3c whereas the positive control, S3I-201, inhibited its dimerization (**Figure 11B**). To further confirm this observation, a co-IP analysis of HA- and FLAG-tagged STAT3 was performed. **Figure 11C** shows that HA- and FLAG-tagged STAT3 can be co-expressed and co-immunoprecipitated successfully in H1299 cells. The dimerization between HA- and FLAG-tagged STAT3 was not affected following inS3-54 treatment while S3I-201 abrogated STAT3 dimerization (**Figure 11D**). Although the decline of STAT3 dimerization is less distinct as that found using STAT3c (**Figure 11B**), it is possibly due to the potential re-association of STAT3 molecules during the process of co-IP lacking S3I-201. The results indicate that inS3-54 does not inhibit STAT3 dimerization and likely does not bind to the SH2 domain of STAT3.

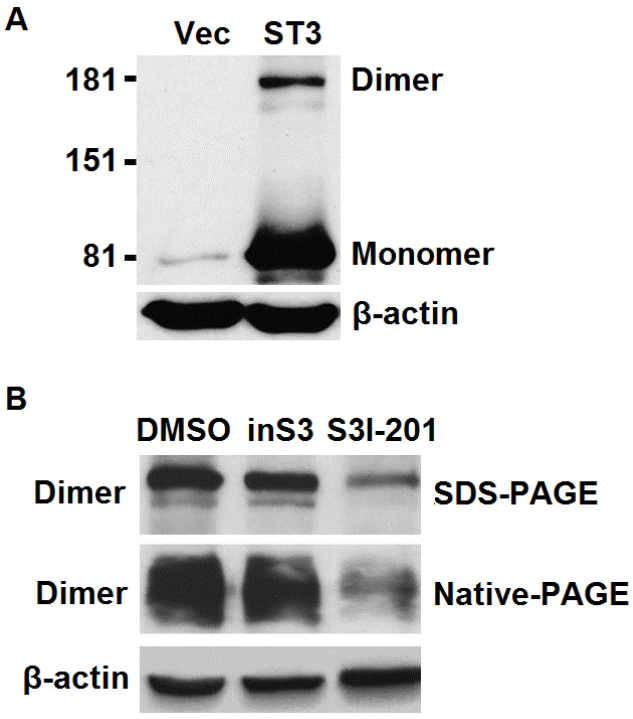

Figure 11. (Continued)

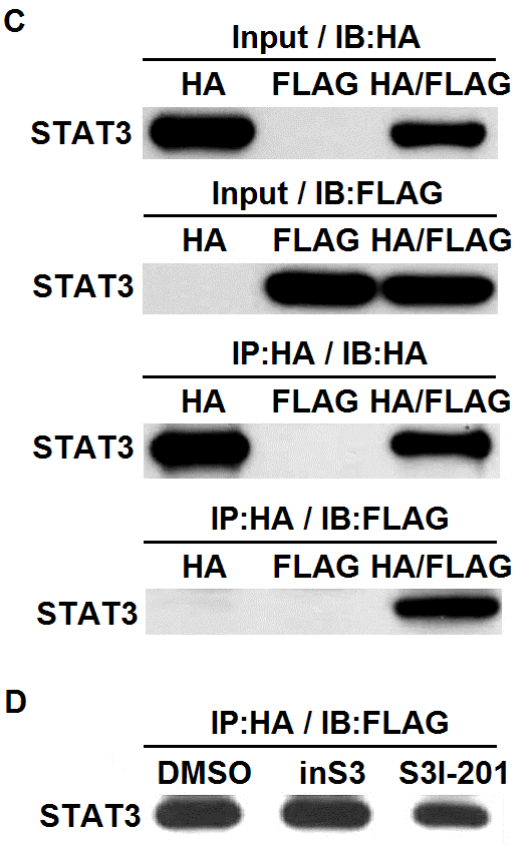

Figure 11. InS3-54 does not affect STAT3 dimerization.

(A) H1299 cells were transiently transfected with vector control (Vec) or constitutively dimerizable FLAG-STAT3c (ST3) followed by Western blot analysis. β-actin was used as a loading control. Dimeric STAT3 was spontaneously formed. (B) FLAG-STAT3c-transfected H1299 cells were treated with DMSO (0.1%), 20 μM inS3-54 or 20 μM S3I-201 followed by Western blot analysis of STAT3 status. InS3-54 did not affect STAT3 dimerization. S3-201 was used as a positive control. (C) Lysates extracted from H1299 cells transfected with HA-tagged, FLAG-tagged STAT3 or both were subjected to co-IP and Western blot analyses. (D) H1299 cells co-expressed with HA- and FLAG-tagged STAT3 were exposed to DMSO (0.1%), 20 μM inS3-54 or 20 μM S3I-201 followed by co-IP with anti-HA antibody and

Western blot analysis with anti-FLAG antibody. InS3-54 did not affect the dimerization between HA- and FLAG-tagged STAT3. S3-201 was used a positive control.

E. InS3-54 favorably inhibits cancer cell survival possibly by inducing apoptosis.

To determine whether inS3-54 inhibits the growth and survival of cancer cells harboring constitutively activated STAT3, the viability of two lung cancer cell lines (A549 and H1299) and two breast cancer cell lines (MDA-MB-231 and MDA-MB-468) as well as a normal lung fibroblast (IMR90) and a mammary epithelial cell line (MCF10A1) was evaluated following inS3-54 treatment. Of four cancer cell lines, A549 and H1299 NSCLC cell lines represent a type of lung cancer which is relatively insensitive to chemotherapy, compared to small cell lung carcinoma. And MDA-MB-231 and MDA-MB-468 cell refer to triple-negative breast cancer cell lines which lack effective treatment targets. All these cancer cell lines have been demonstrated to harbor constitutive STAT3 signaling and thereby used in many studies to identify STAT3 inhibitors (72-81). However, the human fibroblast strain IMR-90 was derived from the lungs of a 16-week female fetus and induced to achieve senescence bypass (122). MCF10A1 is a subclone of a spontaneously immortalized non-tumorigenic human breast epithelial cell line established from long term culture of a breast subcutaneous mastectomy (123). Both kinds of cell lines served as the control cell lines due to their low STAT3 background level. As shown in **Figure 12A**, the cancer cells showed persistent STAT3 activity as assessed by the phosphorylation of STAT3 at Tyr705, compared to the non- non-tumorigenic cells. The cancer cells appeared to be more sensitive to inS3-54 with lower IC_{50} than the normal cells (**Figure 12B-C**), suggesting the existence of a therapeutic window for inS3-54.

To determine whether apoptosis contributes to inS3-54 induced loss of tumor cell viability, the exponentially growing lung and breast cancer cells (A549 and MDA-MB-231) were treated with DMSO control (0.1%) or inS3-54 (5, 10 and 20 μM) for 72 hours and analyzed by enzyme-linked immunosorbent assay (ELISA) which determines DNA fragmentation and histone release from the nucleus during the apoptosis process. As shown in **Figure 13**, inS3-54 induced apoptosis in both A549 and MDA-MB-231 cells in a dose-dependent manner.

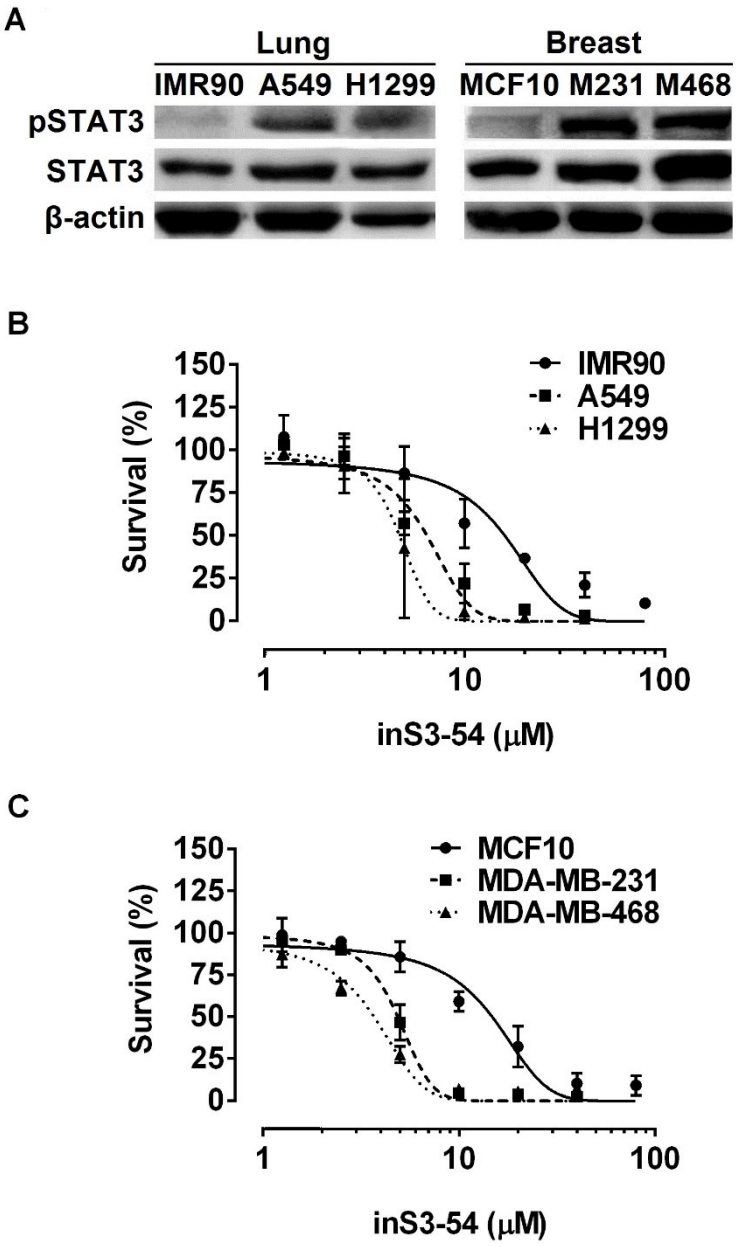

Figure 12. InS3-54 favorably inhibits cancer cell proliferation.

(A) The total and phosphorylated STAT3 in the indicated cell lines were assessed by Western blot analysis. β-actin was used as a loading control. All cancer cell lines showed a higher level of phospho-STAT3 than normal cells. (B-C) Six cell lines were subjected to SRB assay after treatment with increasing concentrations

of inS3-54 for 72 hours. Cancer cells were more sensitive to inS3-54 than normal cells.

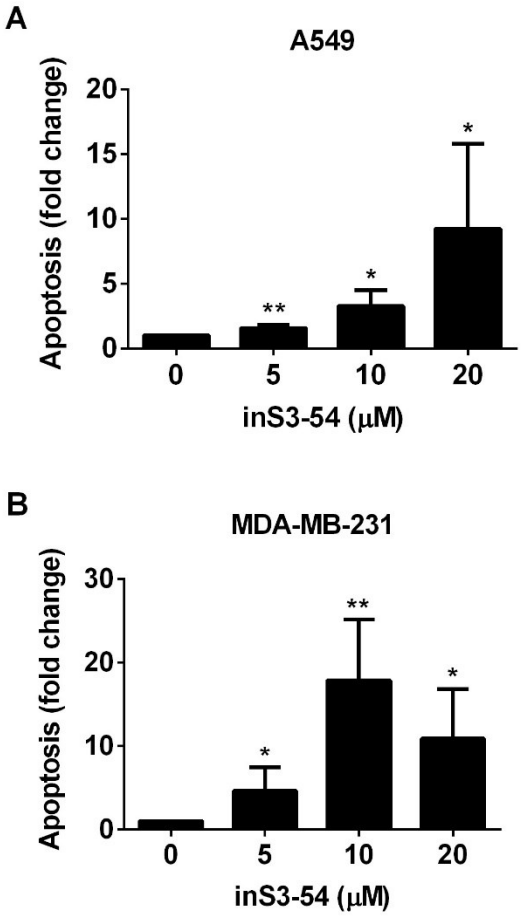

Figure 13. InS3-54 induces apoptosis.

Exponentially growing A549 (A) and MDA-MB-231 (B) cells were treated with DMSO (0.1%), 5, 10 or 20 μM inS3-54 for 72 hours followed by determination of apoptosis using ELISA. InS3-54 induced apoptosis in both cell lines. (N=3; * $p<0.05$, ** $p<0.01$, by Student's t-test as compared with DMSO vehicle control)

F. InS3-54 inhibits cancer cell migration and invasion.

STAT3 plays an important role in promoting cell migration and invasion by regulating the expression of the downstream genes such as MMP-1, 2, 7, 9, 10, twist and VEGF which favor these processes (52, 53). Firstly, the inhibitory effect of inS3-54 on cell migration was determined using wound filling assay which is one of the earliest developed models to study directional cell migration *in vitro*. By creating a "wound" in the cell monolayer, the cells at the edge became motile to close the gap. This method is particularly suitable to assess the effects of any treatment on cell migration. **Figure 14** shows that inS3-54 inhibited migration of both A549 and MDA-MB-231 cells in a dose- and time- dependent manner. At 24 hours, 68% and 95% of wounds were filled in the DMSO control-treated A549 and MDA-MB-231 cells, respectively. However, only 54% and 77% of the wounds were filled in A549 and MDA-MB-231 cells respectively following the treatment with10 μM inS3-54. The wound filling was further reduced to 27% and 29% in the cells treated with 20 μM inS3-54.

Additionally, metastatic tumor cells must be able to break away from the primary tissue, digest the basement membrane as well as invade nearby vessels. To determine the effects of inS3-54 on cell metastatic potential, we used Matrigel invasion assay which provides a reconstituted basement membrane *in vitro* and thereby allows to assess the invasive property of cells. Under the attraction of serum which is essential for cell growth, invasive cells detached from Matrigel matrix and invaded through the pores of the membrane. As shown in **Figure 15**, both A549 and MDA-MB-231 cells exhibited significantly decreased invasion

through Matrigel-coated filter in the presence of 10 or 20 μM inS3-54 as compared with the vehicle control-treated cells. After 6-hour treatment of 10 and 20 μM inS3-54, the invasion was reduced to 67% and 49% in A549 cells and to 52% and 24% in MDA-MB-231 cells, respectively. At 24 hours, the invasion was reduced to 71% and 24% in A549 and MDA-MB-231 cells exposed to 10 μM inS3-54, respectively. At 20 μM, the invasion of A549 and MDA-MB-231 cells was further reduced to 33% and 5% compared to the vehicle control, respectively.

Since inhibition of cell proliferation may contribute to the positive outcome in the above cell migration and cell invasion models, 100% confluent cells and short treatment time were applied to the above assays. To further eliminate this possibility, cell proliferation and apoptosis were analyzed under the same condition as wound filling and Matrigel invasion assays with confluent cultures. As shown in **Figure 16**, treatment with 20 μM inS3-54 for 24 hours had no significant effect on proliferation and apoptosis of confluent A549 cells although 20 μM inS3-54 decreased proliferation and induced apoptosis of MDA-MB-231 cells compared to the control group. However, 10 μM inS3-54 did not significantly affect proliferation or apoptosis of MDA-MB-231 cells, under which condition it significantly reduced the migration and invasion activity of MDA-MB-231 cells (**Figure 14-15**). No apoptosis was also observed when cells were exposed to 20 μM inS3-54 for 6 hours in both cell lines. Furthermore, MDA-MB-231 cells were observed to remain round in morphology at 6 hours. Due to similar phenomena found in both DMSO control and A18-treated cells, it is probably resulted from the specific cell line that costs more time to spread well after invading. Based on the above analyses, inS3-

54 was found to inhibit cancer cell migration and invasion which is unlikely due to its effects on apoptosis and cell proliferation.

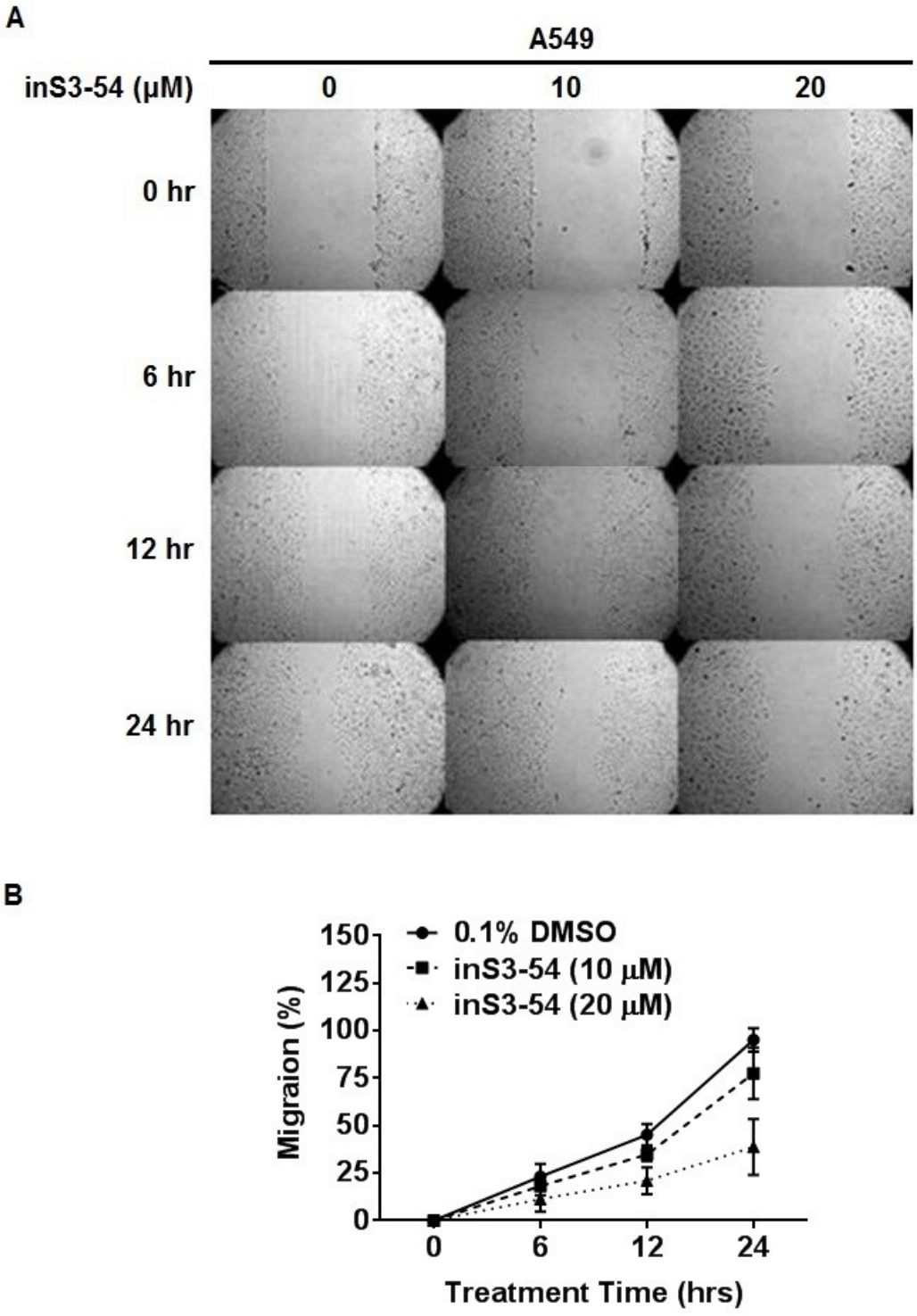

Figure 14. (Continued)

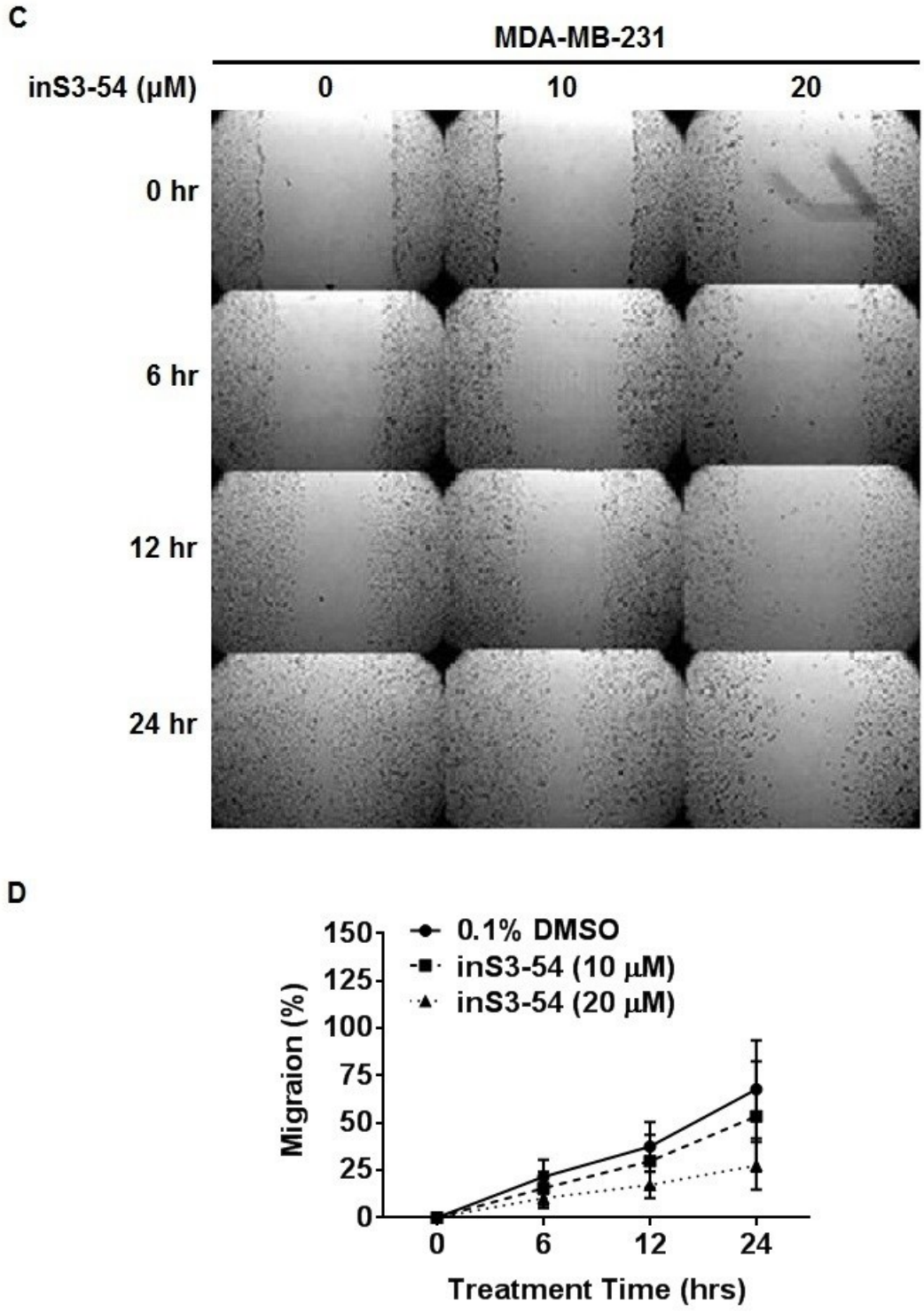

Figure 14. InS3-54 inhibits cancer cell migration.

Cell migration was assessed by wound filling assay in A549 (A-B) and MDA-MB-231 (C-D) cells following treatment with DMSO (0.1%), 10 or 20 μM inS3-54 for 24

hours. Panel B and D show the quantification analysis of wound filling assay from at least three independent experiments. InS3-54 suppressed cell migration in both cell lines.

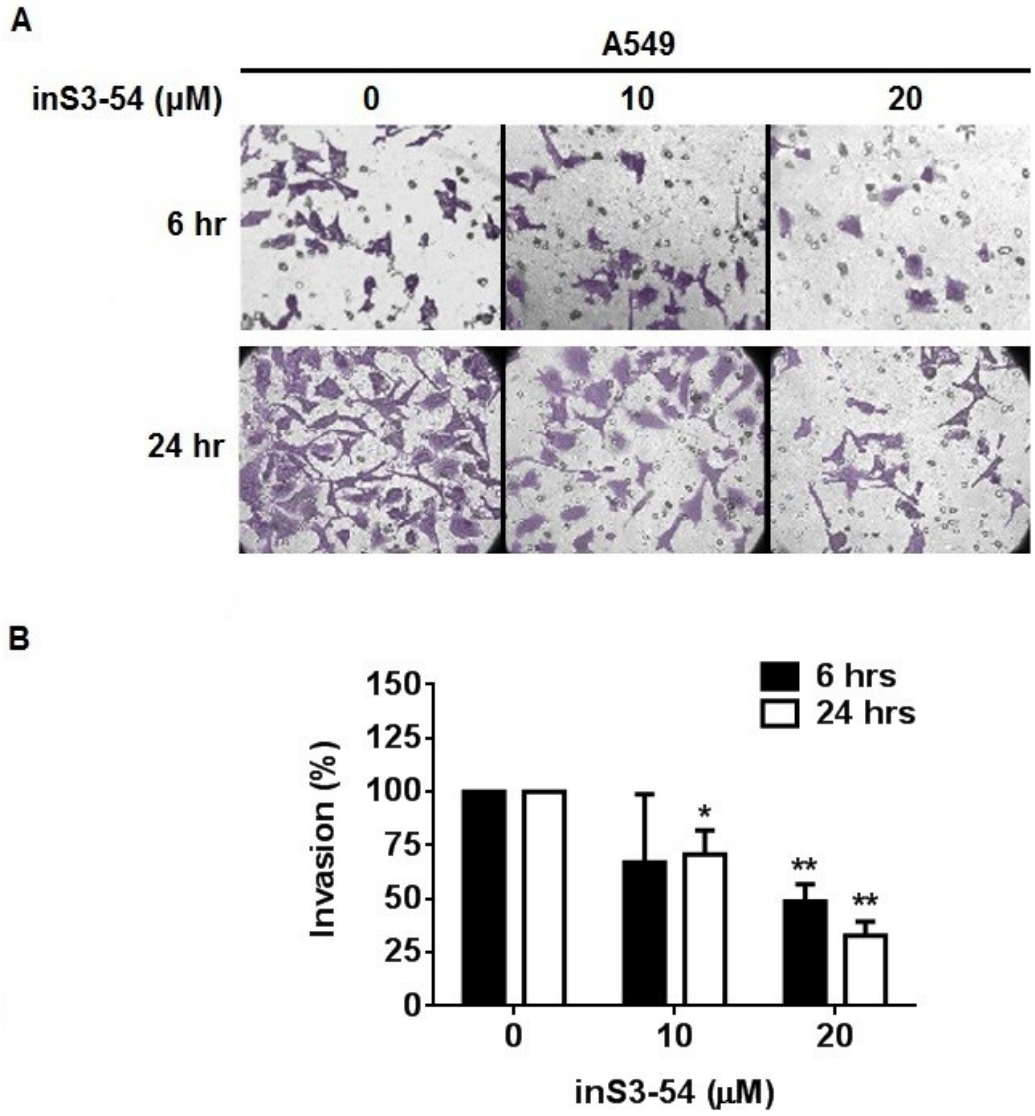

Figure 15. (Continued)

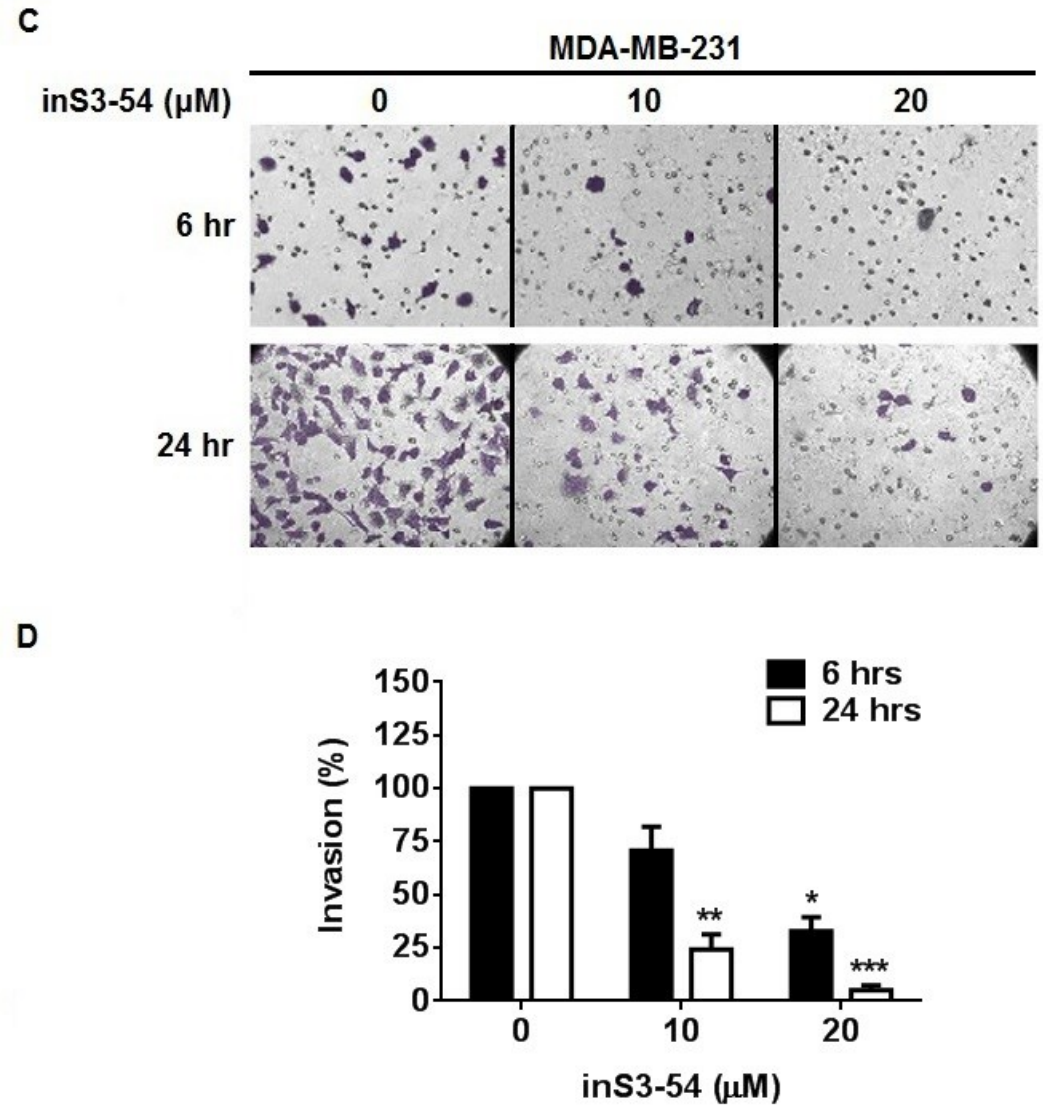

Figure 15. InS3-54 inhibits cancer cell invasion.

Cell invasion was determined in A549 (A-B) and MDA-MB-231 cells (C-D) in presence of DMSO (0.1%), 10 or 20 μM inS3-54 for 6 or 24 hours using Matrigel invasion assay with 10% FBS in the bottom chamber as a chemoattractant. Panel B and D show the quantification of invasion from measurement of 10 random views at each of three independent experiments. InS3-54 repressed cancer invasion in both cell lines. (N=3; * p<0.05, ** p<0.01, *** p<0.001, by Student's t-test as compared with DMSO vehicle control)

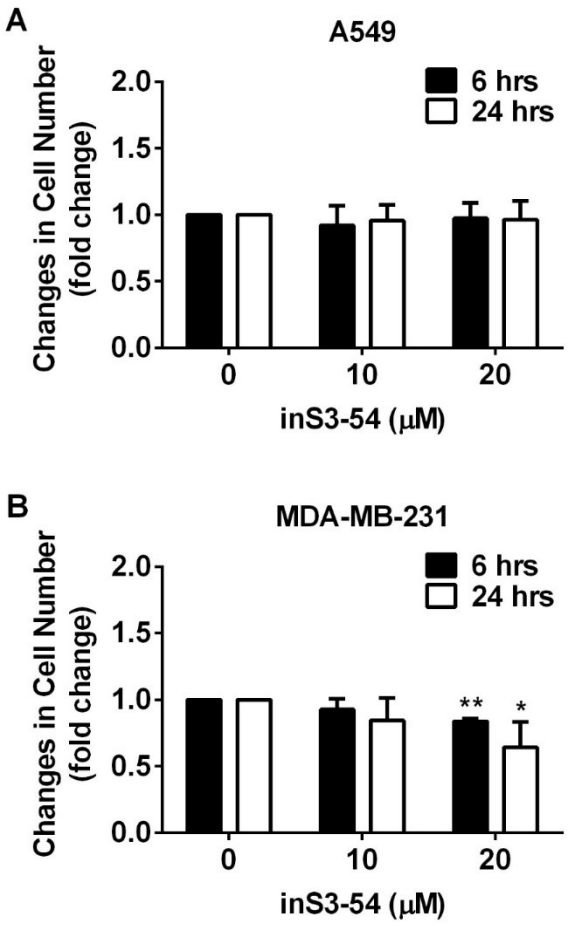

Figure 16. (Continued)

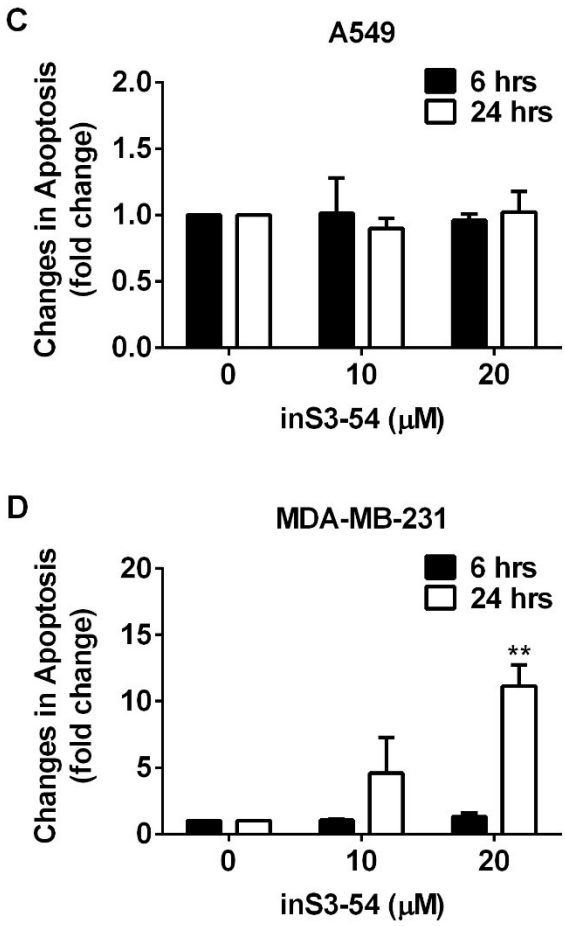

Figure 16. Effects of inS3-54 on cell growth and apoptosis of confluent cells. 100% confluent A549 (A and C) and MDA-MB-231 (B and D) cells were treated with DMSO (0.1%), 10 or 20 μM inS3-54 for 6 or 24 hours followed by determination of change in cell number for proliferation (A-B) or ELISA for apoptosis (C-D). InS3-54 had no effect on confluent A549 cells but MDA-MB-231 cells were affected at 24 hours. (N=3; * $p<0.05$, ** $p<0.01$, by Student's t-test as compared with DMSO vehicle control)

G. InS3-54 inhibits the expression of STAT3 downstream target genes and STAT3 binding to its endogenous target sequences.

To investigate the molecular mechanisms for inhibition of cell proliferation, migration and invasion by inS3-54, the expression of the known STAT3 target genes was examined in A549 and MDA-MB-231 cells following inS3-54 treatment. Immunoblotting analysis of whole-cell lysates showed obvious reduction in expression of cyclin D1, survivin, MMP-2, MMP-9, twist and VEGF in response to inS3-54 treatment (**Figure 17A-C**), indicating that inS3-54 suppresses the expression of cell cycle, anti-apoptotic and metastatic regulatory genes in malignant cells. This observation was also confirmed by real-time PCR analysis of mRNAs in both cancer cell lines (**Figure 17D-E**). It is noteworthy that inS3-54 dramatic reduced the protein levels of STAT3 downstream targets in a dose-dependent manner whereas the changes on the mRNA level were not remarkable. There are many factors that may affect the correlation between protein and mRNA levels. For example, the half-life of different proteins varies from minutes to days while the degradation rate of mRNA falls within a tight range. Other factors include the lower rate of mRNA transcription compared to protein translation in mammalian cells. It is possible that the changes on gene expression level are not reflected at the protein level. Moreover, it is unknown whether inS3-54 has off-target effects that may impact on protein synthesis or protein stability. Importantly, this experiment was intended to detect the changes of STAT3 downstream expression and our data indicate that inS3-54 can repress the expression of STAT3 downstream targets on the protein and mRNA levels.

Additionally, inS3-54 treatments had no effect on the total STAT3 or its phosphorylation at Tyr705 (**Figure 17A**), suggesting that inS3-54 may not affect the expression or activation of STAT3. In addition to constitutively activated STAT3, we also determined whether or not inS3-54 is capable of inhibiting cytokine-induced STAT3 phosphorylation as the level of serum IL-6 has been shown to be elevated in cancer patients and associate with constitutive activation of STAT3 (124, 125). Following serum starvation, A549 cells were pre-treated with 0.1% DMSO control or 20 μM inS3-54 followed by IL-6 stimulation, phospho-STAT3 (Tyr705) expression was observed to be induced to the same level (**Figure 18**). One of the STAT3 target genes, survivin, was also elevated by 17 folds following IL-6 stimulation in the control cells. However, inS3-54 treatment abrogated the IL-6 induced survivin expression by 46% (**Figure 18**). These results indicate that inS3-54, which is designed to target the STAT3 DBD, likely does not affect the expression or activation of constitutive STAT3 or IL-6-induced STAT3 but represses the expression of STAT3 target genes.

Taking into account the EMSA data showing that inS3-54 inhibits the DNA-binding activity of STAT3 *in vitro*, the inS3-54 inhibition of STAT3 target gene expression may be due to blocking the binding of STAT3 to DNA in cells. To test this possibility, A549 and MDA-MB-231 cells were treated with 0.1% DMSO, 10 or 20 μM inS3-54 followed by fractionation of cytosol, soluble nuclear fraction and chromatin-bound proteins. The STAT3 level in these fractions was investigated by Western blot analysis. As shown in **Figure 19**, the chromatin-bound STAT3 decreased while the STAT3 level in soluble nuclear fraction increased with the

increasing concentration of inS3-54, suggesting that inS3-54 effectively inhibits the binding of STAT3 to its endogenous target sequences on genomic DNA *in situ*. Two of the downstream genes, cyclin D1 and twist, were also selected for further verification of inhibition of inS3-54 on the DNA binding of STAT3 using ChIP assay. InS3-54 was found to block the binding of STAT3 to the promoter regions of cyclin D1 and twist (**Figure 20**). Taken together with the results shown above, we conclude that inS3-54 inhibits STAT3 activity in binding to endogenous promoters on genomic DNA, resulting in reduced transcription of its downstream target genes.

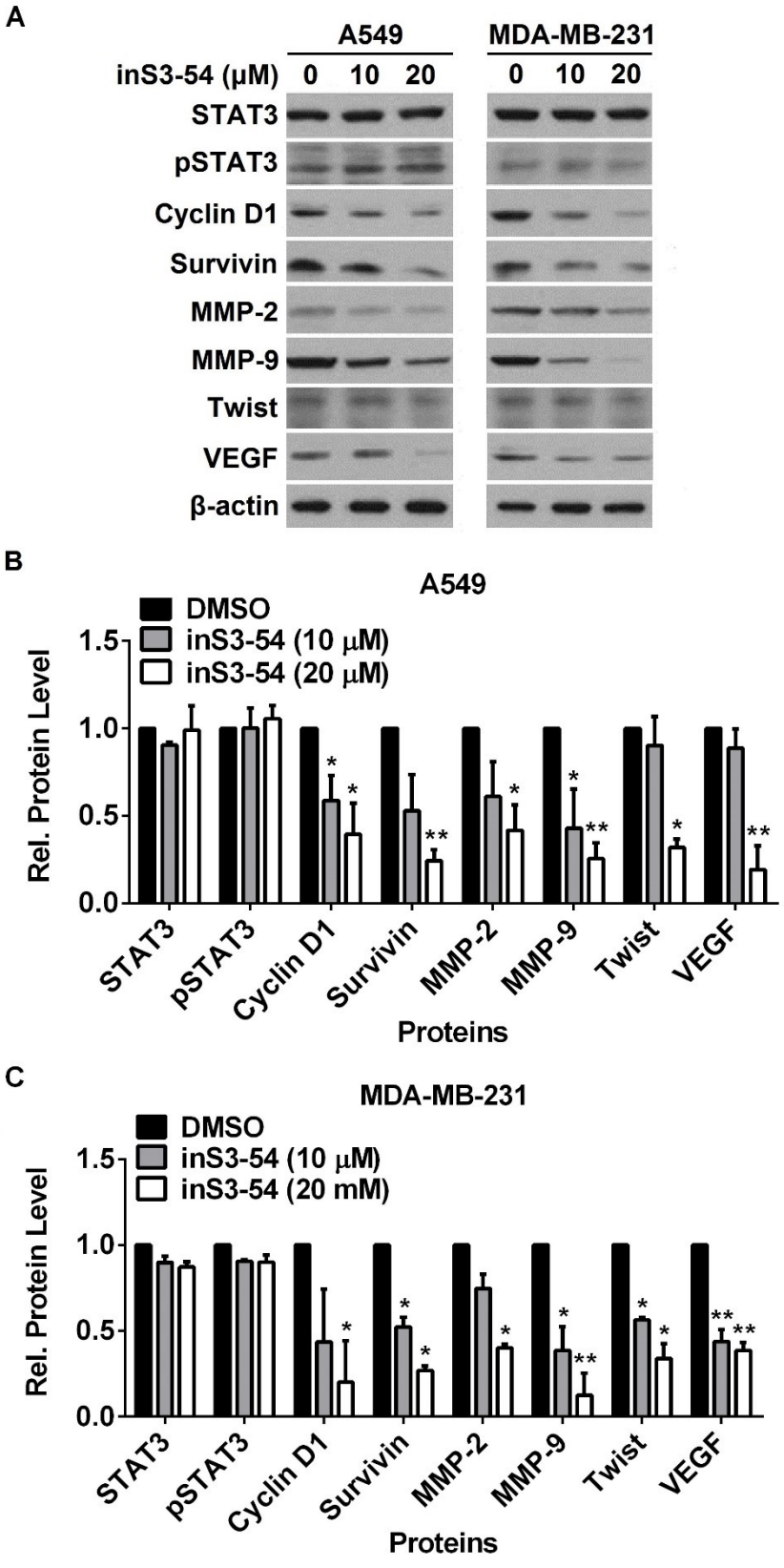

Figure 17. (Continued)

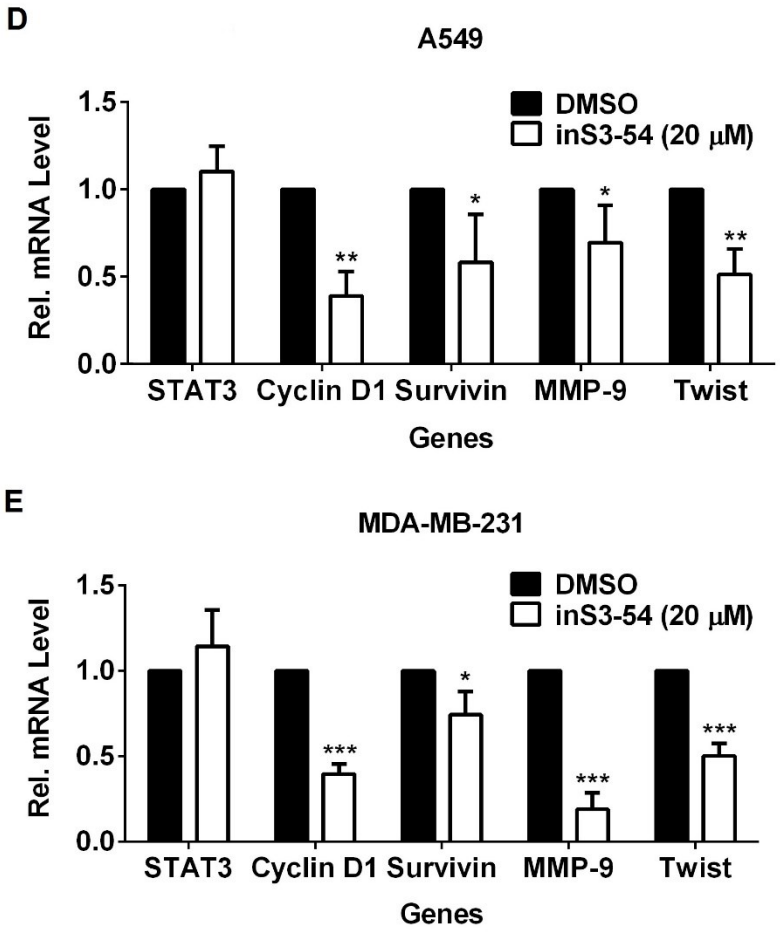

Figure 17. InS3-54 inhibits the expression of STAT3 downstream target genes.

(A-C) A549 and MDA-MB-231 cells were exposed to DMSO (0.1%), 10 or 20 μM inS3-54 followed by lysate preparation and Western blot analysis with antibodies indicated. β-actin was used as a loading control. Panel B and C shows the quantitative data measured by the density of Western blot bands and normalized against the β-actin internal control. Results indicate that inS3-54 inhibited protein expression of STAT3 downstream targets in both cells lines. (N=3; * p<0.05, ** p<0.01, by Student's t-test as compared with DMSO vehicle control) (D-E) A549 (D) and MDA-MB-231 (E) cells were exposed to 0.1% DMSO or 20 μM inS3-54

followed by extracting total RNA and real-time PCR analysis of selected genes. GAPDH was used an internal control. InS3-54 inhibited mRNA level of STAT3 downstream targets in both cells lines. (N=4; * $p<0.05$, ** $p<0.01$, *** $p<0.001$, by Student's t-test as compared with DMSO vehicle control)

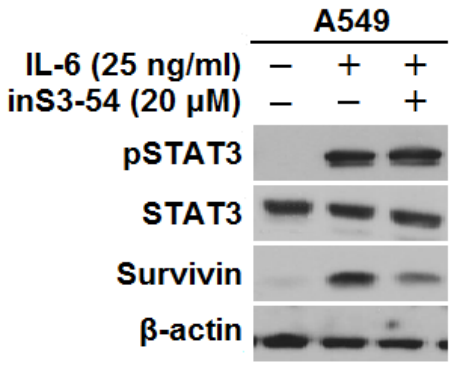

Figure 18. InS3-54 does not affect IL-6 induced STAT3 phosphorylation.

A549 cells were cultured in serum-free medium for 2 days and then pre-treated with 20 μM inS3-54 for 12 hours followed by addition of 25 ng/mL of IL-6 for 30 minutes. After treatment, the expression levels of phospho-STAT3, STAT3 and survivin were examined by Western blot analysis. IL-6 induced phosphorylation of STAT3 was not affected by inS3-54 treatment whereas IL-6 stimulated survivin was still down-regulated by 46%.

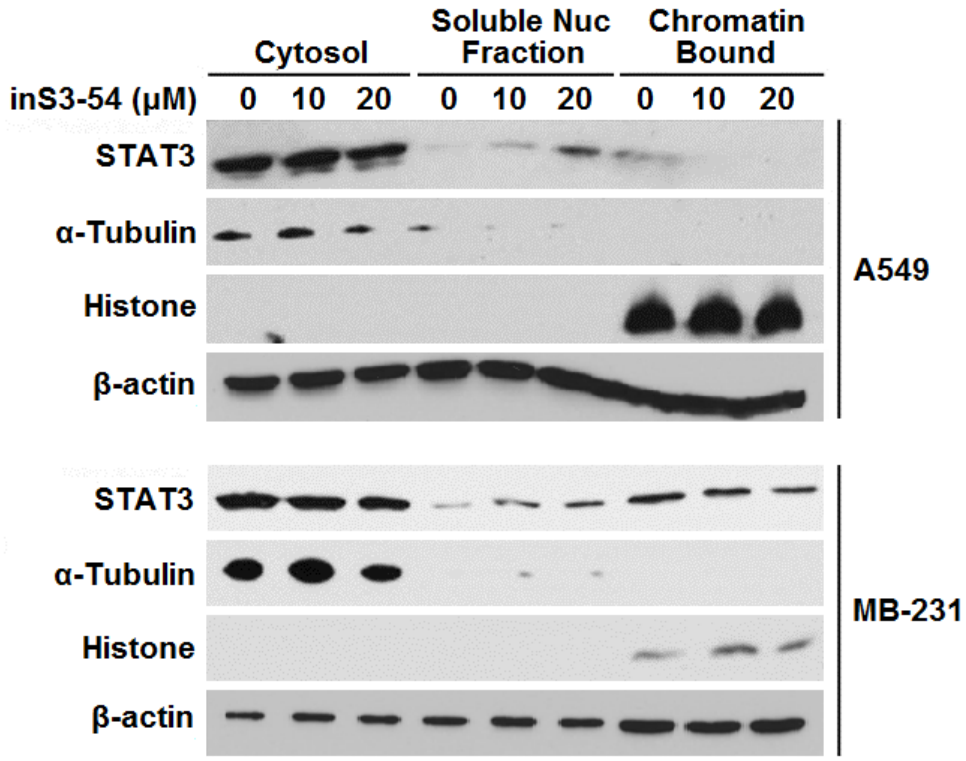

Figure 19. InS3-54 inhibits STAT3 binding to chromatin.

A549 and MDA-MB-231 cells were treated with 0.1% DMSO, 10 or 20 μM inS3-54 for 72 hours followed by fractionation of cytosol, soluble nuclear fraction, and chromatin-bound proteins and Western blot analysis of STAT3 in these fractions. α-Tubulin, histone 2A/3 and β-actin were used as loading controls for various protein fractions. InS3-54 blocked the binding of STAT3 to genomic DNA.

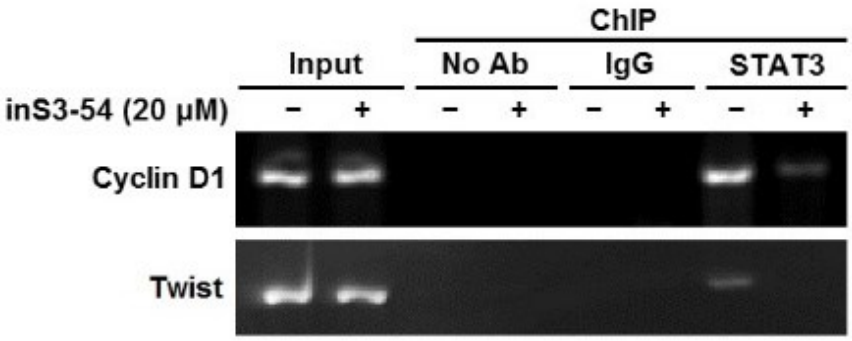

Figure 20. InS3-54 inhibits the binding of STAT3 to the promoter regions of responsive genes.

H1299 cells were treated with 0.1% DMSO or 20 μM inS3-54 for 24 hours followed by ChIP assay and agarose gel electrophoresis. No antibody and IgG were used as background negative controls. The binding of STAT3 to cyclin D1 or twist promoter was abrogated following inS3-54 treatment.

Part II. Development of inS3-54 analogues

A. Analogues of inS3-54 targeting the DBD of STAT3 are developed.

To investigate the structure-activity relationship (SAR) of inS3-54, 79 available analogues of inS3-54 were obtained by searching the Chemdiv database with a criterion of 80% structural similarity using the Chemfinder module in Chemoffice 8.0 (**Table 5**). These compounds were then assessed by a STAT3-dependent luciferase reporter assay in MDA-MB-231-STAT3 cells as we identified inS3-54 previously. Three compounds (named A18, A26 and A69) were more active in inhibiting STAT3-dependent luciferase activity as compared with the parental compound inS3-54 while A18 and A69 showed statistically significant difference (p<0.05) (**Figure 21A**). Further analysis confirmed that A18, A26 and A69 suppressed STAT3 signaling in a dose- and time-dependent manner with IC_{50} of 8.8~10.6 μM (**Figure 21B-C** and **Table 5**) whereas the three analogues did not exert any effect on the reporter expression driven by a p27 promoter containing no STAT3-binding site as previously described (**Figure 21D**), suggesting their specific effects on STAT3-dependent luciferase reporter. Inhibition of the reporter expression by inS3-54 analogues is thus unlikely due to its non-specific effect on the expression or activity of the reporter gene. Interestingly, A18, A26 and A69 had comparable IC_{50} whereas inS3-54 and A69 cost shorter time to achieve 50% inhibition on STAT3-dependent luciferase reporter than A18 and A26, probably due to the higher polarity. Furthermore, 10 analogues of A79 (A80~A89) were synthesized manually in collaboration with Dr. Zhong-Yin Zhang and then tested for their activity in inhibiting STAT3-dependent luciferase reporter activity. As

shown in **Figure 21A** and **Table 5**, none of these 10 derivatives had any inhibitory activity. Therefore, the three analogues of inS3-54 (A18, A26 and A69) from ChemDiv library were selected for more tests to investigate their effects on inhibition of constitute STAT3 signaling.

An *in vitro* colony formation assay using wild-type and conditional STAT3 knock-out bone marrow cells then provide a tool to determine the potential specificity of the compounds on STAT3 protein. Conditional knock-out of STAT3 has been demonstrated to reduce about 50% of colony formation potential in granulocyte macrophage (CFU-GM), erythroid (BFU-E) and multi-potential (CFU-CEMM) hematopoietic progenitor cells compared to wile-type cells as described previously (116, 117). It is assumed that the STAT3-specific compounds suppress colony formation of $STAT3^{+/+}$ cells, but do not further affect the colony formation potentials of progenitor cells from the $STAT3^{-/-}$ mice. Unfortunately, inS3-54 inhibited colony formation of CFU-GM, BFU-E and CFU-GEMM from both control mice (C57BL/B; $STAT3^{+/+}$) and $STAT3^{-/-}$ mice after these progenitor cells isolated from bone marrow were exposed to inS3-54, suggesting a low specificity of inS3-54 for STAT3 (**Figure 22**). However, the three active analogues (A18, A26 and A69) affected colony formation of progenitor cells from only $STAT3^{+/+}$ but not $STAT3^{-/-}$ mice (**Figure 22**), indicating that A18, A26 and A69 are likely specific to STAT3 whereas inS3-54 may also work on other targets in addition to STAT3 that are important for colony formation of hematopoietic progenitor cells.

Taken together, three active analogues of inS3-54 (A18, A26 and A69) show remarkable activity in inhibiting STAT3-dependent luciferase activity as well as are more specific to STAT3 signaling than their parental compound, inS3-54.

Table 5. Chemical properties of inS3-54 and its analogues

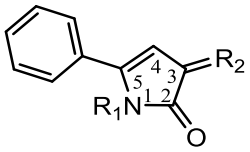

Core Structure

Name	R_1	R_2	Formula	M.W. (g/mol)
inS3-54	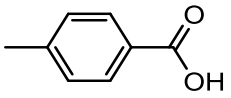	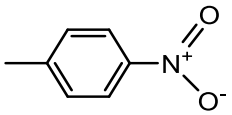	$C_{24}H_{16}N_2O_5$	412.41
A1	—	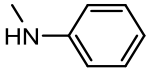	$C_{18}H_{16}N_2O$	276.33
A2	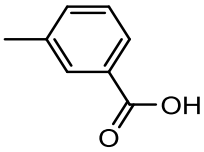	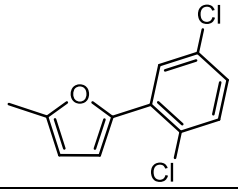	$C_{28}H_{17}Cl_2NO_4$	502.34
A3	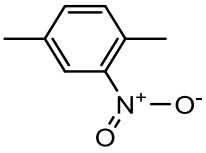	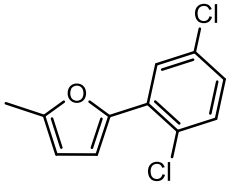	$C_{28}H_{18}ClN_2O_4$	517.36
A4		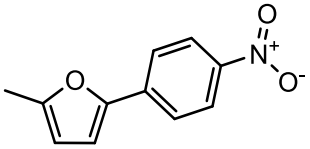	$C_{28}H_{20}N_2O_4$	448.47
A5	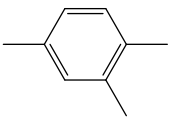	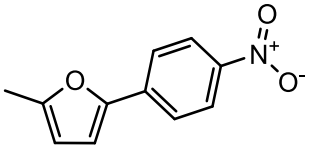	$C_{29}H_{22}N_2O_4$	462.50
A6	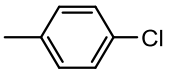	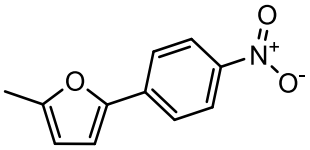	$C_{27}H_{17}ClN_2O_4$	468.89
A7	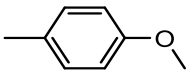	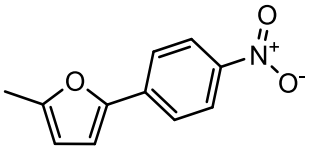	$C_{28}H_{20}N_2O_5$	464.47
A8	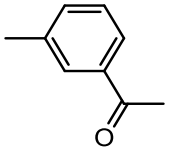	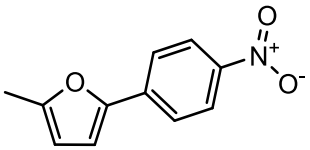	$C_{29}H_{20}N_2O_5$	476.48

A9	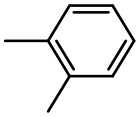	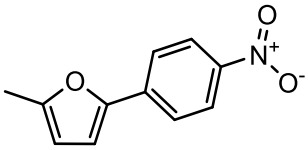	$C_{28}H_{20}N_2O_4$	448.47
A10	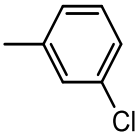	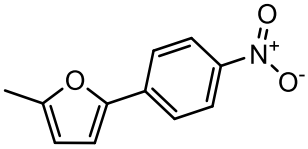	$C_{27}H_{17}ClN_2O_4$	468.88
A11		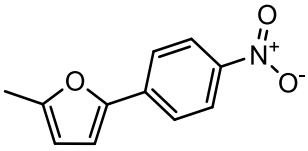	$C_{27}H_{17}FN_2O_4$	452.43
A12	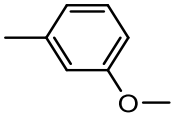	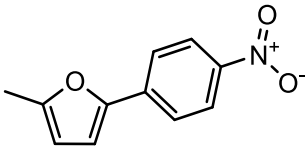	$C_{28}H_{20}N_2O_5$	464.47
A13	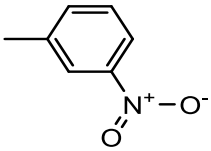	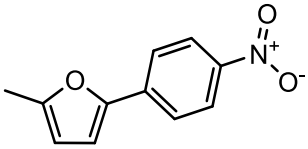	$C_{27}H_{17}N_3O_6$	479.44
A14	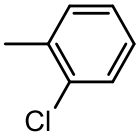	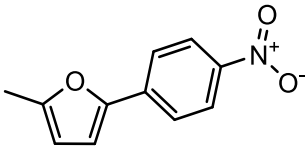	$C_{27}H_{17}ClN_2O_4$	468.89
A15	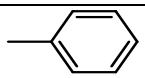	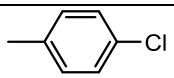	$C_{23}H_{16}ClNO$	357.83
A16	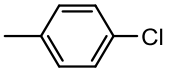	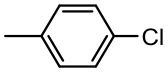	$C_{23}H_{15}Cl_2NO$	392.28
A17	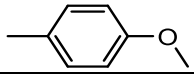	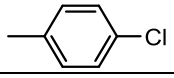	$C_{24}H_{18}ClNO_2$	387.86
A18	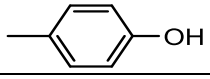	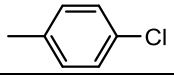	$C_{23}H_{16}ClNO_2$	373.83
A19	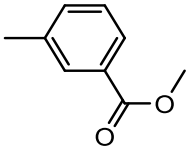	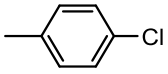	$C_{25}H_{18}ClNO_3$	415.87
A20	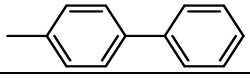	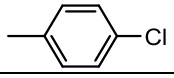	$C_{29}H_{20}ClNO$	433.93
A21	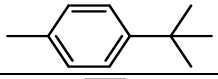	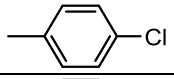	$C_{27}H_{24}ClNO$	413.94
A22	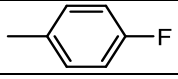	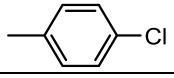	$C_{23}H_{15}ClFNO$	375.82
A23	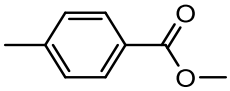	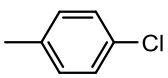	$C_{25}H_{18}ClNO_3$	415.87

A24	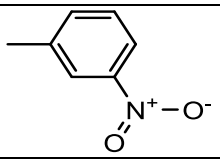	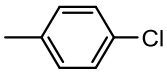	$C_{23}H_{15}ClN_2O_3$	402.83
A25	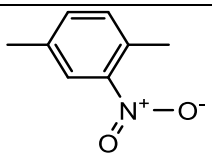	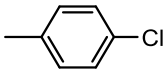	$C_{24}H_{17}ClN_2O_3$	416.86
A26	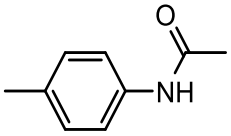	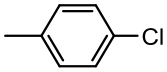	$C_{25}H_{19}ClN_2O_2$	414.88
A27	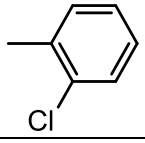	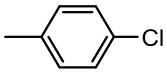	$C_{23}H_{15}Cl_2NO$	392.28
A28	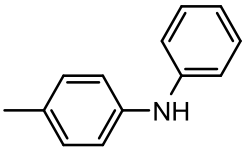	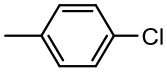	$C_{29}H_{21}ClN_2O$	448.94
A29	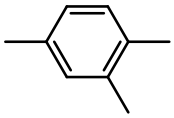	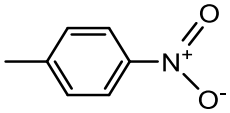	$C_{25}H_{20}N_2O_3$	396.44
A30	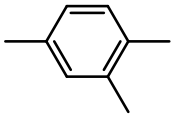	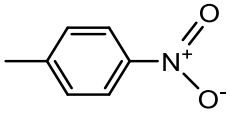	$C_{25}H_{20}N_2O_3$	396.44
A31	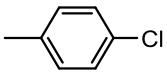	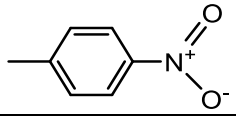	$C_{23}H_{15}ClN_2O_3$	402.83
A32	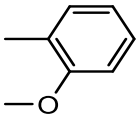	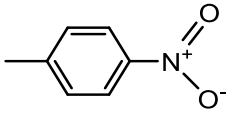	$C_{24}H_{18}N_2O_4$	398.41
A33	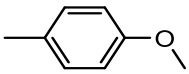	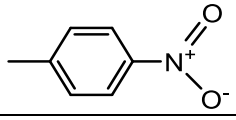	$C_{24}H_{18}N_2O_4$	398.41
A34	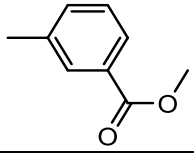	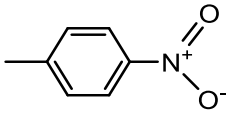	$C_{25}H_{18}N_2O_5$	426.42
A35	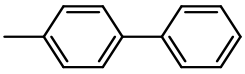	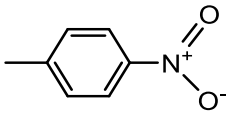	$C_{29}H_{20}N_2O_3$	444.48

A36	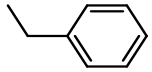	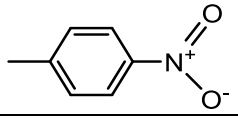	$C_{24}H_{18}N_2O_3$	382.41
A37	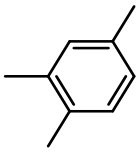	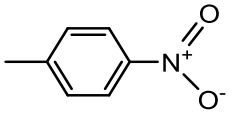	$C_{25}H_{20}N_2O_3$	396.44
A38	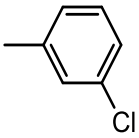	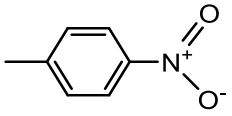	$C_{23}H_{15}ClN_2O_3$	402.83
A39	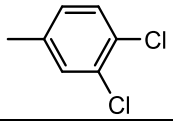	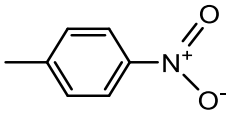	$C_{23}H_{14}Cl_2N_2O_3$	437.27
A40	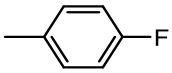	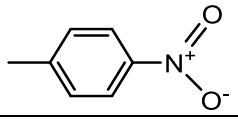	$C_{23}H_{15}FN_2O_3$	386.38
A41	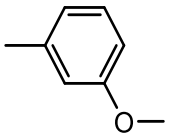	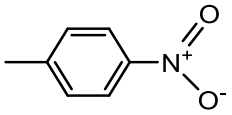	$C_{24}H_{18}N_2O_4$	398.41
A42	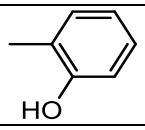	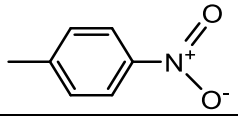	$C_{23}H_{16}N_2O_4$	384.38
A43	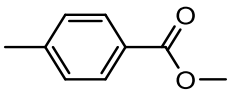	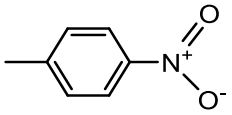	$C_{25}H_{18}N_2O_5$	426.42
A44	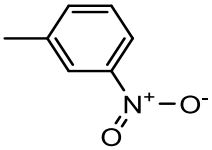	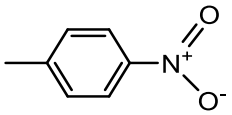	$C_{23}H_{15}N_3O_5$	413.38
A45	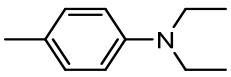	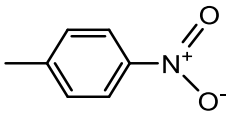	$C_{27}H_{25}N_3O_3$	439.51
A46	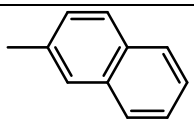	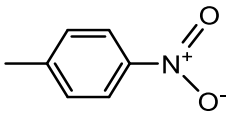	$C_{27}H_{18}N_2O_3$	418.44
A47	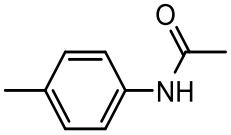	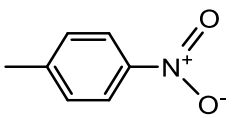	$C_{25}H_{19}N_3O_4$	425.44
A48	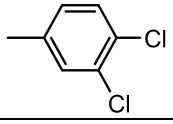	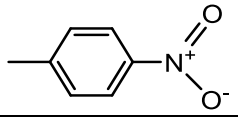	$C_{23}H_{14}Cl_2N_2O_3$	437.27

A49	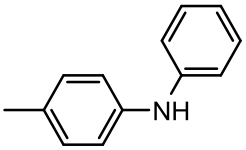	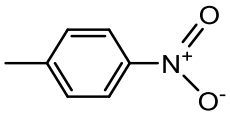	$C_{29}H_{21}N_3O_3$	459.50
A50	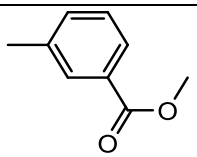	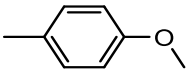	$C_{26}H_{21}NO_4$	411.45
A51	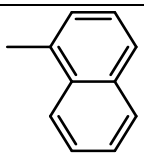	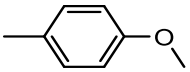	$C_{28}H_{21}NO_2$	403.47
A52	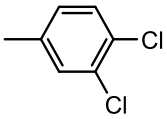	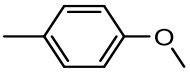	$C_{24}H_{17}Cl_2NO_2$	422.30
A53	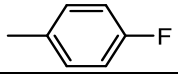	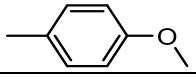	$C_{24}H_{18}FNO_2$	371.40
A54	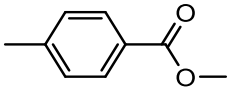	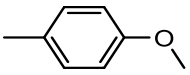	$C_{26}H_{21}NO_4$	411.45
A55	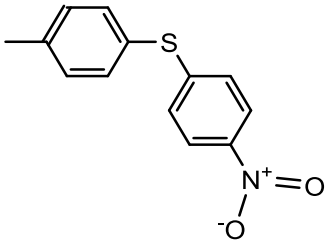	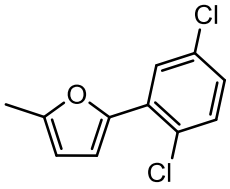	$C_{30}H_{33}N_2O_4S$	506.57
A56	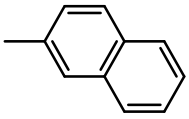	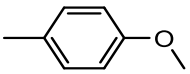	$C_{28}H_{21}NO_2$	403.47
A57	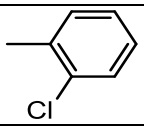	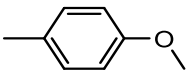	$C_{24}H_{18}ClNO_2$	387.86
A58	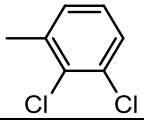	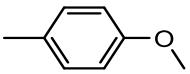	$C_{24}H_{17}ClN_2O_2$	422.30
A59	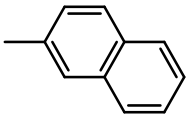	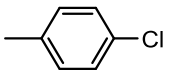	$C_{27}H_{18}ClNO$	407.89
A60	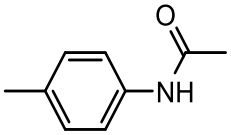	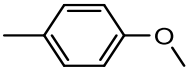	$C_{26}H_{22}N_2O_3$	410.46

A61	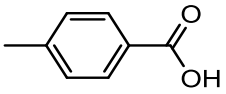	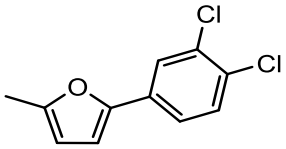	$C_{28}H_{17}Cl_2NO_4$	502.34
A62	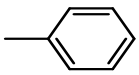	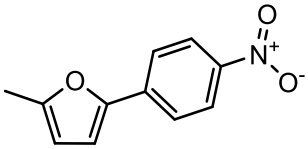	$C_{27}H_{18}N_2O_4$	434.44
A63	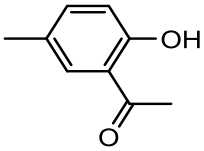	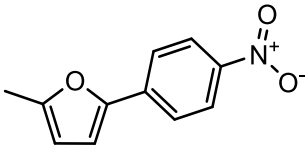	$C_{28}H_{18}N_2O_7$	494.45
A64	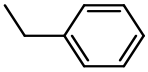	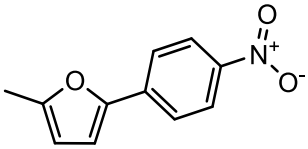	$C_{28}H_{20}N_2O_4$	448.47
A65	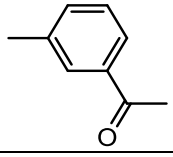	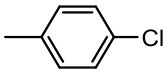	$C_{25}H_{18}ClNO_2$	399.87
A66	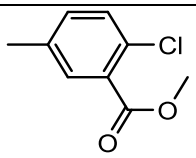	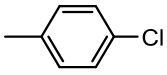	$C_{25}H_{17}Cl_2NO_3$	450.31
A67	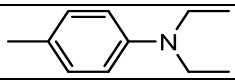	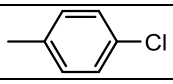	$C_{27}H_{15}ClN_2O$	428.95
A68	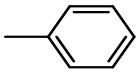	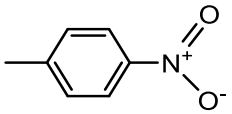	$C_{23}H_{16}N_2O_3$	368.38
A69	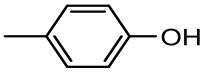	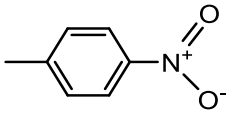	$C_{23}H_{16}N_2O_4$	384.38
A70	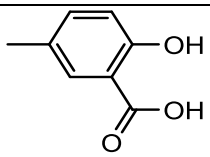	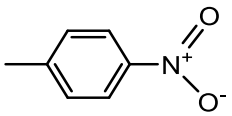	$C_{24}H_{16}N_2O_6$	428.39
A71	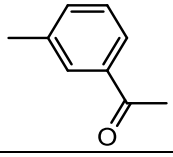	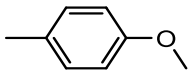	$C_{25}H_{18}N_2O_4$	410.42
A72	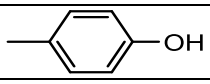	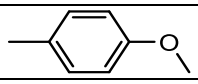	$C_{24}H_{19}NO_3$	369.41

A73	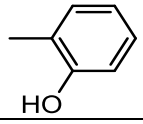	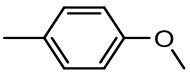	$C_{24}H_{19}NO_3$	369.41
A74	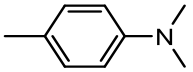	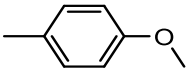	$C_{26}H_{24}N_2O_2$	396.48
A75	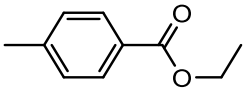	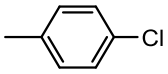	$C_{26}H_{20}ClNO_3$	429.89
A76	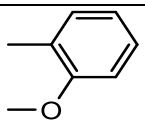	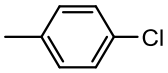	$C_{24}H_{18}ClNO_2$	387.86
A77	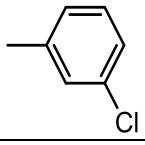	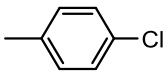	$C_{23}H_{15}Cl_2NO$	392.28
A78	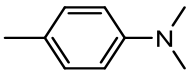	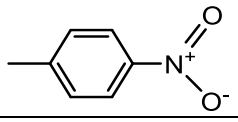	$C_{25}H_{21}N_3O_3$	411.45
A79	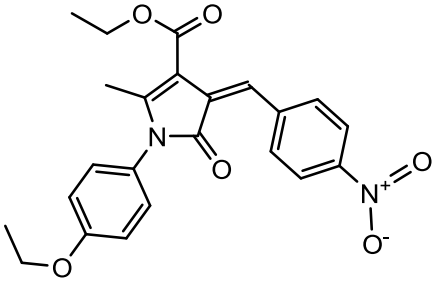		$C_{23}H_{22}N_2O_6$	422.43
	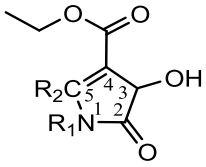 Core Structure			
A80	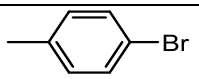	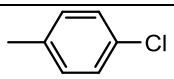	$C_{19}H_{15}ClBrNO_4$	436.68
A81	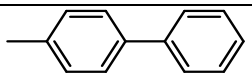	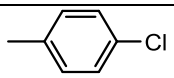	$C_{25}H_{20}ClNO_4$	433.88
A82	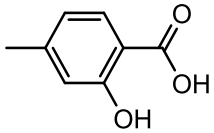	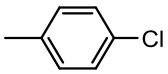	$C_{20}H_{16}ClNO_7$	417.80
A83	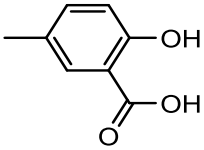	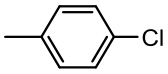	$C_{20}H_{16}ClNO_7$	417.80
A84	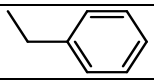	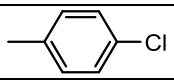	$C_{20}H_{18}ClNO_4$	371.81

A85	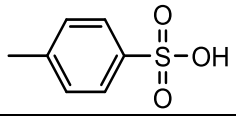	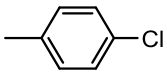	$C_{19}H_{16}ClNO_7S$	437.85
A86	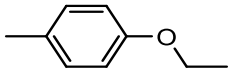	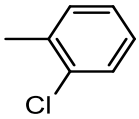	$C_{21}H_{20}ClNO_5$	401.84
A87	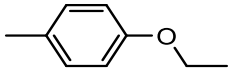	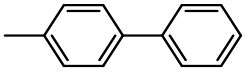	$C_{27}H_{25}NO_5$	443.49
A88	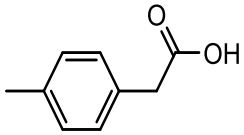	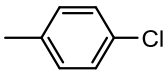	$C_{26}H_{20}ClBrN_2O_6$	571.80
A89	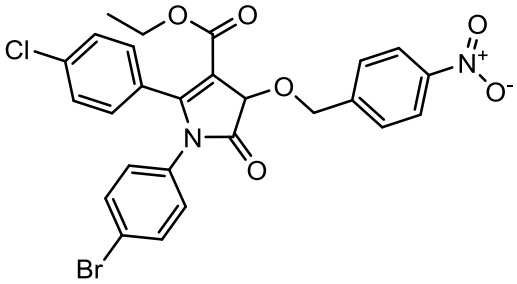		$C_{21}H_{18}ClNO_6$	415.82

Table 6. Summary of inS3-54 and its active analogues

Compounds	Inhibition of STAT3-dependent luciferase activity		Inhibition of cell survival					
			IC_{50} (μM)					
			Lung			Breast		
	IC_{50} (μM)	Half Time (hrs)	IMR90	A549	H1299	MCF10A1	MB-231	MB-468
inS3-54	13.8±0.4	29.2±4.7	10.0±2.3	5.4±0.6*	4.7±1.7*	12.0±1.0	4.8±0.5**	3.2±0.3**
A18	10.6±0.5$^{\#\#}$	38.5±6.6	10.5±0.2	4.0±0.7***	4.7±0.8***	7.0±2.1	3.2±0.6*	3.5±0.6
A26	8.8±1.8$^{\#}$	49.9±9.9$^{\#}$	4.0±0.3	2.6±0.4*	3.4±0.2*	9.2±1.8	3.2±0.4***	1.8±0.2***
A69	12.6±2.2	12.7±0.6$^{\#\#}$	9.2±0.8	5.3±1.0**	5.6±1.4**	10.3±0.8	5.0±0.3**	2.6±0.2**

Data are presented as mean±SD. $^{\#}$ p<0.05, $^{\#\#}$ p<0.01, by Student's t-test as compared with inS3-54. * p<0.05, ** p<0.01, *** p<0.01, by Student's t-test as compared with respective non-cancer cell lines.

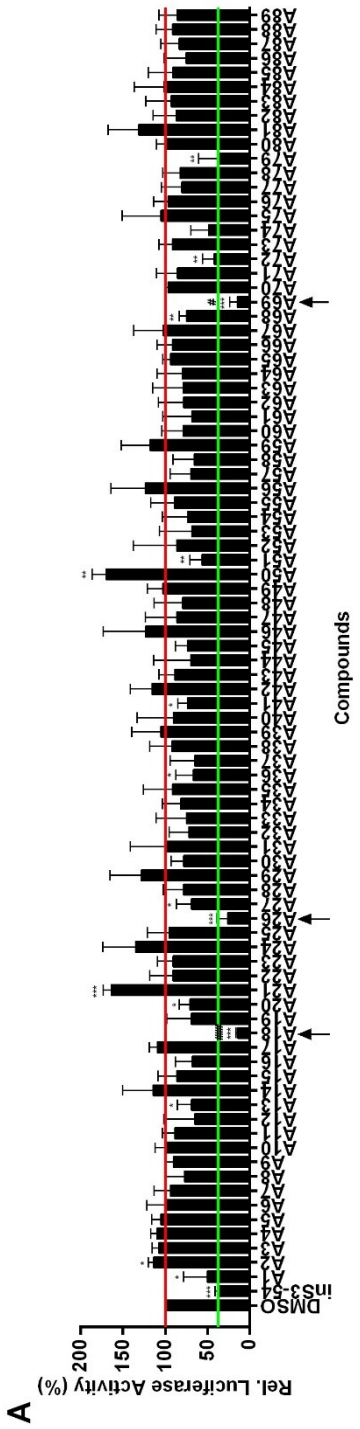

Figure 21. (Continued)

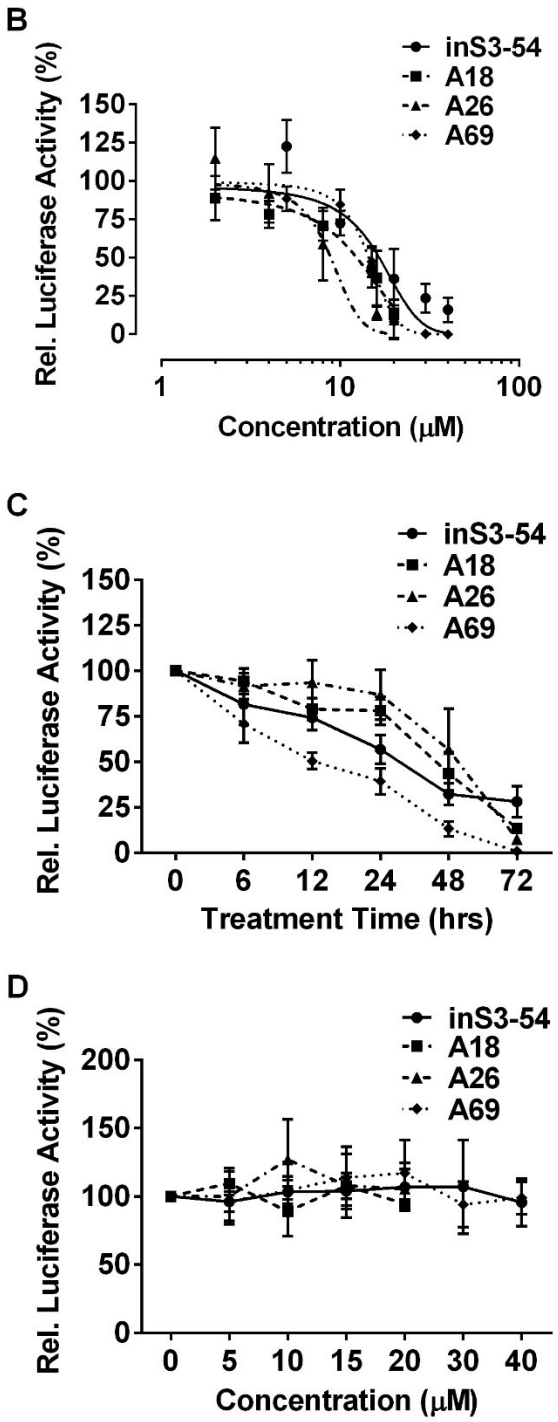

Figure 21. Identification of inS3-54 analogues.

(A) Effects of inS3-54 analogues on STAT3-driven luciferase expression. MDA-MB-231 cells stably transfected with STAT3-dependent luciferase reporter were

treated with vehicle control (0.1% DMSO), 20 μM of inS3-54 or its analogues (A1-A89), followed by measurement of luciferase activity. A18 and A69 are significantly more active than inSTAT3-54. Red line indicates 100% as defined by DMSO vehicle control. Green line indicates the effect of inS3-54 on STAT3-dependent luciferase reporter. (B-C) Effects of three active inS3-54 analogues on STAT3-dependent luciferase reporter expression. MDA-MB-231-STAT3 cells were exposed to increasing concentrations of inS3-54 or its analogues for 72 hours (B) or exposed to 20 μM inS3-54 or its analogues for various time intervals (C) followed by luciferase reporter assay. Three analogues inhibited STAT3-dependent luciferase reporter in a dose- and time-dependent manner. (D) Effects of three active inS3-54 analogues on STAT3-independent luciferase reporter expression. H1299 cells were transiently transfected with a luciferase reporter construct driven by a p27 promoter lacking STAT3-binding sequence followed by treatment with increasing concentrations of inS3-54 or its analogues for 48 hours. (N=3; * $p<0.05$, ** $p<0.01$, *** $p<0.001$, by Student's t-test as compared with DMSO vehicle control; $^{\#}$ $p<0.05$, $^{\#\#\#}$ $p<0.001$, by Student's t-test as compared with inS3-54)

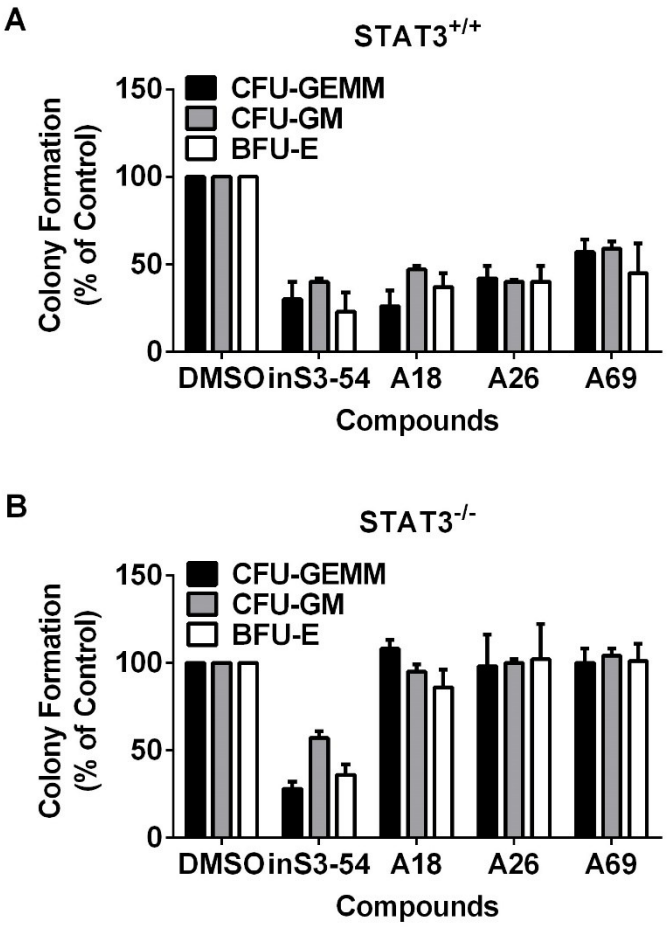

Figure 22. Effects of inS3-54 and its active analogues on colony formation of hematopoietic progenitor cells.

Hematopoietic progenitor cells isolated from $STAT3^{+/+}$ (A) and $STAT3^{-/-}$ (B) mice were cultured in the presence of vehicle control (0.1% DMSO), 20 μM inS3-54 or its analogues (A18, A26 and A69) followed by counting of colonies formed. Three analogues reduced colony formation of CFU-GM, BFU-E, and CFU-GEMM from only $STAT3^{+/+}$ but not $STAT3^{-/-}$ mice.

B. InS3-54 analogues selectively inhibit the DNA-binding activity of STAT3 other than that of STAT1.

Previous studies have revealed that inS3-54 selectively blocks the DNA-binding activity of STAT3, without affecting STAT1. The same EMSA was also performed to evaluate three active analogues. As shown in **Figure 23**, the specific binding of DNA probe to STAT3 or STAT1 was demonstrated using super-shift and competition analyses. A18, A26 and A69 all inhibited the DNA- binding activity of STAT3 in a dose-dependent manner whereas none of them affected the specific binding of DNA probe to STAT1. Overall, inS3-54 analogues selectively block the DNA-binding activity of STAT3 but not that of STAT1.

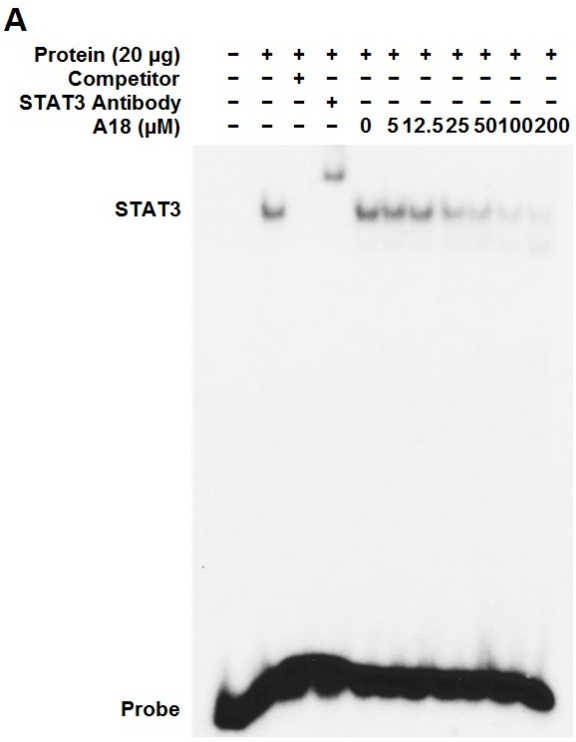

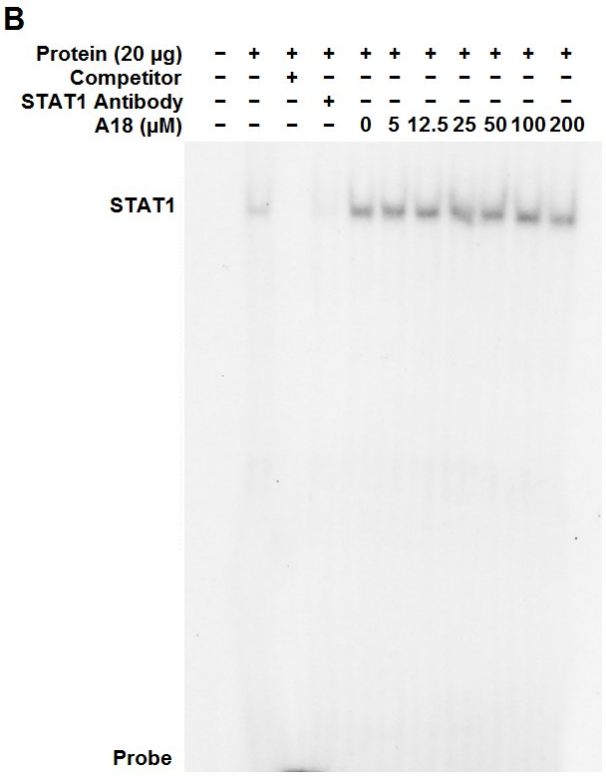

Figure 23. (Continued)

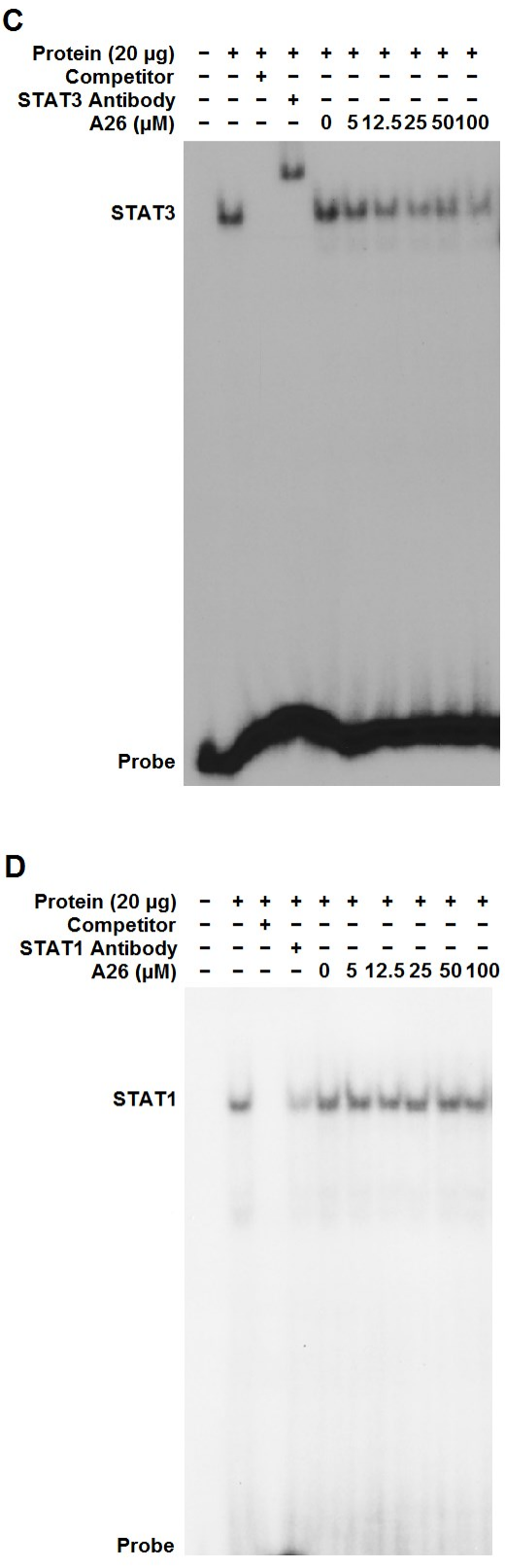

Figure 23. (Continued)

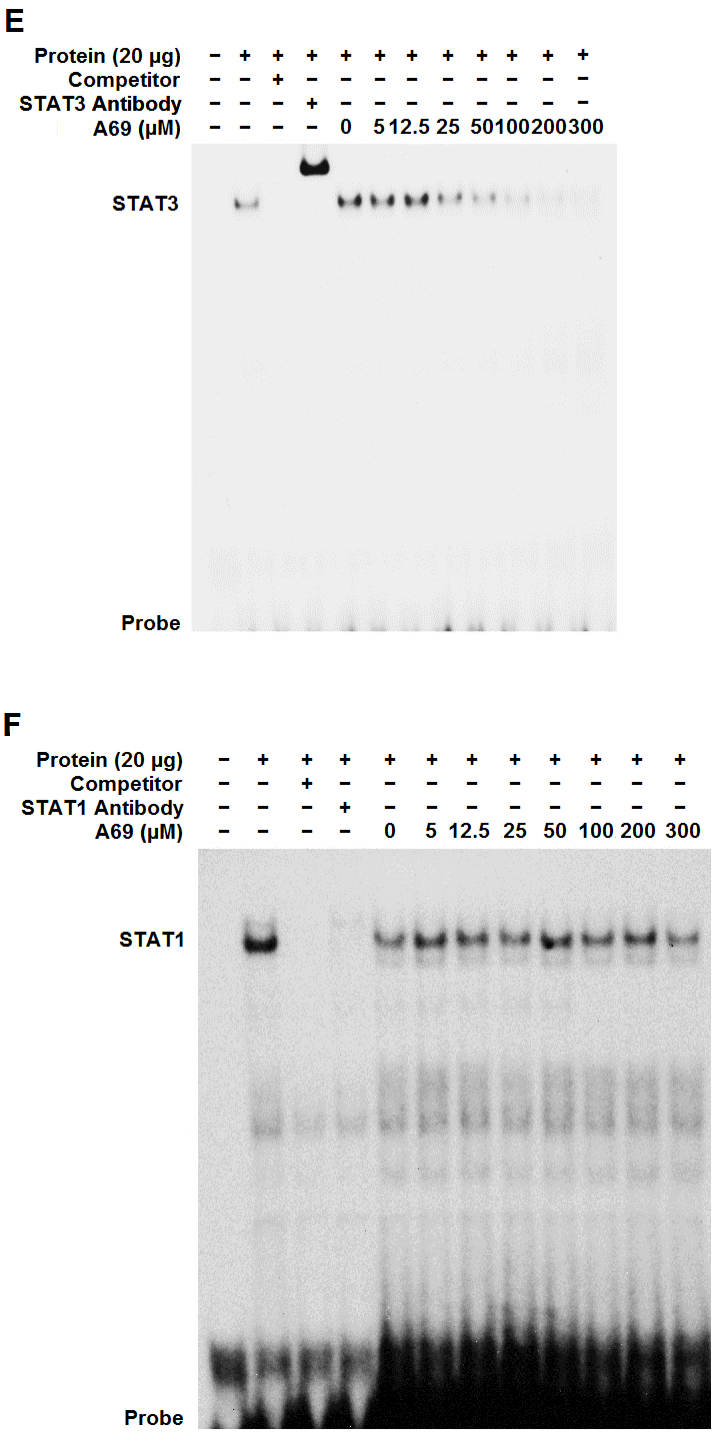

Figure 23. (Legend on next page)

Figure 23. InS3-54 analogues inhibits the DNA-binding activity of STAT3 but not that of STAT1.

The effects of inS3-54 analogues on the DNA-binding activity of STAT3 (A, C and E) and STAT1 (B, D and F) were assessed by EMSA. The whole cell lysates extracted from H1299 cells transiently transfected with constitutively dimerizable FLAG-STAT3 or STAT1 were pre-incubated with increasing concentrations of inS3-54 analogues for 30 minutes prior to addition of [^{32}P]-labeled double strand DNA probe that contains a STAT3 DNA-binding site for 20 minutes at room temperature. The reaction mixtures were then resolved on 6% non-denaturing polyacrylamide gel and detected by autoradiography. The binding of STAT3 to specific probe was inhibited following treatment with three analogues.

C. InS3-54 analogues bind to STAT3.

In the previous studies, inS3-54-conjugated beads pulled down STAT3 from whole cell lysate, suggesting inS3-54 may bind to STAT3. To verify if these analogues (A18, A26 and A69) indeed bind to STAT3, compound-conjugated beads were also used to detect their potential interaction with STAT3 protein. A26 containing an imino group was conjugated to CNBr-activated Sepharose 4B. **Figure 24A** shows that A26-conjugated beads successfully pulled down STAT3 whereas the vehicle control beads (DMSO) or an irrelevant compound control (PHP) did not. Furthermore, pretreatment of the cell lysate using excess free A26 abrogated the pull down of STAT3 by A26-conjugated beads while the inactive analogue had no effect (**Figure 24B**). Although Sepharose beads are available to conjugate A18 and A69, the competitive experiment was used to provide indirect evidence for their potential interaction with STAT3. Results shows that pretreatment of A26-conjugated beads with A18 and A69 also diminished the pull down of STAT3 from cell lysate (**Figure 24C**). Based on the above analyses, the inS3-54 analogues (A18, A26 and A69) may have the potential interaction with STAT3.

Due to the similar property of the chemical structures compared to the STAT3 alkylating agent as previously described, we chose one of inS3-54 analogues, A18, to determine whether it may act as an alkylating agent by using glutathione as a substrate accordingly. Similar to inS3-54, A18 did not affect the level of glutathione in both lung cancer A549 cells and breast cancer MDA-MB-231 cells after exposure to 10 μM A18 for 48 hours (**Figure 25**), suggesting that

the interaction between A18 and STAT3 may not due to alkylation of cysteine residues in STAT3 under the condition tested.

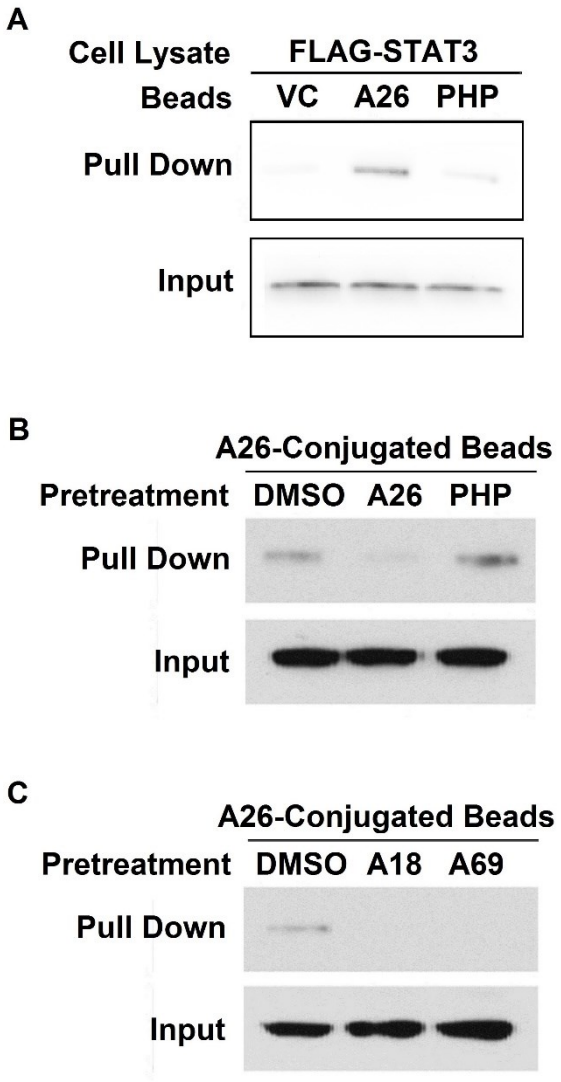

Figure 24. Binding of inS3-54 analogues to STAT3.

(A) Pull-down assay of STAT3 from total lysate of constitutively dimerizable FLAG-STAT3-transfected H1299 cells using CNBr-activated Sepharose 4B-conjugated with vehicle control, A26 or irrelevant negative control compound (PHP). Pull-down samples were analyzed using SDS-PAGE and Western blotting probed with anti-FLAG antibody. (B) Competition of STAT3-binding to A26-conjugated CNBr-activated Sepharose 4B beads by excess free A26, an irrelevant compound control or vehicle control (DMSO). (C) Competition of STAT3-binding to A26-conjugated

CNBr-activated Sepharose 4B beads by excess free A18, A69 or vehicle control (DMSO). Unbound flow-through samples were used as the input control. All three compounds show the potential to bind to STAT3 protein.

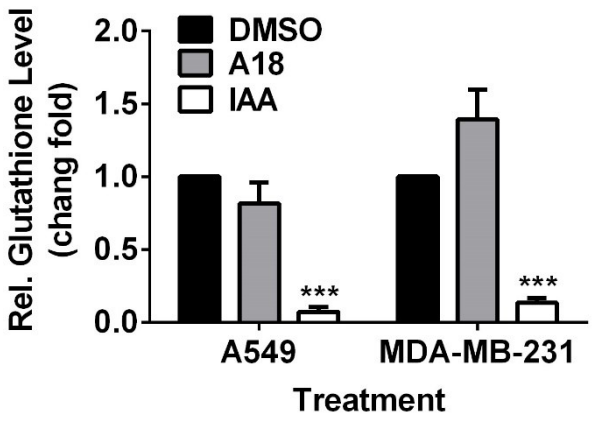

Figure 25. A18 does not alkylate cysteine using glutathione as a substrate. After A549 and MDA-MB-231 cells were exposed to DMSO (0.1%) or 10 μM A18 for 48 hours or 15 mM IAA for 30 minutes, the level of glutathione was assessed by GSH-Glo™ glutathione assay following the manufacturer's instructions. IAA was used as a positive control. The level of glutathione was not significantly affected by A18 under the condition tested. (N=3; *** p<0.001, by Student's t-test as compared with DMSO vehicle control)

D. InS3-54 analogues favorably inhibit cancer cell survival possibly by inducing apoptosis.

To determine whether the analogues (A18, A26 and A69) inhibit the survival of cancer cells with constitutive STAT3 signaling, the effects of various analogues on cell viability were analyzed in two lung cancer cell lines (A549 and H1299) and two breast cancer cell lines (MDA-MB-231 and MDA-MB-468) as well as a normal lung fibroblast cell line (IMR90) and a normal mammary epithelial cell line (MCF10A1) as measured by SRB assay. Our previous study demonstrated that these cancer cells harbor constitutively activated STAT3 as assessed by its phosphorylation status at Tyr705 compared to the normal cells (**Figure 12A**). Cancer cells appeared to be more sensitive to the analogues than the non-tumorigenic cells with lower IC_{50} (1.8~5.6 μM vs 4.0~12.0 μM; **Table 6**), consistent with inS3-54. However, all three analogues showed comparable or more potent activity on inhibition of cancer cell proliferation as compared to the parental compound inS3-54 (**Figure 26** and **Table 6**).

To investigate whether apoptosis contributes to loss of tumor cell viability, the same ELISA which was used to determine the effect of inS3-54 on apoptosis was also used to evaluate the three analogues following treatment in exponentially growing cells. After A549 and MDA-MB-231 cells were exposed to DMSO control (0.1%), A18 or A69 for 72 hours, a remarkable induction of apoptosis was induced in both lung and breast cancer cells, suggesting that apoptosis probably contributes to suppression of cancer cell survival (**Figure 27**).

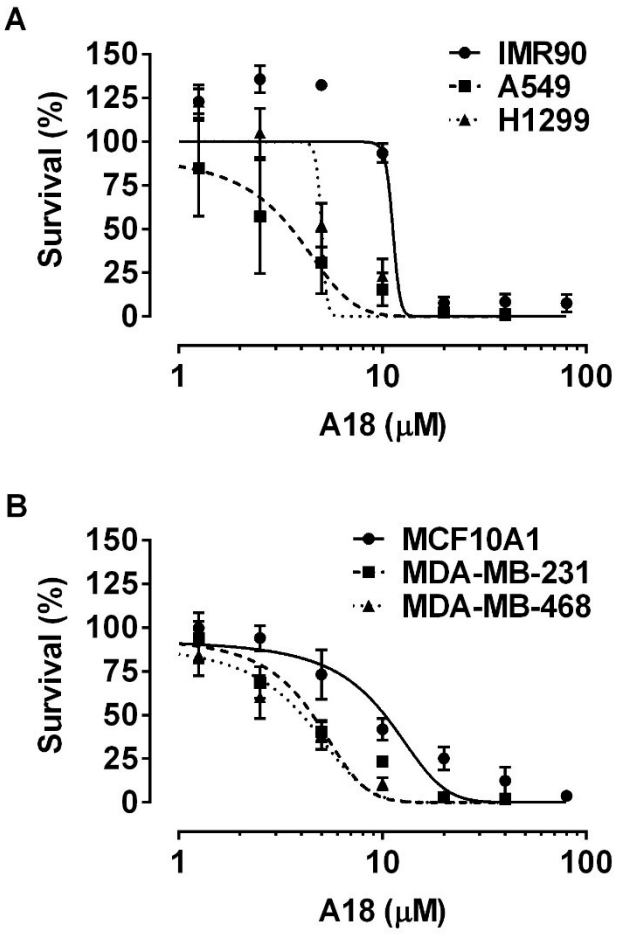

Figure 26. (Continued)

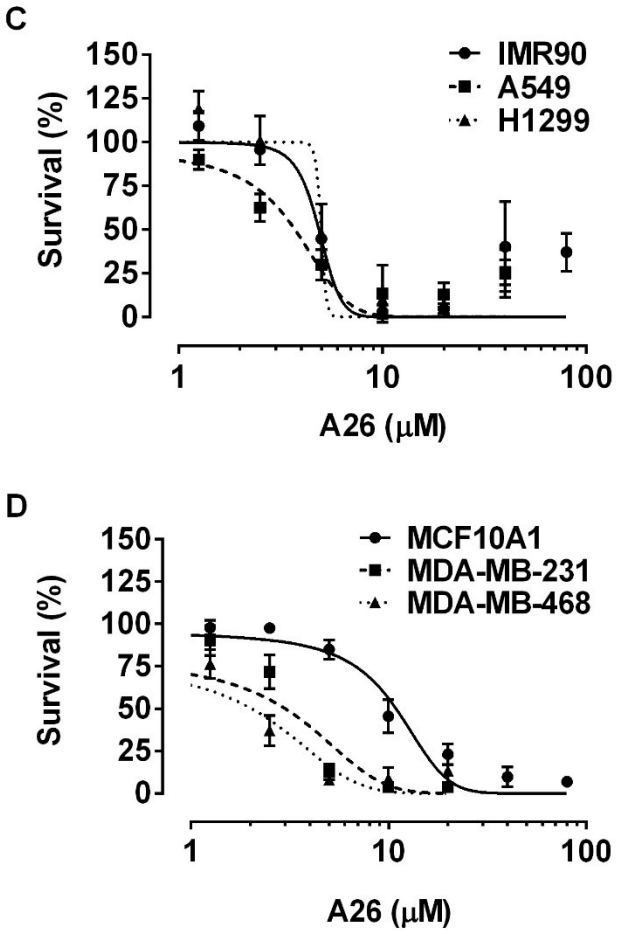

Figure 26. (Continued)

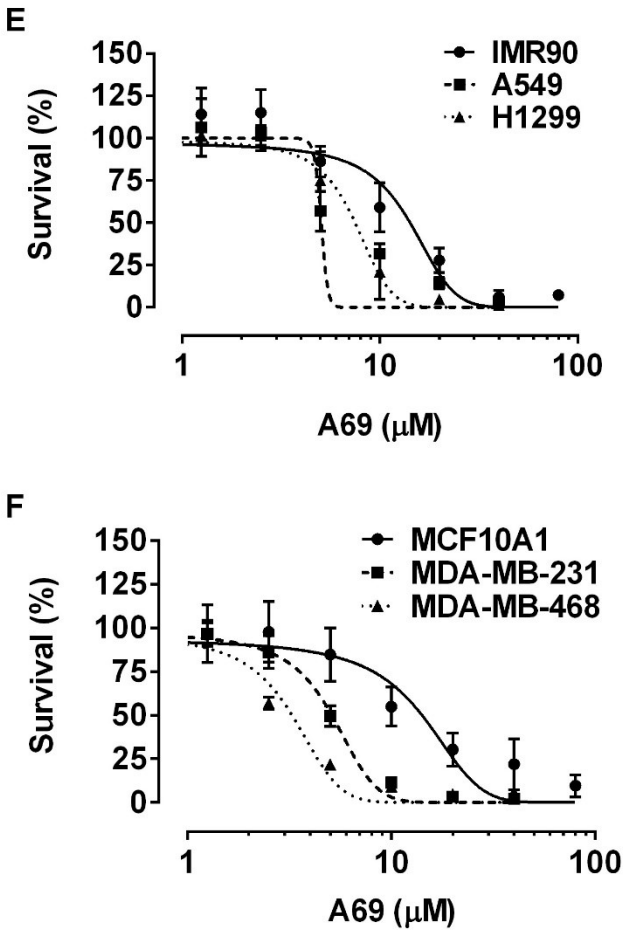

Figure 26. InS3-54 analogues inhibit cancer cell proliferation.

A variety of lung and breast cell lines were treated with the indicated concentrations of A18 (A-B), A26 (C-D) or A69 (E-F) for 72 hours followed by SRB assay. Cancer cell lines are more sensitive to inS3-54 analogues compared to normal cell lines.

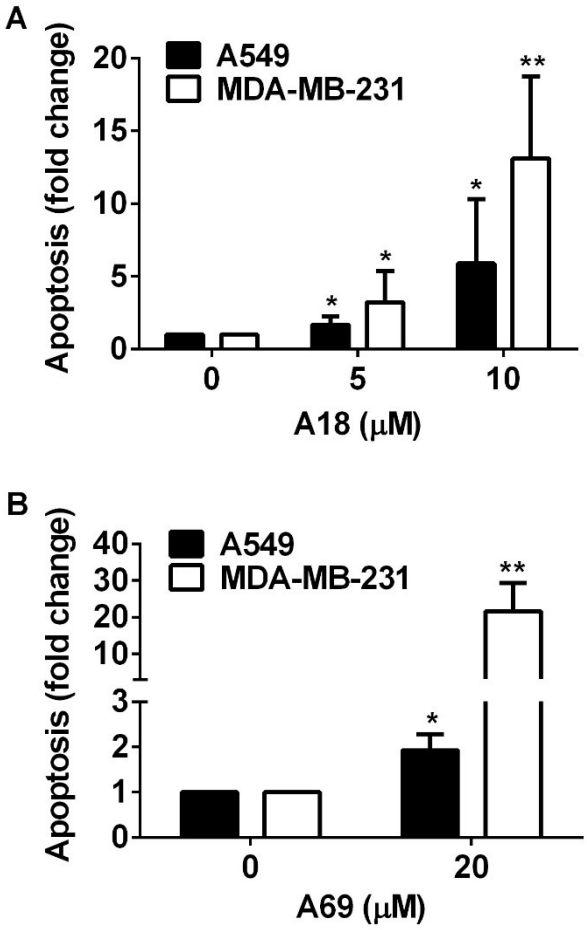

Figure 27. InS3-54 analogues induce apoptosis.

Exponentially growing A549 and MDA-MB-231 cells were treated with A18 (A) or A69 (B) for 72 hours followed by determination of apoptosis using ELISA. Apoptosis was induced after exposure to both compounds in A549 and MDA-MB-231 cells. (N=3; * $p<0.05$, ** $p<0.01$, by Student's t-test as compared with DMSO control)

E. Rationale for focusing on A18 in the following experiments

Although inS3-54 represents our first attempt to develop small molecule compounds targeting the DBD of STAT3, it may not be an ideal candidate compound for further development of specific STAT3 inhibitors due to low specificity for the DBD of STAT3 protein. Fortunately, all three active analogues (A18, A26 and A69) are likely specific to STAT3 protein as determined by *in vitro* colony formation assay using cells isolated from wild-type and $STAT3^{-/-}$ mice. Their effects on DNA-binding activity of STAT3 and cell survival are also more potent or comparable than inS3-54. Of four compounds, inS3-54, A26 and A69 have very poor solubility in available vehicles used for *in vivo* animal studies although they can be completely solubilized in DMSO for *in vitro* experiments, suggesting their limitation for *in vivo* efficacy test (**Table 7**). A pilot toxicity study found that A69 was toxic as low as 0.5 mg/Kg. Moreover, despite inS3-54 and A26 may be tolerant in mice up to 100 mg/Kg and 200 mg/Kg respectively, a pilot PK study indicated that the maximum plasma concentration of inS3-54 only achieved 445~456 ng/mL (equivalent to ~2 μM) by one-time dosing of inS3-54 in homemade or commercial formulations (**Table 8**). The plasma concentration of A26 was even undetectable when mice were administrated by intraperitoneal injection of 200 mg/Kg A26. However, A18 can be completely solubilized in a commercial oral dosing formulation up to 100 mg/mL, facilitating the following efficacy studies (**Table 7**). Combined with the data obtained from the above cellular assays, we decided to focus on A18 in the following studies.

Table 7. Observation of solubility of each compound in formulations commonly used for *in vivo* studies

Formulation	inS3-54	A18	A26	A69
4% ethanol:cremophor (1:1)	Partially dissolved, best in homemade formulations tested	Partially dissolved	Partially dissolved, best in homemade formulations tested	/
20% PEG 400	Not dissolved	Partially dissolved	Partially dissolved	/
50% PEG 400, 10% ethanol, 10% cremophor	Partially dissolved	Partially dissolved	Partially dissolved	/
20% PEG 400, 10% cremophor	Partially dissolved	Partially dissolved	Not dissolved	/
20% PEG400, 10% ethanol, 1% Tween-80	Partially dissolved	Partially dissolved	Not dissolved	/
15% DMSO	Not dissolved	Not dissolved	Not dissolved	/
Methylcellulose	Not dissolved	Not dissolved	Not dissolved	/
2-hydroxy-β-cyclodextrin	Partially dissolved	Partially dissolved	Partially dissolved	/
Hot Rod Chemistry Kit 1-Formulation 1 (HRC-K1-1)	Milk-like suspension	Milk-like suspension	/	Milk-like suspension
Hot Rod Chemistry Kit 1-Formulation 2 (HRC-K1-2)	Milk-like suspension	Milk-like suspension	/	Milk-like suspension
Hot Rod Chemistry Kit 1-Formulation 3 (HRC-K1-3)	Milk-like suspension	Milk-like suspension	/	Milk-like suspension
Hot Rod Chemistry Kit 1-Formulation 4 (HRC-K1-4)	Milk-like suspension	Milk-like suspension	/	Milk-like suspension
Hot Rod Chemistry Kit 1-Formulation 5 (HRC-K1-5)	Milk-like suspension	Milk-like suspension	/	Milk-like suspension
Hot Rod Chemistry Kit 1-Formulation 6 (HRC-K1-6)	Milk-like suspension	Milk-like suspension	/	Milk-like suspension
Hot Rod Chemistry Kit 1-Formulation 7 (HRC-K1-7)	Milk-like suspension, best in Kit 1	Milk-like suspension	/	Milk-like suspension, best in Kit 1

Hot Rod Chemistry Kit 1-Formulation 8 (HRC-K1-8)	Milk-like suspension	Milk-like suspension	/	Milk-like suspension
Hot Rod Chemistry Kit 2-Formulation 1 (HRC-K2-1)	Partially dissolved	Completely dissolved up to 100 mg/mL	Partially dissolved	/
Hot Rod Chemistry Kit 2-Formulation 2 (HRC-K2-2)	Partially dissolved	Partially dissolved	Partially dissolved	/
Hot Rod Chemistry Kit 2-Formulation 3 (HRC-K2-3)	Partially dissolved	Partially dissolved	Partially dissolved	/
Hot Rod Chemistry Kit 2-Formulation 4 (HRC-K2-4)	Partially dissolved	Partially dissolved	Partially dissolved	/
Hot Rod Chemistry Kit 2-Formulation 5 (HRC-K2-5)	Partially dissolved	Partially dissolved	Partially dissolved	/
Hot Rod Chemistry Kit 2-Formulation 6 (HRC-K2-6)	Partially dissolved	Partially dissolved	Partially dissolved	/
Hot Rod Chemistry Kit 2-Formulation 7 (HRC-K2-7)	Partially dissolved	Partially dissolved	Partially dissolved	/
Hot Rod Chemistry Kit 2-Formulation 8 (HRC-K2-8)	Partially dissolved	Partially dissolved	Partially dissolved	/

Table 8. Toxicity and PK characteristics of inS3-54 and its analogues

Compound	Formulation	Route of administration	Tolerance	Maximum plasma concentration
inS3-54	Hot Rod Chemistry Kit 1-Formulation 7 (HRC-K1-7)	i.p.	Up to 100 mg/Kg	445 ng/mL*
	4% ethanol:cremophor (1:1)	i.p.	Up to 100 mg/Kg	456 ng/mL*
A18	Hot Rod Chemistry Kit 2-Formulation 1 (HRC-K2-1)	p.o.	Up to 200 mg/Kg	/
A26	4% ethanol:cremophor (1:1)	p.o.	Up to 200 mg/Kg	Undetectable
A69	Hot Rod Chemistry Kit 1-Formulation 7 (HRC-K1-7)	i.p.	Lower than 0.5 mg/Kg	/

* Equivalent to ~2 μM calculated on ~2 mL of total blood volume in mice.

F. A18 inhibits cancer cell migration and invasion.

Our previous study has suggested that the parental compound inS3-54 inhibits cancer cell migration and invasion by down-regulating the expression of STAT3 downstream targets. To assess the effects of A18 on cancer cell migration and invasion, wound-filling assay was first performed in A549 and MDA-MB-231 cells following the treatment with 0.1% DMSO, 5 and 10 μM A18 for 24 hours. **Figure 28** shows that A18 inhibited migration of both A549 and MDA-MB-231 cells in a dose- and time-dependent manner. At 24 hours, 71% and 99% of wound were filled in absence of A18 in A549 and MDA-MB-231 cells, respectively; whereas 64% and 76% of wound were filled following 5 μM A18 treatment in both cell lines, respectively. Moreover, the wounds were only covered 47% and 39% respectively after both cell lines were exposed to 10 μM A18.

Cell invasion was determined using Matrigel invasion assay after A549 or MDA-MB-231 cells were exposed to 0.1% DMSO, 5 and 10 μM A18 for 6 or 24 hours. As shown in **Figure 29**, 5 μM A18 inhibited 66% and 51% of invasion at 6 hours in A549 and MDA-MB-231 cells, respectively, as compared to the vehicle control. After 24-hour treatment, the cell invasion was reduced to 60% and 36% in both cell lines, respectively. 10 μM A18 suppressed cell invasion to 35% and 13% at 6 hours in both cell lines, respectively, compared to DMSO control, while the cell invasion only achieved 25% and 11% after 24 hours. Significant difference ($p<0.05$) between A18 and DMSO vehicle was evident by 6 hours in A549 and MDA-MB-231 cells.

Similar to inS3-54, although 100% confluent cells and relative short incubation time were applied to the above assays, A18 inhibition of proliferation may still contribute to the above observed outcome. To eliminate this possibility, we analyzed cell proliferation and apoptosis under the same condition as wound filling and Matrigel invasion assays with confluent cultures. **Figure 30** showed that treatment with 5 and 10 μM A18 for 6 or 24 hours had no significant effect on proliferation and apoptosis of confluent A549. Although total cell number decreased following the treatment with 10 μM A18 for 24 hours in MDA-MB-231 cells, the fold change remained at only 20% and cell migration and cell invasion were significantly reduced under this condition (**Figure 28-29**). Thus, it is concluded that A18 inhibition of migration and invasion is unlikely due to its effect on apoptosis and cell proliferation and A18 can inhibit migration and invasion of lung and breast carcinoma cells.

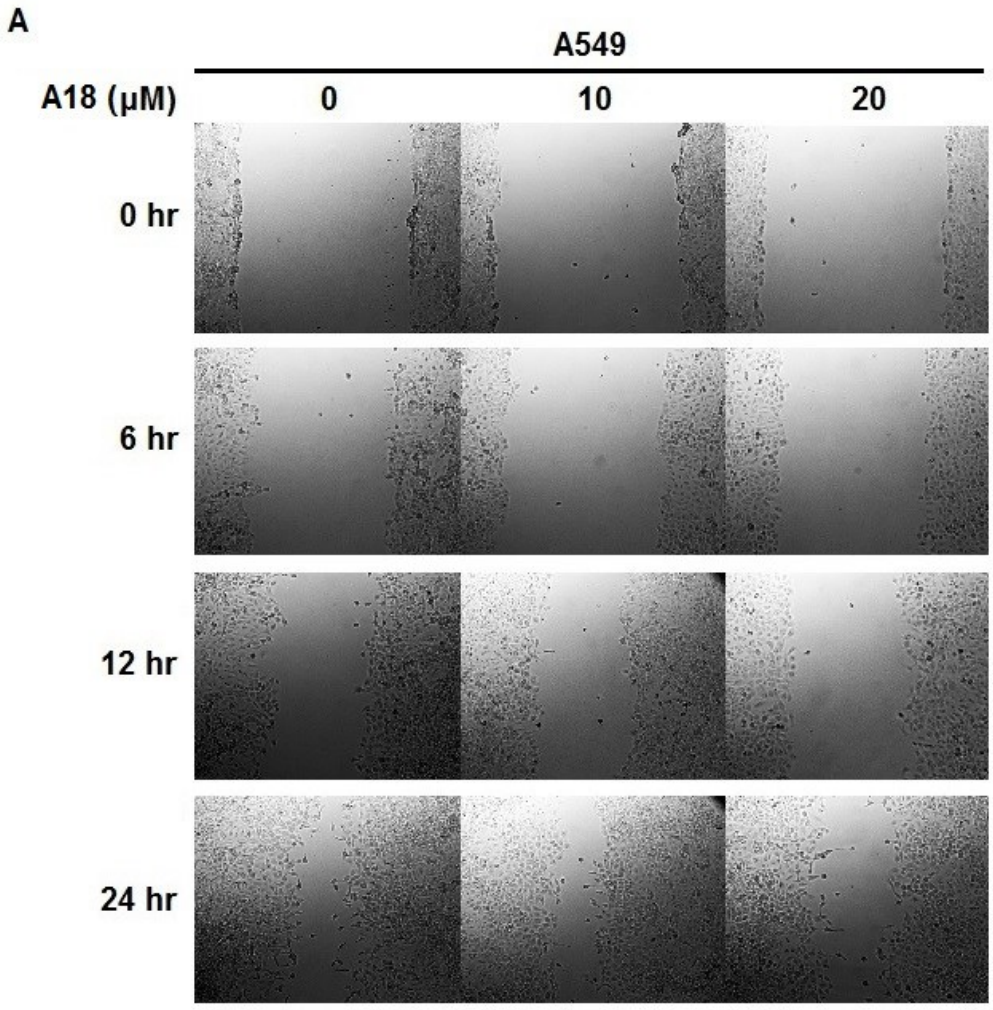

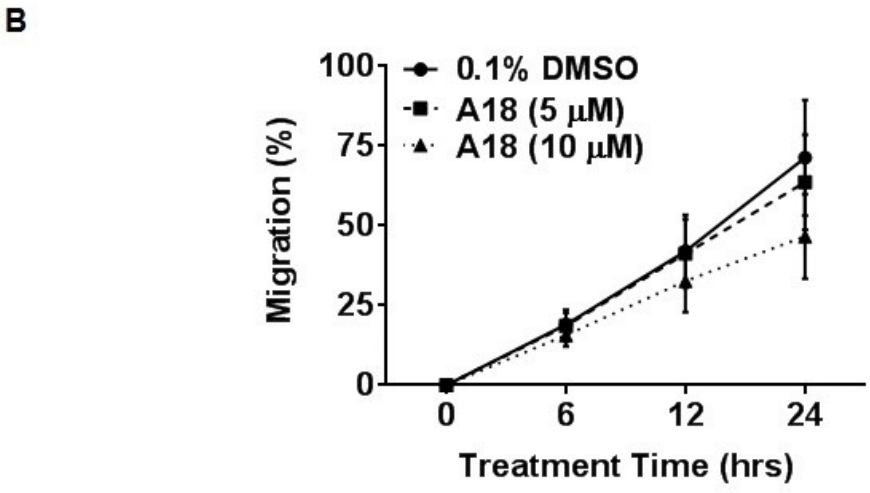

Figure 28. (Continued)

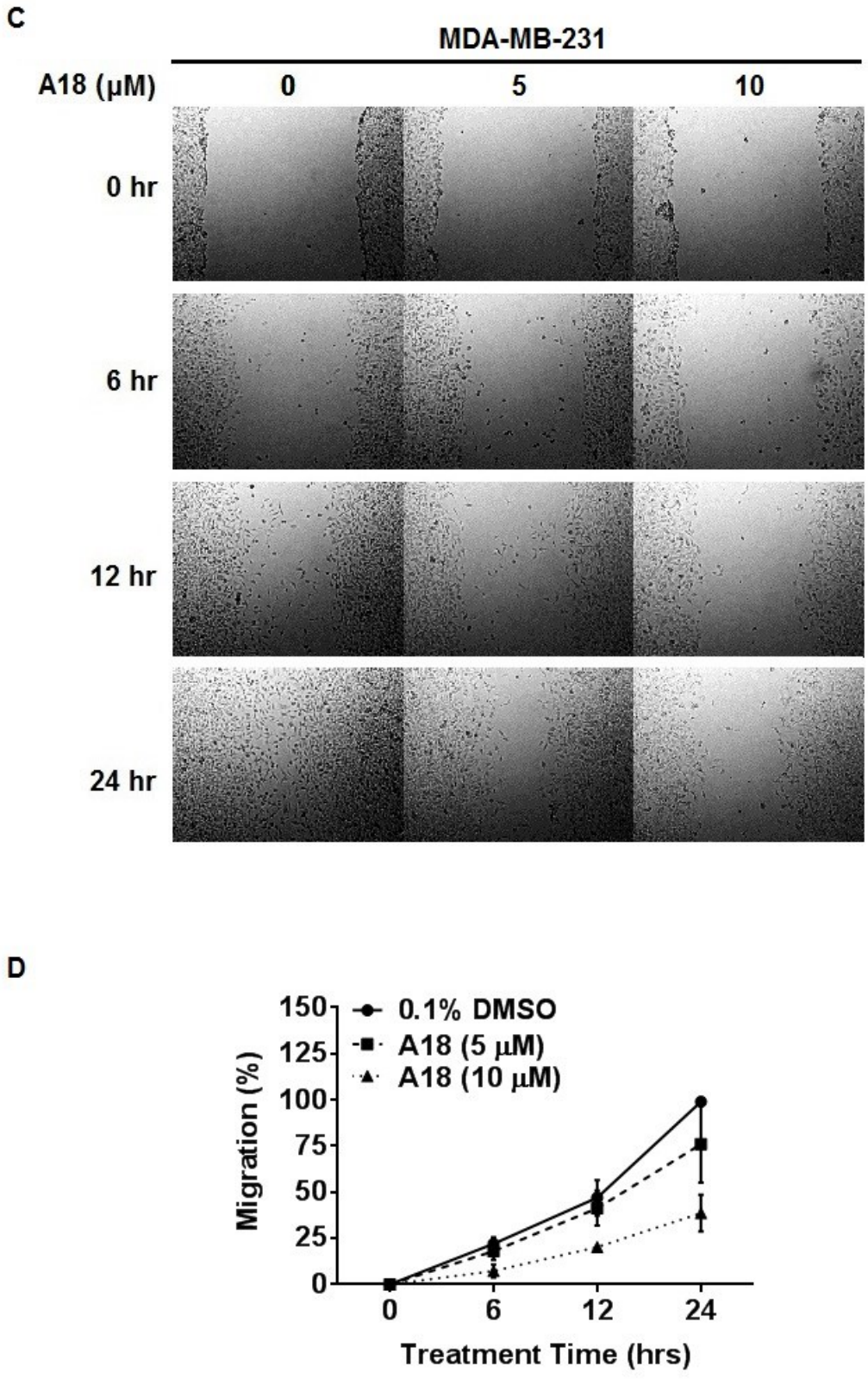

Figure 28. (Legend on next page)

Figure 28. A18 inhibits cancer cell migration.

Migration of A549 (A-B) and MDA-MB-231 (C-D) cells was assessed by wound filling assay in the presence of 0.1% DMSO or A18 for 24 hours. Quantification analyses of wound filling assay were derived from three independent experiments as shown in Panel B and D. Cell migration was reduced following A18 treatment in both cell lines.

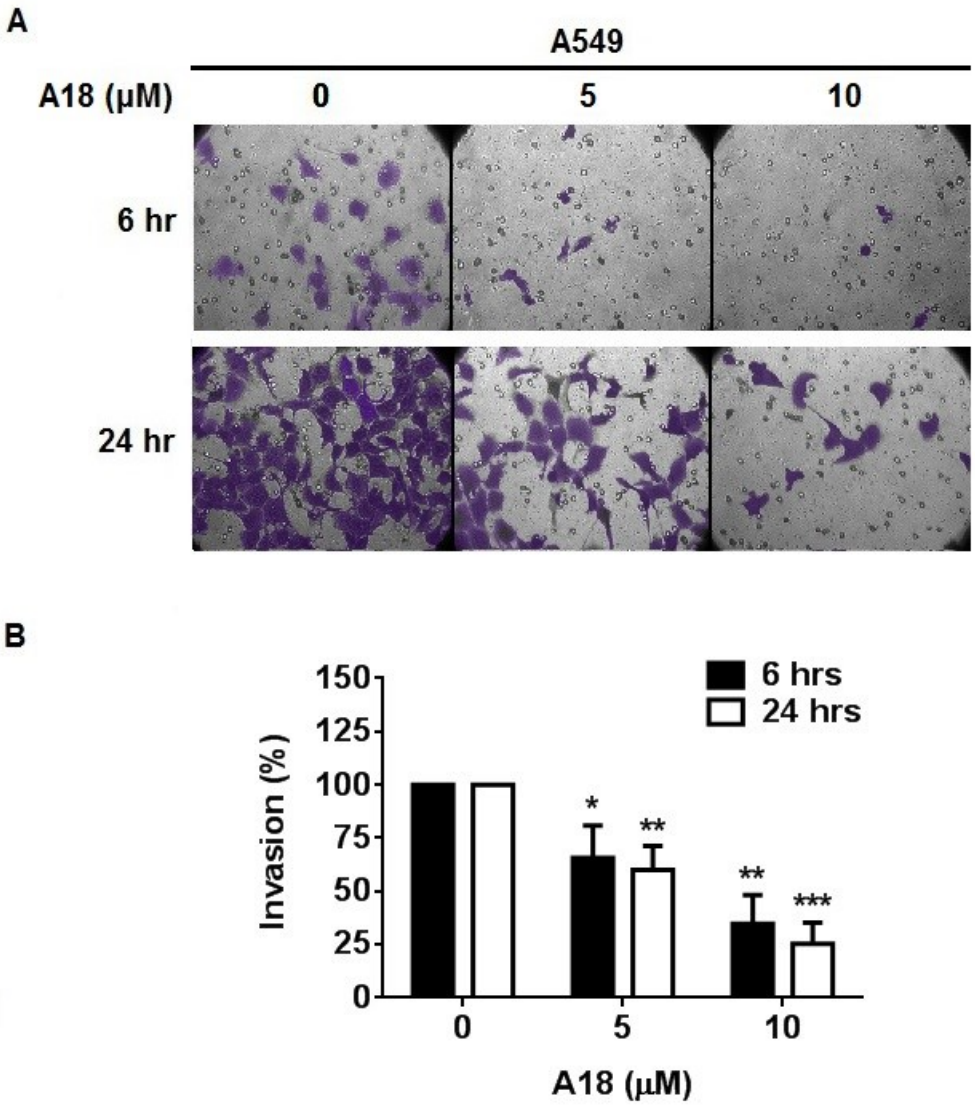

Figure 29. (Continued)

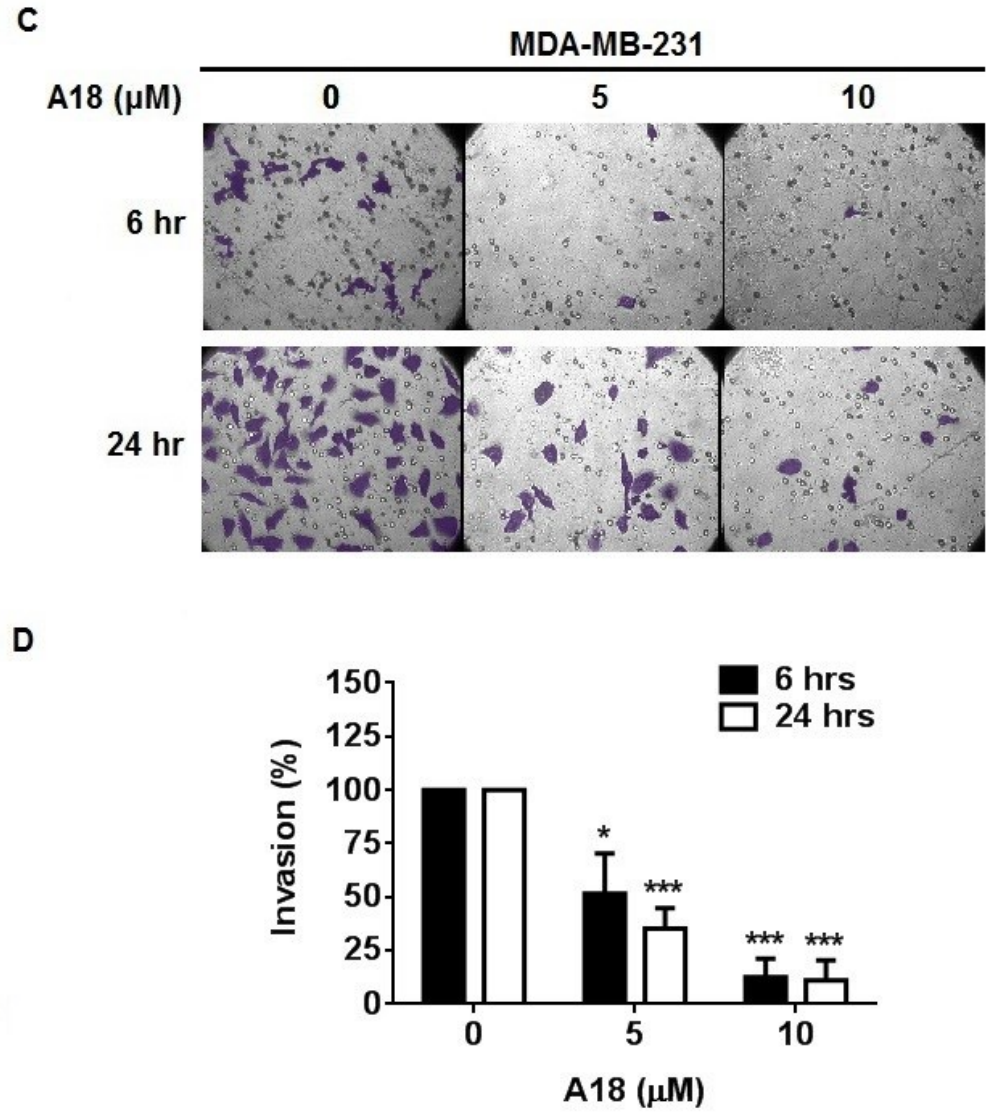

Figure 29. A18 inhibits cancer cell invasion.

The invasion of A549 (A-B) and MDA-MB-231 (C-D) cells were determined in the presence of DMSO (0.1%), 5 or 10 μM A18 for 6 or 24 hours using Matrigel invasion assay with 10% FBS in the bottom chamber as a chemoattractant. As shown in Panel B and D, quantification of invasion came from measurement of 10 random views each of three independent experiments. Cell invasion was suppressed after exposure to A18 in both cell lines. (N=3; * p<0.05, ** p<0.01, *** p<0.001, by Student's t-test as compared with DMSO vehicle control)

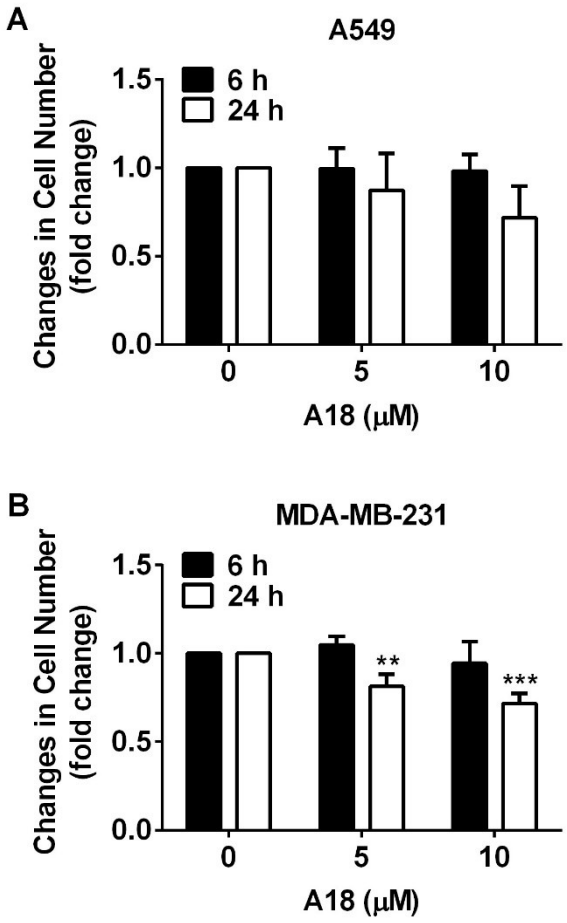

Figure 30. (Continued)

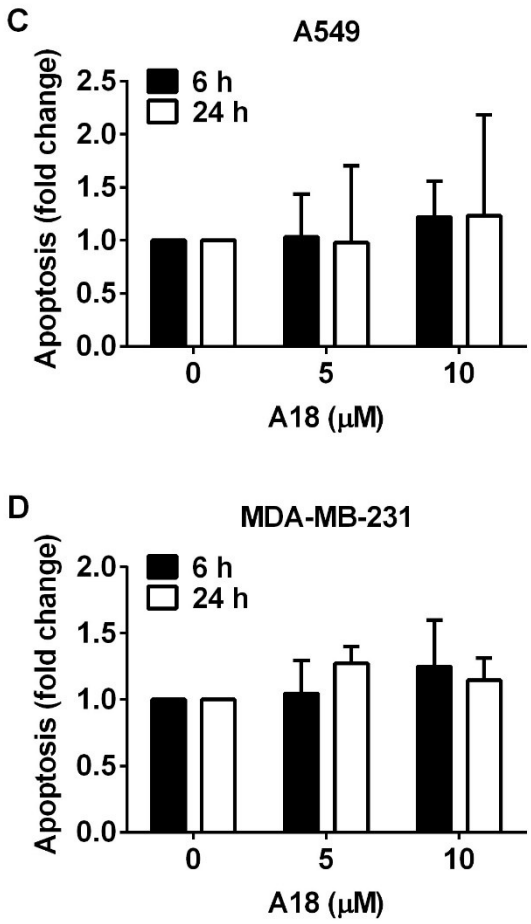

Figure 30. Effects of A18 on cell growth and apoptosis of confluent cells.

100% confluent A549 (A and C) and MDA-MB-231 (B and D) cells were treated with DMSO (0.1%), 5 or 10 μM A18 for 6 or 24 hours followed by determination of change in cell number for proliferation (A-B) or ELISA for apoptosis (C-D). In addition to 10 μM treatment in MDA-MB-231 cells for 24 hours, A18 had no effect on the growth and apoptosis of confluent cells. (N=3; ** p<0.01, ** p<0.001, by Student's t-test as compared with DMSO vehicle control)

G. A18 inhibits the expression of STAT3 downstream target genes and STAT3 binding to its endogenous target sequences.

To investigate the potential effect of A18 on STAT3 downstream targets and thereby verify its inhibitory effect on STAT3 in cells, we further examined the expression level of known STAT3 downstream targets by using Western blot and real-time PCR analyses following A18 treatment in A549 and MDA-MB-231 cells. As shown in **Figure 31A-C**, the expression of cyclin D1, survivin, MMP-9 and VEGF were all decreased in the presence of A18 in both cell lines whereas the levels of phospho-STAT3 (Tyr705) and total STAT3 were not affected. Selected genes were also confirmed by real-time PCR in both cell lines (**Figure 31D-E**).

In addition to constitutively activated STAT3, we also determined whether or not A18 is capable of inhibiting cytokine-induced STAT3 phosphorylation. After starved A549 cells were pre-treated with DMSO control (0.1%) or 10 μM A18 followed by IL-6 stimulation, phospho-STAT3 (Tyr705) expression was not changed obviously with or without A18 pretreatment. One of STAT3 target genes, survivin, was elevated by 14 folds in IL-6 treated cells pre-treated with DMSO, whereas IL-6 induced survivin expression was also abrogated by 41% following A18 treatment (**Figure 32**). The results indicate that A18, which is designed to target the STAT3 DBD, may not affect the expression or activation of constitutive STAT3 or IL-6-induced STAT3 but represses the expression of STAT3 target genes.

To further demonstrate that A18 inhibits the DNA-binding activity of STAT3 in cells, A549 and MDA-MB-231 cells were exposed to DMSO (0.1%), 5 or 10 μM

A18 followed by fractionation of cytosol, soluble nuclear fraction and chromatin-bound proteins. The STAT3 levels in these fractions were investigated by Western blot analysis. As shown in **Figure 33**, the chromatin-bound STAT3 decreased while the STAT3 level in soluble nuclear fraction increased with the increasing concentrations of A18. This result was also verified by determination of STAT3 binding to the promoter regions of two STAT3 downstream targets (cyclin D1 and twist) using ChIP assay. Data indicate that A18 effectively inhibits the binding of STAT3 to its endogenous target sequences on genomic DNA *in situ* (**Figure 34**). Taken together with the results shown above, we conclude that A18 specifically inhibits STAT3 activity in binding to endogenous promoters on genomic DNA, resulting in reduced transcription of its downstream target genes.

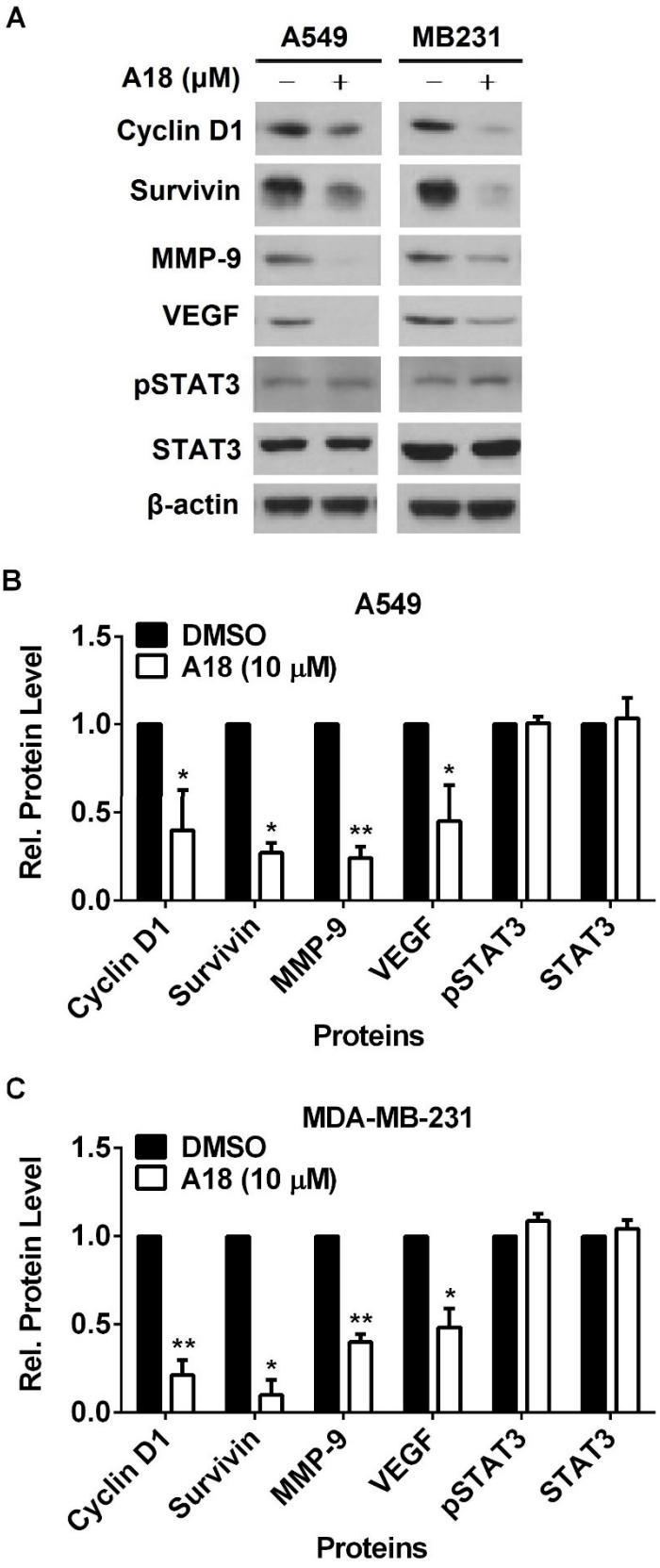

Figure 31. (Continued)

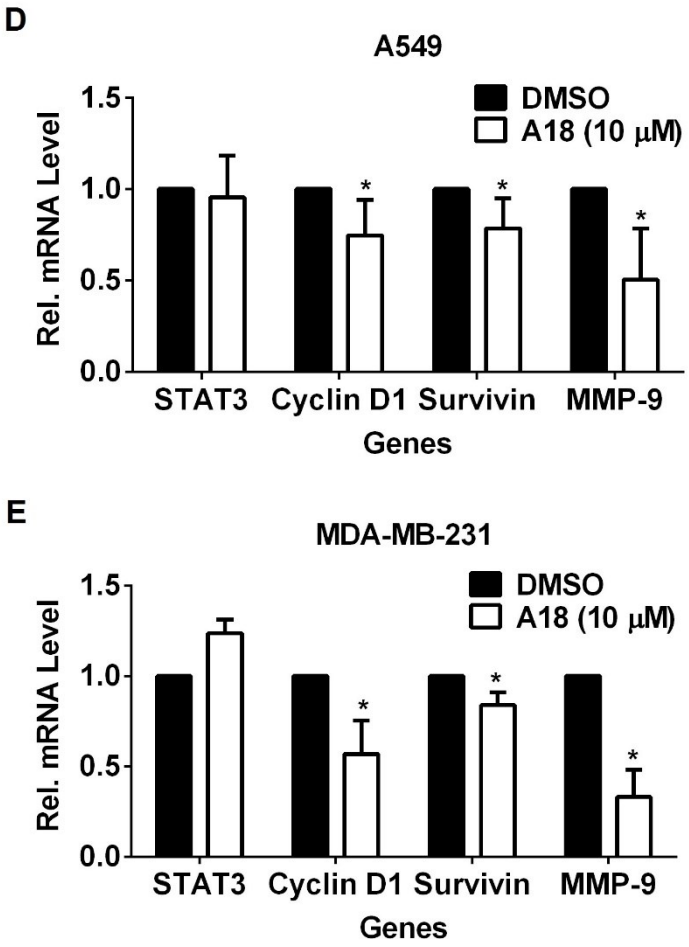

Figure 31. A18 inhibits the expression of STAT3 downstream target genes.

(A-C) A549 and MDA-MB-231 cells were exposed to DMSO (0.1%) or 10 μM A18 followed by lysate preparation and Western blot analysis with antibodies indicated. β-actin was used as a loading control. Panel B and C shows the quantitative data of each protein measured by the density of Western blot bands and normalized against the β-actin internal control. (N=3; * p<0.05, ** p<0.01, by Student's t-test as compared with DMSO vehicle control) (D-E) A549 and MDA-MB-231 cells were treated with DMSO (0.1%) or 10 μM A18 followed by total RNA extraction and real-time PCR analysis. Data show the relative mRNA levels normalized to the internal control, GAPDH. (N=4; * p<0.05, by Student's t-test as compared with DMSO

vehicle control) All results suggest that A18 inhibited the protein and mRNA levels of STAT3 downstream targets in both cells lines.

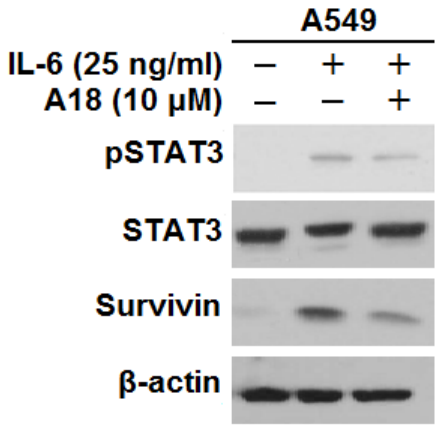

Figure 32. A18 does not affect IL-6 induced STAT3 phosphorylation.

A549 cells were cultured in serum-free medium for 2 days and then pre-treated with 10 μM A18 for 12 hours followed by 25 ng/mL of IL-6 for 30 minutes. After treatment, the expression levels of phospho-STAT3, STAT3 and survivin were examined by Western blot analysis. A18 had no effect on IL-6-induced activation of STAT3. However, IL-6 stimulated survivin was reduced by 41% following A18 treatment.

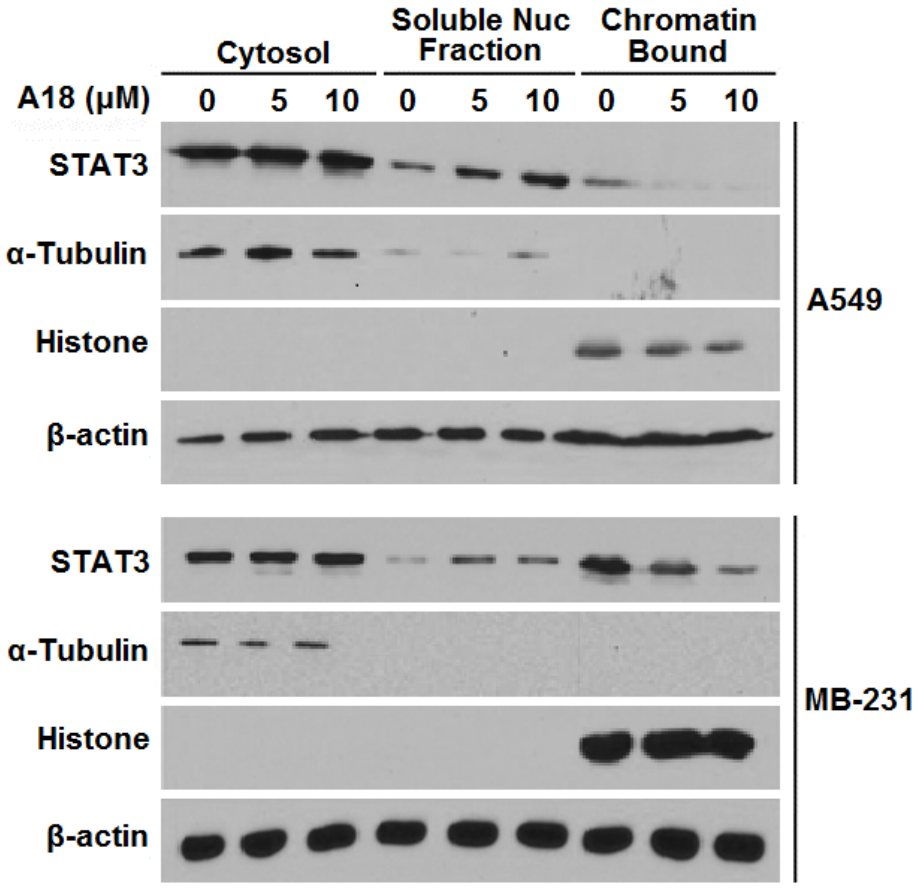

Figure 33. A18 inhibits STAT3 binding to chromatin.

A549 and MDA-MB-231 cells were treated with DMSO (0.1%), 5 or 10 μM A18 for 72 hours followed by fractionation of cytosol, soluble nuclear fraction, and chromatin-bound proteins and Western blot analysis of STAT3 in these fractions. A18 blocked the binding of STAT3 to genomic DNA.

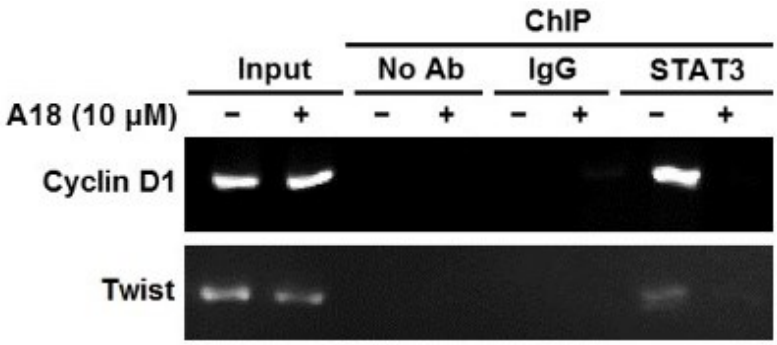

Figure 34. A18 inhibits the binding of STAT3 to the promoter regions of responsive genes.

H1299 cells were treated with 0.1% DMSO or 10 μM A18 for 24 hours followed by ChIP assay and agarose gel electrophoresis. No antibody and IgG were used as background negative control. A18 suppressed the binding of STAT3 to the promoter regions of cyclin D1 and twist.

H. A18 inhibits tumor growth *in vivo*.

A mouse xenograft model of human lung cancer was used to investigate the *in vivo* efficacy of A18. Mice were treated with vehicle or A18 every other day for 30 days and tumor volume was measured overtime by caliper. On day 35 post-implantation, the mice were euthanized and the tumor tissues were harvested, weighed, and processed for immunohistochemistry analyses. One mouse in each group (vehicle and A18) was found dead during drug administration and thus excluded from data analyses. Due to variation in mice, outlier data were also rejected by Dixon's Q test at 95% confidence. Following oral dosing of 200 mg/Kg A18, the tumor volume in the A18-treated group reduced to 237.1 mm^3 whereas that in the vehicle-treated group achieved 438.2 mm^3 (**Figure 35A**). The tumor weight of A18-treated group (0.239±0.076 g) was also lower than that of vehicle control group (0.561±0.266 g) with p=0.53. However, the body weight had no significant difference between both groups during drug administration (**Figure 35B**). Furthermore, necropsy found that no obvious abnormality was visible in the heart, lungs, kidneys, liver and spleen. The weight of each organ also showed no statistically significant difference although the liver weight of A18-treated group is slightly lower than that of vehicle control group (**Figure 35C**). H&E staining and histology evaluation showed that 3 of 5 mice in the vehicle control group developed secondary tumors in lung tissues with extension into the peripancreatic adipose tissues and the adjacent peripancreatic lymph nodes while none of A18-treated mice showed tumor metastasis in lungs (**Figure 36**).

Furthermore, expression of STAT3, survivin and VEGF in the xenograft tumors was determined by immunohistochemistry staining. As shown in **Figure 37**, total STAT3 showed no difference in tissues obtained from both vehicle control group and A18-treated group. Importantly, two STAT3 downstream targets, survivin and VEGF showed decreased staining in A18-treated tumors. Given that A18 was found to inhibit STAT3-depedent gene expression by blocking the binding of STAT3 to the promoter regions of downstream genes whereas the total STAT3 level was not affected following A18 treatment as demonstrated by a variety of cellular assays, these results may also indicate the *in vivo* inhibition of A18 on the expression of STAT3 downstream genes. Taken together, these data suggest the potential value of A18 for development of specific STAT3 inhibitor as a novel anti-neoplastic drug.

Although the pilot study is usually designed based on experience or guess work, the results of the pilot study can also be used to determine the minimal sample size in the future animal studies. The sample size required in each group for further studies was finally estimated as described previously (126). While comparing the means μ_1 and μ_2 from two independent groups, it is assumed to follow normal distribution, homogeneous variances, equal sample sizes and a two-sided test. The false positive rate is set to α, and the power to detecting a difference $\Delta = |\mu_1 - \mu_2|$ is set to $1-\beta$, where β is the false negative rate. Defining α=0.05 and β=0.20, the sample size required in each group (n) is:

$$n = \frac{2\,(Z_{\alpha/2} + Z_{1-\beta})^2}{(\frac{\Delta}{\sigma})^2}$$

where the constant $Z_{\alpha/2}$ represents the desired level of statistical significance (typically 1.96 for 0.05 significance), the constant $Z_{1-\beta}$ represents the desired power (typically 0.84 for 80% power), $\sigma = \sqrt{\frac{\sigma_1^2 + \sigma_2^2}{2}}$, representing the standard deviation of the outcome variable, and $\Delta = |\mu_1 - \mu_2|$, representing the effect size (the difference in means).

Based on the pilot study, μ_1=0.561 g, μ_2=0.239 g, σ_1=0.266 g, σ_2=0.076 g, thus

$$n = \frac{2\times(1.96 + 0.84)^2}{(\frac{0.561-0.239}{0.196})^2} = 5.80$$

Considering 10% drop-out rate, n = 5.80 × 110% = 6.39 ≈ 7.

Therefore, the minimal 7 mice per group shall be used in the following studies, giving 80% power at the 0.05 level of significance.

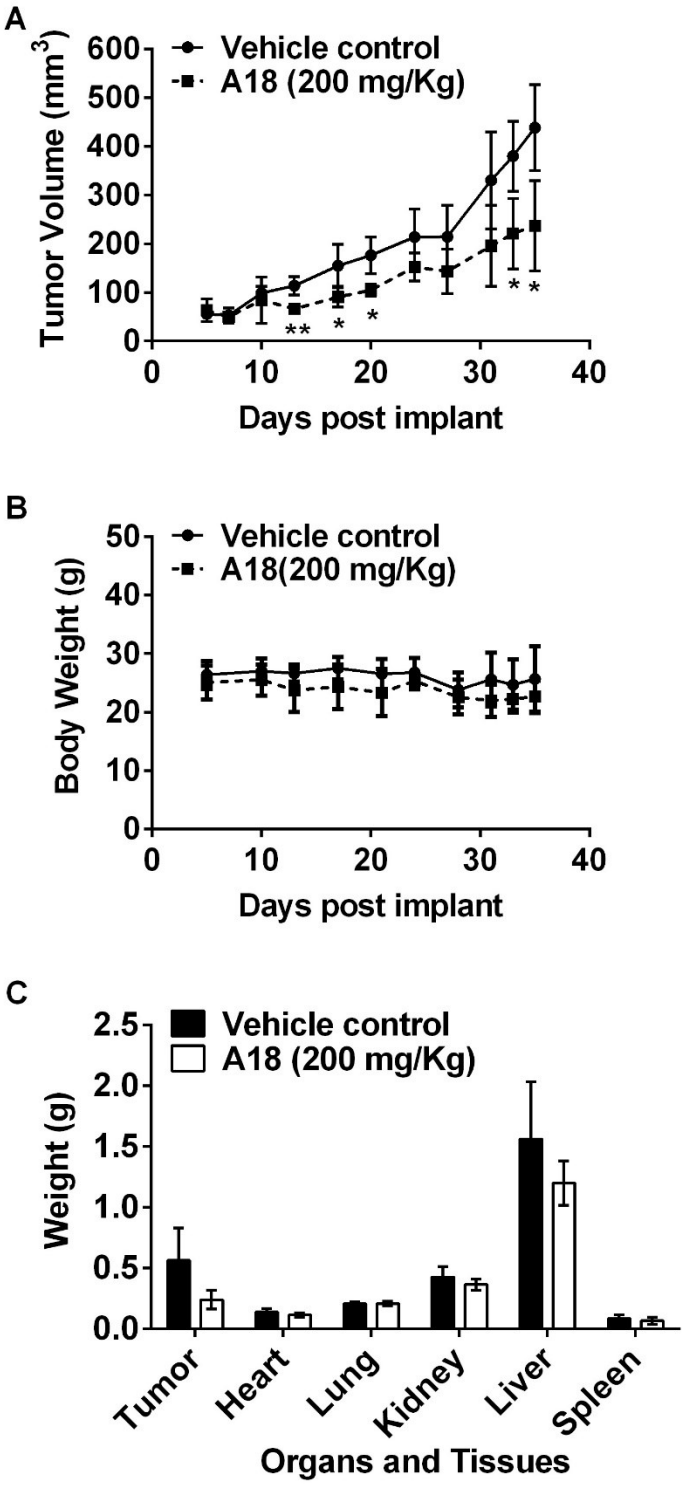

Figure 35. (Legend on next page)

Figure 35. A18 reduces tumor growth *in vivo*.

Six mice in each group were administrated with oral dosing of vehicle control or 200 mg/Kg A18 every other day. Tumor volume and body weight were recorded twice per week during drug treatment. The tumor weight was measured on the 35th day post-implantation. Outliers (one mice in each group) were rejected by Dixon's Q test at 95% confidence. A18 reduced tumor growth with little effect on body weight or indicated organs. (N=4; * p<0.05, by Student's t-test as compared with vehicle control)

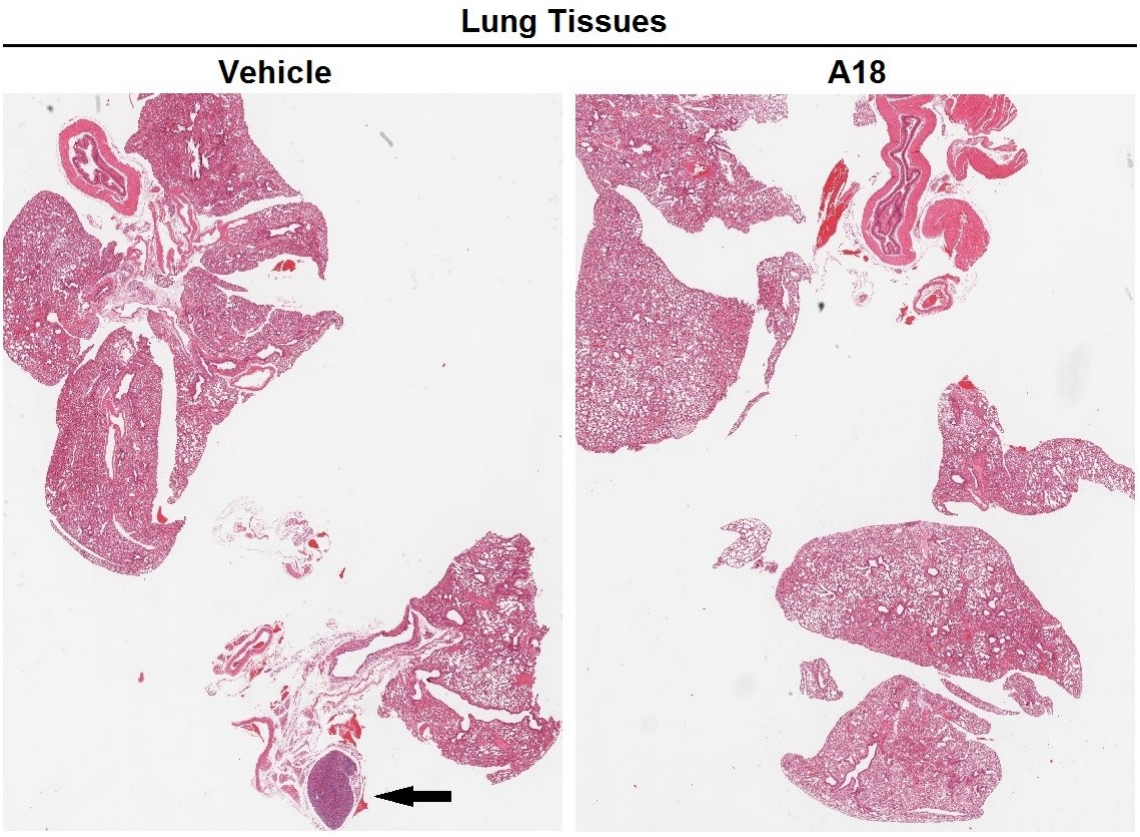

Figure 36. A18 reduces lung metastases in a mouse xenograft model of lung cancer.

A549 cells were implanted in the flanks of 12 NOD/SCID mice. 30 days after drug administration, lung tissues were harvested and prepared for paraffin-embedded tissue sections, followed by H&E staining. H&E-stained paraffin sections of lung tissues obtained from vehicle control group and A18-treated group were finally evaluated by an experienced pathologist. Arrow indicates a solitary tumor developed in the lung tissue of a vehicle control mice.

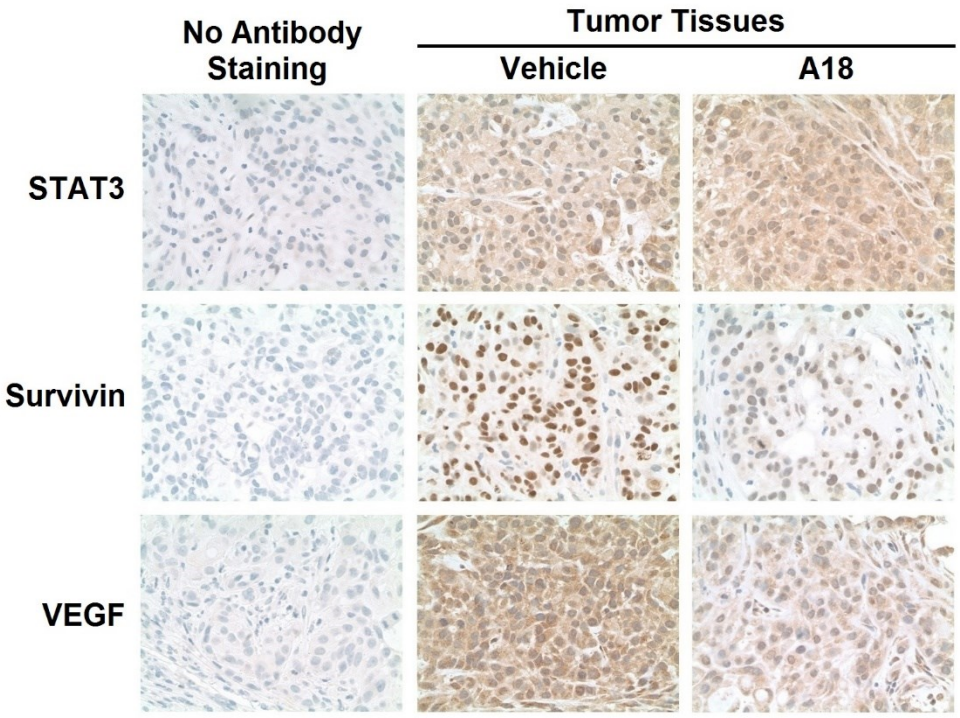

Figure 37. A18 reduces the expression of STAT3 downstream targets *in vivo*. A549 cells were implanted in the flanks of 12 NOD/SCID mice. 30 days after drug administration, tumor tissues were harvested and prepared for paraffin-embedded tissue sections, followed by immunohistochemistry staining. A18-treated groups showed decreased expression of surviving and VEGF. Total STAT3 showed no difference in both groups of mice.

IV. Discussion

A. Contribution of the present study

The present study demonstrates the feasibility of computational screening approach to identify potential small molecule inhibitors that target the DBD of STAT3. Of a total of about 200,000 virtual compounds, inS3-54 showed remarkable inhibition on STAT3-dependent luciferase reporter activity, DNA-binding activity of STAT3, cancer cell survival, cell migration and invasion as well as STAT3-mediated gene expression. By directly binding to STAT3, inS3-54 prevented the binding of STAT3 to the promoter regions of responsive genes, thereby resulting in down-regulation of expression of STAT3-dependent genes such as cyclin D1 and twist. Furthermore, inS3-54 did not affect STAT3 dimerization or the constitutive/IL-induced activation of STAT3. Subsequently, the analogues of inS3-54 were also developed to investigate the structure-activity relationship. Of 89 analogues, A18, A26 and A69 showed more potent or comparable effects on persistent STAT3 signaling. In particular, the three active analogues were more selective to STAT3 protein than inS3-54 as demonstrated by *in vitro* colony formation assay using cells isolated from $STAT3^{+/+}$ and $STAT3^{-/-}$ mice. We further investigated the molecular mechanism of A18 because of its acceptable solubility for animal studies and then verified its inhibitory effects on DNA-binding activity of STAT3 in cells. Importantly, A18 reduced tumor growth in a mouse xenograft model of lung cancer and had little effects on body weight with no abnormality on heart, lungs, kidneys, liver and spleen. Collectively, these data provide compelling evidence that A18 represents a potential lead compound for

further development to inhibit the constitutively activated STAT3 signaling by targeting the DBD of STAT3.

B. Challenges to target STAT3

Irregular transcription factor activity leads to profound and sustained phenotypic effects in cells by altering the gene expression, thereby making this class of proteins highly desirable targets for therapy. An increased knowledge of the transcription mechanisms and the transcriptional regulatory networks has led to a better understanding of their critical roles in cancers. Generally, strategies for targeting transcription factors include inhibiting their functional domains and inhibiting the post-translational modifications that modulate their function. However, successfully blocking the activity of transcription factors remains challenging. The protein-protein interactions or the protein-DNA interfaces usually have large or flat surface area of the target, thereby providing insufficient cavities to develop small molecule antagonists with high affinity. The complexity of the interactions involving multi-point contact over large surfaces leads to difficulties to design small molecular inhibitors. It is very likely to require a large molecule to block the entire surface, leading to the poor membrane permeability and the consequential low biological activity in cells. Furthermore, a transcription factor which binds to negatively charged DNA may tend to be positively charged. A molecule targeting a transcription factor thus needs to be negatively charged, causing the potential poor membrane permeability. Despite these obstacles, a few of these efforts towards targeting transcription factors have been reported, including targeting

nuclear factor-κb (NF-κb), p53, Notch, Nrf2, *etc* (127-129). Approximately 10% of currently prescribed drugs directly target the nuclear receptor class of transcription factors such as tamoxifen and bicalutamide (130). Although no inhibitors targeting transcription factors outside the nuclear receptor family has been approved, clinical trials targeting p53 or NF-κb are currently performed for several types of cancer (127-129).

STAT3 is a well-known oncogenic protein which acts as a transcription activator in cells. Obviously, the intense development of STAT3 inhibitors never ceases. A large number of STAT3 inhibitors obtained from peptidomimetic design, high-throughput screening, fragment-based drug design and structure-based virtual screening, reflecting a significant research area (56, 61, 62). The majority of STAT3 inhibitors are directed at the SH2 domain, which is important for receptor recognition and dimerization of STAT3 by reciprocal binding to Tyr705 (69-81). However, most inhibitors targeting SH2 domain are still not close to clinical application due to their moderate cellular activity. One of the important issues may be attributed to the protein-protein interaction as a targeting site. Since the classic phosphotyrosine residue-SH2 domain interface is located at Lys591, Arg609, Ser611 and Ser613 via direct interaction, most SH2 inhibitors usually target these critical residues (36). However, structural similarity with other proteins may be also challenging for development of specific inhibitors. SH2 domain of STAT3 is a highly conserved region which has a high sequence similarity to other proteins including Src, phospholipase C-γ, phosphatidylinositol 3-kinase and other STATs (131, 132). Moreover, STAT1 and STAT3 share extensive structural homology and their

crystal structures are virtually superimposable, however, they appear to play opposite roles in tumorigenesis (119). STAT3 inhibitors thus have to be assessed for the selectivity on STAT3 over STAT1. And the specificity of inhibitors is a key issue that must be clearly addressed. In addition, it has been recently found that unphosphorylated STAT3 can bind to specific enhancer sequences and thereby contribute to gene expression (82-85). Unphosphorylated STAT3 may have a mechanism distinct from phospho-STAT3. For example, it was found to activate NF-κb-regulated genes by directly binding to unphosphorylated NF-κb via its SH2 domain (84). Although more studies are needed to investigate the detailed mechanism and the potential interaction with other proteins, we may speculate that the disruption of protein-protein interactions may be complicated and thus challenging. Therefore, disrupting the dimerization of STAT3 molecules alone may not be enough to completely inhibit aberrant STAT3 activity in cancer cells.

On the other hand, DBD has gotten far less attention to date than the dimerization disruption. As mentioned above, many DNA-binding proteins such as transcription factors are considered undruggable because their active DNA-binding sites are too shallow or too similar to permit specific and tight binding of small molecules to their DBDs. Nevertheless, the inhibition of the DNA-binding activity of STAT3 for drug discovery has been tested. In particular, the Phase 0 clinical trial of STAT3 decoy ODN has been recently reported to demonstrate the feasibility of blocking DNA binding of STAT3 in humans (99). The main limitation of decoy ODNs remains their pharmaceutical properties due to the nature of these biological agents. Some compounds are presumed to inhibit aberrant STAT3

signaling by blocking the protein-DNA interaction, however, a few successful strategic plans directed at this site have been reported. Either the exact modes of inhibition of STAT3 remain unclear or the compounds may interact with other proteins or affect other signaling pathways (86-93). More efforts to develop effective and selective STAT3 inhibitors may achieve success to develop the clinically appropriate drugs.

C. Targeting of inS3-54 and its analogues to STAT3

Specificity is one of the critical challenges to develop an ideal STAT3 inhibitor which targets STAT3 protein without affecting other proteins such as upstream molecules or other STAT members. In this study, we made a great effort to develop a small molecule STAT3 inhibitor with good efficacy and specificity. Screening of large chemical libraries is expected to acquire compounds with drug-like, assay-compatible and toxicity-free properties. In the process of virtual screening, the initial hit, inS3-54, was originally identified by virtual compound screening and STAT3-dependent luciferase reporter assay to bind to the DBD of STAT3. To ensure the membrane permeability in cells, the small molecule compounds that contain phosphate groups mimicking phosphates in DNA were eliminated. We also docked the potential candidate compounds onto the DBD of STAT1 to eliminate any compounds that may bind to STAT1. Subsequently, 100 potentially specific candidates were selected for *in vitro* screening using STAT3-dependent luciferase reporter assay. After the initial hit inS3-54 and its analogues (A18, A26 and A69) were identified, these compound were also tested by STAT3-

independent luciferase reporter assay. The finding that inS3-54 and three analogues did not inhibit the promoter activity of p27 indicates that these compounds may not exhibit the inhibition of luciferase reporter due to non-specific effects on the expression or activity of reporter gene.

A series of experiments were then performed to verify whether or not inS3-54 and its analogues target STAT3 specifically. First of all, *in-silico* analysis shows that inS3-54 binds to the residues Met331, Val343, Met420, Ile467 and Met470 of STAT3 via hydrophobic interaction with the aid of Lys340 and Asn466 to stabilize the carboxyl group of inS3-54 by favorable electrostatic interaction. Meanwhile, inS3-54 could not bind to STAT1 due to physical hindrance from residue Pro326 and Thr327, leading to a much lower affinity to STAT1. Moreover, EMSA demonstrates that inS3-54 and three analogues appear to be selective to STAT3 over STAT1. The less cytotoxic effect of these compounds on normal lung fibroblast and mammary epithelial cells than malignant cells harboring persistent activation of STAT3 further confirms the above observation, as determined by SRB assay. It is noteworthy that these compounds showed IC_{50} of 8.8~13.8 μM in luciferase reporter assay. However, the IC_{50} of inS3-54 in cytotoxicity assay is ranged from 1.8~5.6 μM in cancer cells to 4.0~12.0 μM in normal cells. Currently, it is unknown why the compounds are more effective in inhibiting cell survival than inhibiting luciferase reporter expression. It is possible that the cytotoxicity assay is more sensitive as it measures both proliferation and cell death induced by the compounds, which is an amplified result of reduced expression of STAT3 downstream target genes. It is also possible that the compounds may have off-

target effects that may impact on cell survival. Additionally, we attempted to investigate the direct interaction between these compounds and STAT3 protein. The compound-conjugated beads were prepared for a pull down assay to identify the potential binding between STAT3 and these compounds. The finding that inS3-54 or A26-conjugated beads pulled down STAT3 from whole cell lysate verifies the potential compound-protein interaction. Although there are no available beads for conjugation of A18 and A69, a competition assay indicates they may bind to STAT3 by using A26-conjugated beads with pretreatment of excess A18 or A69. It is noted that the commercial human recombinant STAT3 protein was observed to bind to inS3-54-conjugated beads, suggesting the direct interaction between inS3-54 and STAT3 protein. However, the silver staining result of pull down assays using whole cell lysates revealed multiple bands for inS3-54. It is possible that multiple proteins come with STAT3 pull-down or inS-54 causes off-target effects by binding to other proteins. Thus, we suspected whether these compounds have promiscuous multi-target effects eventually based on the above results. Subsequently, a STAT3-dependent colony formation assay using bone marrow hematopoietic progenitor cells offers a useful tool to identity the specificity profile that correlates with the blockade of constitute STAT3 activity on basis that specific STAT3 inhibitors do not affect the colony formation of mouse bone marrow cells from mice with conditional knock-out of STAT3. In addition to the initial hit, inS3-54, all three analogues were found to inhibit colony formation of $STAT3^{+/+}$ hematopoietic progenitor cells but not $STAT3^{-/-}$ cells, suggesting their selectivity on STAT3 relative to other targets that are important for colony formation of

hematopoietic progenitor cells. Furthermore, as determined in **Figure 22**, inhibition on colony formation of wild-type hematopoietic progenitor cells may predict the potential toxicity of these compounds in animals, e.g. myelosuppression. However, no significant toxicity was observed in A18-treated mice. Indeed, the dosage of A18 (200 mg/Kg), which is equivalent to ~5 μM calculated on ~2 mL of blood volume in mice, may not be comparable to the concentration (20 μM) used in colony formation assay even though the bioavailability achieves 100% in mice. Overall, our studies provide an attempt on preclinical studies and we believe these observations suggest A18 may emerge as a promising antineoplastic agent with further exploration.

All specific inhibitors identified from virtual screening need to be further characterized to elucidate their actual binding mode. A troubling trend is the fact that a number of small molecule inhibitors of STAT3 have a reactive chemical moiety in common (56, 61, 62). Various STAT3 inhibitors can be classified as Michael acceptors processing vinyl sulfone and α,β-unsaturated ketone functionalities. For example, it is possible that C18 which alkylates Cys468 on the DBD is capable of modifying cysteine residues through the Michael reaction, which could result in any surface-exposed cysteine residues being available for inhibitor-medicated alkylation as well (93). Interestingly, many SH2 inhibitors also exhibit similar features, e.g. S3I-201 and stattic. Some compounds identified by such structural features appear to be identified frequently by high throughput screening. These compounds are promising for initial exploration, whereas they usually do not progress fun in the analysis pipeline. Despite containing a Michael acceptor

group, inS3-54 and A18 do not alkylate the thiol group of cysteine as determined by the glutathione assay and the binding of STAT3 to inS3-54-conjugated beads can be reversed by elution with excess free compound. These data indicate that the binding of STAT3 to compound-conjugated beads is not due to covalent binding and our compounds most likely do not act as an alkylating agent. In the future, nuclear magnetic resonance spectrum analysis or protein-ligand binding assay such as surface plasmon resonance analysis will facilitate more critical evaluation of these compounds and drive more information regarding their key structural determinants in the future.

D. Structure-activity relationship of inS3-54 and its analogues

Based on the current results of cellular assays, a further structure-activity relationship analysis reveals the features of these compounds that bind to the DBD of STAT3 (**Figure 38**). Firstly, inS3-54 and most of analogues contain a core structure of 5-phenyl-1*H*-pyrrol-2(3*H*)-ketone. Interestingly, the manual modification of the core structure to ethyl-4-hyrodroxy-5-oxo-4,5-dihydro-1*H*-pyrrole-3-carbonylate (A80~89) caused loss of activity of the compounds (**Table 6**). Secondly, it appears that the activity of these compounds in inhibiting STAT3 varies based on the modification of the R_1 and R_2 side groups in the core structure. As shown in **Figure 7**, the nitrobenzene at the R_2 position of inS3-54 contributes to the binding of the residues Met331, Val343, Met420, Ile467 and Met470 of STAT3 via hydrophobic interaction. The carboxyl group on the benzene ring at R_1 position stabilizes the binding via electrostatic interaction with the residues Lys340

and Asn466 of STAT3. However, the docking of inS3-54 onto STAT1 is unfavorable with physical hindrance. Therefore, both R_1 and R_2 groups may be critical for the activity and specificity of these compounds. A general review of inS3-54 analogues reveals that the STAT3 inhibitory activity of the compounds increased with the R_2 group being nitrobenzene, *p*-chlorobenzene, benzenamine and *p*-methoxylbenzene, but decreased with R_2 group being and 5-phenylfuran (**Figure 21A** and **Table 5**). The R_1 group is also one of the important determinants of STAT3-inhibiting activity. The existence of *p*-hydroxyl, *p*-carboxyl and *p*-amide side groups on the benzene ring facilitated the activity of these compounds (**Figure 21A** and **Table 5**). However, this relationship is not absolute; the activity of the compounds is more likely to depend on the combination of R_1 and R_2 side groups in the core structure. All three active analogues of inS3-54 exhibited more potent or comparable activity on inhibition of STAT3-dependent signaling, DNA-binding activity, and cancer cell survival than the initial hit and all compounds are specific to STAT3 protein as demonstrated by the colony formation assay of $STAT3^{+/+}$ and $STAT3^{-/-}$ cells. It is also noteworthy that the specificity of the three active inS3-54 analogues appears to be determined by the side group on 1-benzene ring at 4'-position. While the STAT3 specific inhibitors A18, A26 and A69 have hydroxyl or amide groups at this position, the non-specific inhibitor inS3-54 has carboxyl group. Replacing the hydroxyl or amide groups by carboxyl group at this position may abolish the specificity of these compounds to STAT3 and enable them to bind to other proteins. Besides, the combination of various R groups may affect the *in vivo* properties. For example, a pilot pharmacokinetic study revealed a very low plasma

concentration of inS3-54 and A26 due to their poor solubility and absorption with much deposit in peritoneal cavity. A69 appears to work on STAT3 faster than other compounds with shortest time to achieve 50% inhibition on STAT3-dependent luciferase reporter (**Figure 21C**), but a pilot toxicity study reveals that the compound is toxic to mice with a tolerance dose of less than 0.5 mg/Kg (**Table 8**). However, A18 has acceptable activity on STAT3 signaling and good solubility of up to 100 mg/mL in a commercial vehicle for animal studies (**Table 7**). Eventually, the *in vivo* efficacy of A18 was assessed by a mouse xenograft model of lung cancer. The compound inhibited tumor growth in mice harboring A549 xenograft tumors via oral administration whereas it had little effect on total body weight and five main organs (**Figure 35**). However, additional SAR studies are needed to test the hypothesis that the various side groups determine the activity of compounds.

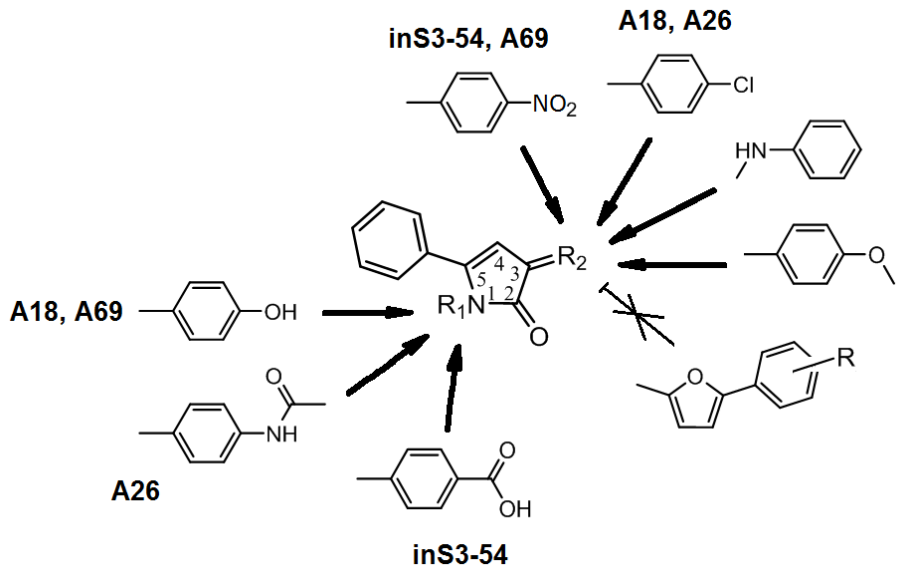

Figure 38. SAR analysis of inST3-54 analogues.

Schematic core structure of inST3-54 and its peripheral groups. Representational functional groups are shown with indication of favorable (thick arrows) or unfavorable substitutions (thin-crossed arrows).

E. Mechanism of inS3-54 and its analogues

As expected, these compounds inhibited constitutive STAT3 signaling by blocking the binding of STAT3 to the promoter regions of STAT3 responsive genes. In this study, inS3-54 and its analogues were found to inhibit cancer cell survival, migration and invasion as well as induce apoptosis after lung and breast cancer cells were exposed to the compounds. We thereby suggest that inhibition of STAT3 binding is a primary mechanism by which these compound exert antitumor effects in A594 and MDA-MB-231 cells. Firstly, STAT3 activation occurs by ligand binding to specific cell surface receptors (16). InS3-54 and A18 were found not to affect IL-6-induced STAT3 activation by detecting the phosphorylation status of STAT3, however, one of the STAT3 downstream targets, survivin, was still suppressed by inS3-54 or A18 in absence and presence of IL-6, suggesting these compounds have little effect on STAT3 activation. Furthermore, direct inhibition of STAT3 can be achieved via targeting one of three structural domains of STAT3 such as SH2, DBD or N-terminal domains, resulting in inhibition of STAT3 signaling. InS3-54 was found not to inhibit STAT3 dimerization, indicating that it may not bind to the susceptible SH2 domain. To verify the inhibitory effects of these compounds on DNA-binding activity of STAT3 in cells, different cellular fractions were isolated from A549 and MDA-MB-231 cells following inS3-54 or A18 treatment. We are not surprised to find that inS3-54 and A18 blocked the binding of STAT3 protein to chromatin in both lung and breast cancer cells. The total level of STAT3 and the level of STAT3 in cytosol fraction remained stable after treatment in both A549 and MDA-MB-231 cells, however, these compounds blocked the binding of STAT3 to

chromatin, causing an increment of STAT3 in soluble nuclear protein fraction and a decline of STAT3 in chromatin-bound fraction. It was also observed that inS3-54 and A18 suppressed the binding of STAT3 to the promoter regions of STAT3 responsive genes in cancer cells with constitutively active STAT3 in ChIP assay which specifically tested two STAT3-regulated genes, cyclin D1 and twist. Moreover, the expression levels of STAT3 downstream targets were determined because STAT3 is a nuclear transcription factor that regulate the expression of diverse genes. InS3-54 and A18 showed inhibition of STAT3-regulated genes as well. Therefore, the inhibitory effects of InS3-54 and A18 on tumor cells harboring constitutive activation of STAT3 are demonstrated to be due to inhibition of STAT3 downstream target expression including cyclin D1, survivin, MMP-2, -9, twist and VEGF. Importantly, this observation was verified in xenograft tumors as well.

Based on the above results, we conclude tentatively that inS3-54 and its analogues favorably inhibit persistent STAT3 signaling by disruption of STAT3 binding to DNA. As a result, these compounds inhibit cell proliferation, migration and invasion and induce apoptosis in cells with constitutively activated STAT3. Although the initial hit, inS3-54, may not be specific to STAT3 protein, it provides a good attempt for development of novel STAT3 inhibitors. A structure-activity analysis of inS3-54 analogues subsequently establishes a basis for further design and optimization of novel small molecule compounds that effectively and selectively block DNA-binding activity of STAT3. Of three active analogues, A18 showed preference for STAT3 but little effect on other proteins as well as *in vitro* and *in vivo* effects on inhibition of aberrant STAT3 signaling. Our study supports

the computational modeling application in structure-based virtual screening for identifying STAT3 inhibitors targeting DBD and offers a promising approach to a new therapeutic agent for the treatment of cancer. Further studies directed at this strategy are currently in progress and will provide more insights into the novel molecular approaches to interrupt STAT3 signaling pathway for potential cancer therapies. Each report of a novel STAT3 inhibitor will bring an increasing optimism for the development of clinically useful drugs. And more in-depth analyses will benefit to achieving this goal, providing a promising and viable strategy for patient care.

V. Summary and Conclusion

The experimental results of this dissertation can be summarized as follows:

1. Using *in-silico* screening of a virtual compound database by docking onto the DNA-binding site of human STAT3, inS3-54 is identified to disrupt STAT3-dependent signaling.

2. InS3-54 inhibits the DNA-binding activity of STAT3 but not that of STAT1.

3. InS3-54 directly binds to STAT3 but may also have other targets.

4. InS3-54 may not affect activation and dimerization of STAT3.

5. InS3-54 favorably inhibits cancer cell survival, cell migration and invasion in breast and lung carcinoma cells harboring constitutively active STAT3.

6. InS3-54 prevents the binding of STAT3 to responsive DNA region via interaction with STAT3 protein, leading to negative regulation of STAT3 downstream targets.

7. InS3-54 is not applicable for further studies due to less specificity on STAT3 protein and poor absorption in mice; however, it can be used as an *in vitro* tool to study STAT3 function.

8. Three active analogues of inS3-54 (A18, A26 and A69) have more potent or comparable activity on STAT3 signaling as compared with the initial hit, depending on the combination of R_1 and R_2 side groups in the core structure of inS3-54.

9. A18, A26 and A69 are more specific to STAT3 protein than their parental compound, inS3-54.

10. A18 exerts anti-tumor effects by suppressing the DNA-binding activity of STAT3, causing prevention of STAT3 binding to its endogenous target sequences as well as down-regulation of STAT3-dependent target genes.

11. A18 is suitable for further studies because of acceptable solubility, absorption and tolerance in mice. Administration of A18 in a lung tumor xenograft model suppressed tumor growth with little effect on body weight or organs of heart, lungs, kidneys, liver and spleen.

VI. Future Plans

Based on the present work, we conclude that it is possible to inhibit STAT3 by targeting DBD for discovery of anticancer therapeutics. Future directions that may extend the current work contain:

1. To further determine the direct interaction between A18 and DBD of STAT3 using purified protein and direct protein-ligand binding assays. The determination of affinity of compounds to protein will bring a better understanding of active determinants in these compounds in order to identify more potent and specific STAT3 inhibitors.

2. To identify the potential off-target effects of A18 and to verify the specificity of A18 on STAT3 protein. Further studies of A18 will provide more evidence for development of A18 as a novel STAT3 inhibitor as well as demonstrate the feasibility of targeting the DBD of STAT3 *in vivo*.

3. To further verify the *in vivo* effect of A18 on tumor growth and investigate whether or not A18 represses expression of STAT3 downstream targets in tumor tissues through more pharmacokinetic/pharmacodynamic studies. The pilot toxicity and efficacy studies exhibit the *in vivo* inhibition of A18 on tumor growth. PK studies will inspire optimal dosing regimens by determination of the fate of the compound after administration, probably improving *in vivo* efficacy of the compound.

4. To determine the effects of A18 on metastasis and angiogenesis in animals. The current data indicate A18 inhibits cell migration and cell invasion as well as reduces the production of VEGF, suggesting its inhibitory effects on

metastasis and angiogenesis *in vitro*. More animal studies on metastasis and angiogenesis may be helpful in investigating *in vivo* effects and thereby determining the potential subjects who may benefit from our studies.

5. To further optimize the structure of A18 for more potent and more specific STAT3 inhibitors. Although A18 emerges as a promising antineoplastic agent, further exploration on chemical structure will bring more evidence with respect to designing inhibitors targeting the DBD of STAT3.

VII. References

1. Stark GR, Darnell JE, Jr. The JAK-STAT pathway at twenty. Immunity. 2012;36(4):503-14.
2. Dale TC, Imam AM, Kerr IM, Stark GR. Rapid activation by interferon alpha of a latent DNA-binding protein present in the cytoplasm of untreated cells. Proceedings of the National Academy of Sciences of the United States of America. 1989;86(4):1203-7.
3. Schindler C, Fu XY, Improta T, Aebersold R, Darnell JE, Jr. Proteins of transcription factor ISGF-3: one gene encodes the 91-and 84-kDa ISGF-3 proteins that are activated by interferon alpha. Proceedings of the National Academy of Sciences of the United States of America. 1992;89(16):7836-9.
4. Shuai K, Schindler C, Prezioso VR, Darnell JE, Jr. Activation of transcription by IFN-gamma: tyrosine phosphorylation of a 91-kD DNA binding protein. Science. 1992;258(5089):1808-12.
5. Shuai K, Stark GR, Kerr IM, Darnell JE, Jr. A single phosphotyrosine residue of Stat91 required for gene activation by interferon-gamma. Science. 1993;261(5129):1744-6.
6. Adamkova L, Souckova K, Kovarik J. Transcription protein STAT1: biology and relation to cancer. Folia biologica. 2007;53(1):1-6.
7. Chan SR, Vermi W, Luo J, Lucini L, Rickert C, Fowler AM, et al. STAT1-deficient mice spontaneously develop estrogen receptor alpha-positive luminal mammary carcinomas. Breast cancer research : BCR. 2012;14(1):R16.
8. Au-Yeung N, Mandhana R, Horvath CM. Transcriptional regulation by STAT1 and STAT2 in the interferon JAK-STAT pathway. Jak-Stat. 2013;2(3):e23931.
9. Chowdhury FZ, Farrar JD. STAT2: A shape-shifting anti-viral super STAT. Jak-Stat. 2013;2(1):e23633.
10. Zhong Z, Wen Z, Darnell JE, Jr. Stat3 and Stat4: members of the family of signal transducers and activators of transcription. Proceedings of the National Academy of Sciences of the United States of America. 1994;91(11):4806-10.
11. Wurster AL, Tanaka T, Grusby MJ. The biology of Stat4 and Stat6. Oncogene. 2000;19(21):2577-84.
12. Mui AL, Wakao H, Harada N, O'Farrell AM, Miyajima A. Interleukin-3, granulocyte-macrophage colony-stimulating factor, and interleukin-5 transduce signals through two forms of STAT5. Journal of leukocyte biology. 1995;57(5):799-803.
13. Liu X, Robinson GW, Gouilleux F, Groner B, Hennighausen L. Cloning and expression of Stat5 and an additional homologue (Stat5b) involved in prolactin signal transduction in mouse mammary tissue. Proceedings of the National Academy of Sciences of the United States of America. 1995;92(19):8831-5.
14. Buitenhuis M, Coffer PJ, Koenderman L. Signal transducer and activator of transcription 5 (STAT5). The International Journal of Biochemistry & Cell Biology. 2004; 36(11):2120-4.
15. Goenka S, Kaplan MH. Transcriptional regulation by STAT6. Immunologic research. 2011;50(1):87-96.

16. Zhong Z, Wen Z, Darnell JE, Jr. Stat3: a STAT family member activated by tyrosine phosphorylation in response to epidermal growth factor and interleukin-6. Science. 1994;264(5155):95-8.
17. Ihle JN. STATs: signal transducers and activators of transcription. Cell. 1996;84(3):331-4.
18. Darnell JE, Jr. STATs and gene regulation. Science. 1997;277(5332):1630-5.
19. Bromberg J, Darnell JE, Jr. The role of STATs in transcriptional control and their impact on cellular function. Oncogene. 2000;19(21):2468-73.
20. Levy DE, Darnell JE, Jr. Stats: transcriptional control and biological impact. Nature reviews Molecular cell biology. 2002;3(9):651-62.
21. Klosek SK, Nakashiro K, Hara S, Li C, Shintani S, Hamakawa H. Constitutive activation of Stat3 correlates with increased expression of the c-Met/HGF receptor in oral squamous cell carcinoma. Oncology reports. 2004;12(2):293-6.
22. Vij N, Sharma A, Thakkar M, Sinha S, Mohan RR. PDGF-driven proliferation, migration, and IL8 chemokine secretion in human corneal fibroblasts involve JAK2-STAT3 signaling pathway. Molecular vision. 2008;14:1020-7.
23. Yu CL, Meyer DJ, Campbell GS, Larner AC, Carter-Su C, Schwartz J, et al. Enhanced DNA-binding activity of a Stat3-related protein in cells transformed by the Src oncoprotein. Science. 1995;269(5220):81-3.
24. Leslie K, Lang C, Devgan G, Azare J, Berishaj M, Gerald W, et al. Cyclin D1 is transcriptionally regulated by and required for transformation by activated signal transducer and activator of transcription 3. Cancer research. 2006;66(5):2544-52.
25. Kiuchi N, Nakajima K, Ichiba M, Fukada T, Narimatsu M, Mizuno K, et al. STAT3 is required for the gp130-mediated full activation of the c-myc gene. The Journal of experimental medicine. 1999;189(1):63-73.
26. Gritsko T, Williams A, Turkson J, Kaneko S, Bowman T, Huang M, et al. Persistent activation of stat3 signaling induces survivin gene expression and confers resistance to apoptosis in human breast cancer cells. Clinical cancer research : an official journal of the American Association for Cancer Research. 2006;12(1):11-9.
27. Itoh M, Murata T, Suzuki T, Shindoh M, Nakajima K, Imai K, et al. Requirement of STAT3 activation for maximal collagenase-1 (MMP-1) induction by epidermal growth factor and malignant characteristics in T24 bladder cancer cells. Oncogene. 2006;25(8):1195-204.
28. Zugowski C, Lieder F, Muller A, Gasch J, Corvinus FM, Moriggl R, et al. STAT3 controls matrix metalloproteinase-1 expression in colon carcinoma cells by both direct and AP-1-mediated interaction with the MMP-1 promoter. Biological chemistry. 2011;392(5):449-59.
29. Xie TX, Wei D, Liu M, Gao AC, Ali-Osman F, Sawaya R, et al. Stat3 activation regulates the expression of matrix metalloproteinase-2 and tumor invasion and metastasis. Oncogene. 2004;23(20):3550-60.

30. Yuan G, Qian L, Shi M, Lu F, Li D, Hu M, et al. HER2-dependent MMP-7 expression is mediated by activated STAT3. Cellular signalling. 2008;20(7):1284-91.
31. Dechow TN, Pedranzini L, Leitch A, Leslie K, Gerald WL, Linkov I, et al. Requirement of matrix metalloproteinase-9 for the transformation of human mammary epithelial cells by Stat3-C. Proceedings of the National Academy of Sciences of the United States of America. 2004;101(29):10602-7.
32. Zhang X, Yin P, Di D, Luo G, Zheng L, Wei J, et al. IL-6 regulates MMP-10 expression via JAK2/STAT3 signaling pathway in a human lung adenocarcinoma cell line. Anticancer research. 2009;29(11):4497-501.
33. Cheng GZ, Zhang WZ, Sun M, Wang Q, Coppola D, Mansour M, et al. Twist is transcriptionally induced by activation of STAT3 and mediates STAT3 oncogenic function. The Journal of biological chemistry. 2008;283(21):14665-73.
34. Wei D, Le X, Zheng L, Wang L, Frey JA, Gao AC, et al. Stat3 activation regulates the expression of vascular endothelial growth factor and human pancreatic cancer angiogenesis and metastasis. Oncogene. 2003;22(3):319-29.
35. Niu G, Wright KL, Huang M, Song L, Haura E, Turkson J, et al. Constitutive Stat3 activity up-regulates VEGF expression and tumor angiogenesis. Oncogene. 2002;21(13):2000-8.
36. Becker S, Groner B, Muller CW. Three-dimensional structure of the Stat3beta homodimer bound to DNA. Nature. 1998;394(6689):145-51.
37. Xu X, Sun YL, Hoey T. Cooperative DNA binding and sequence-selective recognition conferred by the STAT amino-terminal domain. Science. 1996;273(5276):794-7.
38. Haan S, Hemmann U, Hassiepen U, Schaper F, Schneider-Mergener J, Wollmer A, et al. Characterization and binding specificity of the monomeric STAT3-SH2 domain. The Journal of biological chemistry. 1999;274(3):1342-8.
39. Horvath CM, Wen Z, Darnell JE, Jr. A STAT protein domain that determines DNA sequence recognition suggests a novel DNA-binding domain. Genes & development. 1995;9(8):984-94.
40. Wen Z, Zhong Z, Darnell JE, Jr. Maximal activation of transcription by Stat1 and Stat3 requires both tyrosine and serine phosphorylation. Cell. 1995;82(2):241-50.
41. Bild AH, Turkson J, Jove R. Cytoplasmic transport of Stat3 by receptor-mediated endocytosis. The EMBO Journal. 2002;21(13):3255-63.
42. Tenev T, Bohmer SA, Kaufmann R, Frese S, Bittorf T, Beckers T, et al. Perinuclear localization of the protein-tyrosine phosphatase SHP-1 and inhibition of epidermal growth factor-stimulated STAT1/3 activation in A431 cells. European journal of cell biology. 2000;79(4):261-71.
43. Kim H, Baumann H. Dual signaling role of the protein tyrosine phosphatase SHP-2 in regulating expression of acute-phase plasma proteins by interleukin-6 cytokine receptors in hepatic cells. Molecular and cellular biology. 1999;19(8):5326-38.
44. Sun S, Steinberg BM. PTEN is a negative regulator of STAT3 activation in human papillomavirus-infected cells. J Gen Virol. 2002;83:1651-8.

45. Gunaje JJ, Bhat GJ. Involvement of tyrosine phosphatase PTP1D in the inhibition of interleukin-6-induced Stat3 signaling by alpha-thrombin. Biochemical and biophysical research communications. 2001;288(1):252-7.
46. Chung CD, Liao J, Liu B, Rao X, Jay P, Berta P, et al. Specific inhibition of Stat3 signal transduction by PIAS3. Science. 1997;278(5344):1803-5.
47. Krebs DL, Hilton DJ. SOCS proteins: negative regulators of cytokine signaling. Stem cells. 2001;19(5):378-87.
48. Bowman T, Garcia R, Turkson J, Jove R. STATs in oncogenesis. Oncogene. 2000;19(21):2474-88.
49. Cao X, Tay A, Guy GR, Tan YH. Activation and association of Stat3 with Src in v-Src-transformed cell lines. Molecular and cellular biology. 1996;16(4):1595-603.
50. Turkson J, Bowman T, Garcia R, Caldenhoven E, De Groot RP, Jove R. Stat3 activation by Src induces specific gene regulation and is required for cell transformation. Molecular and cellular biology. 1998;18(5):2545-52.
51. Bromberg JF, Horvath CM, Besser D, Lathem WW, Darnell JE, Jr. Stat3 activation is required for cellular transformation by v-src. Molecular and cellular biology. 1998;18(5):2553-8.
52. Devarajan E, Huang S. STAT3 as a central regulator of tumor metastases. Current molecular medicine. 2009;9(5):626-33.
53. Chen Z, Han ZC. STAT3: a critical transcription activator in angiogenesis. Medicinal research reviews. 2008;28(2):185-200.
54. Lee H, Pal SK, Reckamp K, Figlin RA, Yu H. STAT3: a target to enhance antitumor immune response. Current topics in microbiology and immunology. 2011;344:41-59.
55. Siegel R, Naishadham D, Jemal A. Cancer Statistics, 2013. CA: A cancer journal for clinicians. 2013; 63(1):11–30.
56. Debnath B, Xu S, Neamati N. Small molecule inhibitors of signal transducer and activator of transcription 3 (Stat3) protein. Journal of medicinal chemistry. 2012;55(15):6645-68.
57. Sun W, Song L, Ai T, Zhang Y, Gao Y, Cui J. Prognostic value of MET, cyclin D1 and MET gene copy number in non-small cell lung cancer. The Journal of biomedical research. 2013;27(3):220–30.
58. Xu YH, Lu S. A meta-analysis of STAT3 and phospho-STAT3 expression and survival of patients with non-small-cell lung cancer. European Journal of surgical oncology. 2013; [Epub ahead of print].
59. Dolled-Filhart M, Camp RL, Kowalski DP, Smith BL, Rimm DL. Tissue microarray analysis of signal transducers and activators of transcription 3 (Stat3) and phospho-Stat3 (Tyr705) in node-negative breast cancer shows nuclear localization is associated with a better prognosis. Clinical cancer research : an official journal of the American Association for Cancer Research. 2003;9(2):594-600.

60. Diaz N, Minton S, Cox C, Bowman T, Gritsko T, Garcia R, et al. Activation of stat3 in primary tumors from high-risk breast cancer patients is associated with elevated levels of activated SRC and survivin expression. Clinical cancer research : an official journal of the American Association for Cancer Research. 2006;12(1):20-8.
61. Deng J, Grande F, Neamati N. Small molecule inhibitors of Stat3 signaling pathway. Current cancer drug targets. 2007;7(1):91-107.
62. Yue P, Turkson J. Targeting STAT3 in cancer: how successful are we? Expert opinion on investigational drugs. 2009;18(1):45-56.
63. Bharti AC, Shishodia S, Reuben JM, Weber D, Alexanian R, Raj-Vadhan S, et al. Nuclear factor-kappaB and STAT3 are constitutively active in CD138+ cells derived from multiple myeloma patients, and suppression of these transcription factors leads to apoptosis. Blood. 2004;103(8):3175-84.
64. Dobi E, Monnien F, Kim S, Ivanaj A, N'Guyen T, Demarchi M, et al. Impact of STAT3 phosphorylation on the clinical effectiveness of anti-EGFR-based therapy in patients with metastatic colorectal cancer. Clinical colorectal cancer. 2013;12(1):28-36.
65. Wang W, Edington HD, Rao UN, Jukic DM, Wang H, Shipe-Spotloe JM, et al. STAT3 as a biomarker of progression in atypical nevi of patients with melanoma: dose-response effects of systemic IFNalpha therapy. The Journal of investigative dermatology. 2008;128(8):1997-2002.
66. Eto M, Kamba T, Miyake H, Fujisawa M, Kamai T, Uemura H, et al. STAT3 polymorphism can predict the response to interferon-alpha therapy in patients with metastatic renal cell carcinoma. European urology. 2013;63(4):745-52.
67. Ito N, Eto M, Nakamura E, Takahashi A, Tsukamoto T, Toma H, et al. STAT3 polymorphism predicts interferon-alfa response in patients with metastatic renal cell carcinoma. Journal of clinical oncology : official journal of the American Society of Clinical Oncology. 2007;25(19):2785-91.
68. Han Z, Feng J, Hong Z, Chen L, Li W, Liao S, et al. Silencing of the STAT3 signaling pathway reverses the inherent and induced chemoresistance of human ovarian cancer cells. Biochemical and biophysical research communications. 2013;435(2):188-94.
69. Turkson J, Ryan D, Kim JS, Zhang Y, Chen Z, Haura E, et al. Phosphotyrosyl peptides block Stat3-mediated DNA binding activity, gene regulation, and cell transformation. The Journal of biological chemistry. 2001;276(48):45443-55.
70. Ren Z, Cabell LA, Schaefer TS, McMurray JS. Identification of a high-affinity phosphopeptide inhibitor of Stat3. Bioorganic & medicinal chemistry letters. 2003;13(4):633-6.
71. Turkson J, Kim JS, Zhang S, Yuan J, Huang M, Glenn M, et al. Novel peptidomimetic inhibitors of signal transducer and activator of transcription 3 dimerization and biological activity. Molecular cancer therapeutics. 2004;3(3):261-9.

72. Song H, Wang R, Wang S, Lin J. A low-molecular-weight compound discovered through virtual database screening inhibits Stat3 function in breast cancer cells. Proceedings of the National Academy of Sciences of the United States of America. 2005;102(13):4700-5.
73. Schust J, Sperl B, Hollis A, Mayer TU, Berg T. Stattic: a small-molecule inhibitor of STAT3 activation and dimerization. Chemistry & biology. 2006;13(11):1235-42.
74. Siddiquee K, Zhang S, Guida WC, Blaskovich MA, Greedy B, Lawrence HR, et al. Selective chemical probe inhibitor of Stat3, identified through structure-based virtual screening, induces antitumor activity. Proceedings of the National Academy of Sciences of the United States of America. 2007;104(18):7391-6.
75. Siddiquee KA, Gunning PT, Glenn M, Katt WP, Zhang S, Schrock C, et al. An oxazole-based small-molecule Stat3 inhibitor modulates Stat3 stability and processing and induces antitumor cell effects. ACS chemical biology. 2007;2(12):787-98.
76. Hao W, Hu Y, Niu C, Huang X, Chang CP, Gibbons J, et al. Discovery of the catechol structural moiety as a Stat3 SH2 domain inhibitor by virtual screening. Bioorganic & medicinal chemistry letters. 2008;18(18):4988-92.
77. Fletcher S, Singh J, Zhang X, Yue P, Page BD, Sharmeen S, et al. Disruption of transcriptionally active Stat3 dimers with non-phosphorylated, salicylic acid-based small molecules: potent in vitro and tumor cell activities. Chembiochem : a European journal of chemical biology. 2009;10(12):1959-64.
78. Lin L, Deangelis S, Foust E, Fuchs J, Li C, Li PK, et al. A novel small molecule inhibits STAT3 phosphorylation and DNA binding activity and exhibits potent growth suppressive activity in human cancer cells. Molecular cancer. 2010;9:217.
79. Lin L, Hutzen B, Li PK, Ball S, Zuo M, DeAngelis S, et al. A novel small molecule, LLL12, inhibits STAT3 phosphorylation and activities and exhibits potent growth-suppressive activity in human cancer cells. Neoplasia. 2010;12(1):39-50.
80. Lin L, Hutzen B, Zuo M, Ball S, Deangelis S, Foust E, et al. Novel STAT3 phosphorylation inhibitors exhibit potent growth-suppressive activity in pancreatic and breast cancer cells. Cancer research. 2010;70(6):2445-54.
81. Bill MA, Fuchs JR, Li C, Yui J, Bakan C, Benson DM, Jr., et al. The small molecule curcumin analog FLLL32 induces apoptosis in melanoma cells via STAT3 inhibition and retains the cellular response to cytokines with anti-tumor activity. Molecular cancer. 2010;9:165.
82. Nkansah E, Shah R, Collie GW, Parkinson GN, Palmer J, Rahman KM, et al. Observation of unphosphorylated STAT3 core protein binding to target dsDNA by PEMSA and X-ray crystallography. FEBS letters. 2013;587(7):833-9.
83. Timofeeva OA, Chasovskikh S, Lonskaya I, Tarasova NI, Khavrutskii L, Tarasov SG, et al. Mechanisms of unphosphorylated STAT3 transcription factor binding to DNA. The Journal of biological chemistry. 2012;287(17):14192-200.
84. Yang J, Liao X, Agarwal MK, Barnes L, Auron PE, Stark GR. Unphosphorylated STAT3 accumulates in response to IL-6 and activates transcription by binding to NFkappaB. Genes & development. 2007;21(11):1396-408.

85. Yang J, Chatterjee-Kishore M, Staugaitis SM, Nguyen H, Schlessinger K, Levy DE, et al. Novel roles of unphosphorylated STAT3 in oncogenesis and transcriptional regulation. Cancer research. 2005;65(3):939-47.
86. Weidler M, Rether J, Anke T, Erkel G. Inhibition of interleukin-6 signaling by galiellalactone. FEBS letters. 2000;484(1):1-6.
87. Hellsten R, Johansson M, Dahlman A, Dizeyi N, Sterner O, Bjartell A. Galiellalactone is a novel therapeutic candidate against hormone-refractory prostate cancer expressing activated Stat3. The Prostate. 2008;68(3):269-80.
88. Buerger C, Nagel-Wolfrum K, Kunz C, Wittig I, Butz K, Hoppe-Seyler F, et al. Sequence-specific peptide aptamers, interacting with the intracellular domain of the epidermal growth factor receptor, interfere with Stat3 activation and inhibit the growth of tumor cells. The Journal of biological chemistry. 2003;278(39):37610-21.
89. Nagel-Wolfrum K, Buerger C, Wittig I, Butz K, Hoppe-Seyler F, Groner B. The interaction of specific peptide aptamers with the DNA binding domain and the dimerization domain of the transcription factor Stat3 inhibits transactivation and induces apoptosis in tumor cells. Molecular cancer research : MCR. 2004;2(3):170-82.
90. Lee YK, Isham CR, Kaufman SH, Bible KC. Flavopiridol disrupts STAT3/DNA interactions, attenuates STAT3-directed transcription, and combines with the Jak kinase inhibitor AG490 to achieve cytotoxic synergy. Molecular cancer therapeutics. 2006;5(1):138-48.
91. Turkson J, Zhang S, Palmer J, Kay H, Stanko J, Mora LB, et al. Inhibition of constitutive signal transducer and activator of transcription 3 activation by novel platinum complexes with potent antitumor activity. Molecular cancer therapeutics. 2004;3(12):1533-42.
92. Turkson J, Zhang S, Mora LB, Burns A, Sebti S, Jove R. A novel platinum compound inhibits constitutive Stat3 signaling and induces cell cycle arrest and apoptosis of malignant cells. The Journal of biological chemistry. 2005;280(38):32979-88.
93. Buettner R, Corzano R, Rashid R, Lin J, Senthil M, Hedvat M, et al. Alkylation of cysteine 468 in Stat3 defines a novel site for therapeutic development. ACS chemical biology. 2011;6(5):432-43.
94. Leong PL, Andrews GA, Johnson DE, Dyer KF, Xi S, Mai JC, et al. Targeted inhibition of Stat3 with a decoy oligonucleotide abrogates head and neck cancer cell growth. Proceedings of the National Academy of Sciences of the United States of America. 2003;100(7):4138-43.
95. Xi S, Gooding WE, Grandis JR. In vivo antitumor efficacy of STAT3 blockade using a transcription factor decoy approach: implications for cancer therapy. Oncogene. 2005;24(6):970-9.
96. Zhang X, Zhang J, Wang L, Wei H, Tian Z. Therapeutic effects of STAT3 decoy oligodeoxynucleotide on human lung cancer in xenograft mice. BMC cancer. 2007;7:149.
97. Zhang X, Zhang J, Wei H, Tian Z. STAT3-decoy oligodeoxynucleotide inhibits the growth of human lung cancer via down-regulating its target genes. Oncology reports. 2007;17(6):1377-82.

98. Zhang X, Liu P, Zhang B, Wang A, Yang M. Role of STAT3 decoy oligodeoxynucleotides on cell invasion and chemosensitivity in human epithelial ovarian cancer cells. Cancer genetics and cytogenetics. 2010;197(1):46-53.
99. Sen M, Thomas SM, Kim S, Yeh JI, Ferris RL, Johnson JT, et al. First-in-human trial of a STAT3 decoy oligonucleotide in head and neck tumors: implications for cancer therapy. Cancer discovery. 2012;2(8):694-705.
100. Huang C, Cao J, Huang KJ, Zhang F, Jiang T, Zhu L, et al. Inhibition of STAT3 activity with AG490 decreases the invasion of human pancreatic cancer cells in vitro. Cancer science. 2006;97(12):1417-23.
101. Kotha A, Sekharam M, Cilenti L, Siddiquee K, Khaled A, Zervos AS, et al. Resveratrol inhibits Src and Stat3 signaling and induces the apoptosis of malignant cells containing activated Stat3 protein. Molecular cancer therapeutics. 2006;5(3):621-9.
102. Ferrajoli A, Faderl S, Van Q, Koch P, Harris D, Liu Z, et al. WP1066 disrupts Janus kinase-2 and induces caspase-dependent apoptosis in acute myelogenous leukemia cells. Cancer research. 2007;67(23):11291-9.
103. Iwamaru A, Szymanski S, Iwado E, Aoki H, Yokoyama T, Fokt I, et al. A novel inhibitor of the STAT3 pathway induces apoptosis in malignant glioma cells both in vitro and in vivo. Oncogene. 2007;26(17):2435-44.
104. Hedvat M, Huszar D, Herrmann A, Gozgit JM, Schroeder A, Sheehy A, et al. The JAK2 inhibitor AZD1480 potently blocks Stat3 signaling and oncogenesis in solid tumors. Cancer cell. 2009;16(6):487-97.
105. Ramakrishnan V, Kimlinger T, Haug J, Timm M, Wellik L, Halling T, et al. TG101209, a novel JAK2 inhibitor, has significant in vitro activity in multiple myeloma and displays preferential cytotoxicity for CD45+ myeloma cells. American journal of hematology. 2010;85(9):675-86.
106. Levitzki A. Tyrphostins: tyrosine kinase blockers as novel antiproliferative agents and dissectors of signal transduction. FASEB journal : official publication of the Federation of American Societies for Experimental Biology. 1992;6(14):3275-82.
107. Nam S, Buettner R, Turkson J, Kim D, Cheng JQ, Muehlbeyer S, et al. Indirubin derivatives inhibit Stat3 signaling and induce apoptosis in human cancer cells. Proceedings of the National Academy of Sciences of the United States of America. 2005;102(17):5998-6003.
108. Ling X, Arlinghaus RB. Knockdown of STAT3 expression by RNA interference inhibits the induction of breast tumors in immunocompetent mice. Cancer research. 2005;65(7):2532-6.
109. Kunigal S, Lakka SS, Sodadasu PK, Estes N, Rao JS. Stat3-siRNA induces Fas-mediated apoptosis in vitro and in vivo in breast cancer. International journal of oncology. 2009;34(5):1209-20.
110. Pettersen EF, Goddard TD, Huang CC, Couch GS, Greenblatt DM, Meng EC, et al. UCSF Chimera--a visualization system for exploratory research and analysis. Journal of computational chemistry. 2004;25(13):1605-12.
111. Lang PT, Brozell SR, Mukherjee S, Pettersen EF, Meng EC, Thomas V, et al. DOCK 6: combining techniques to model RNA-small molecule complexes. Rna. 2009;15(6):1219-30.

112. Graves AP, Shivakumar DM, Boyce SE, Jacobson MP, Case DA, Shoichet BK. Rescoring docking hit lists for model cavity sites: predictions and experimental testing. J Mol Biol. 2008;377(3):914-34.
113. Liu Z, Dong Z, Han B, Yang Y, Liu Y, Zhang JT. Regulation of expression by promoters versus internal ribosome entry site in the 5'-untranslated sequence of the human cyclin-dependent kinase inhibitor p27kip1. Nucleic Acids Res. 2005;33(12):3763-71.
114. Liu JY, Li ZM, Li HA, Zhang JT. Critical Residue That Promotes Protein Dimerization: A Story of Partially Exposed Phe(25) in 14-3-3 sigma. Journal of chemical information and modeling. 2011;51(10):2612-25.
115. Liu H, Liu Y, Zhang JT. A new mechanism of drug resistance in breast cancer cells: fatty acid synthase overexpression-mediated palmitate overproduction. Mol Cancer Ther. 2008;7(2):263-70.
116. Welte T, Zhang SS, Wang T, Zhang Z, Hesslein DG, Yin Z, et al. STAT3 deletion during hematopoiesis causes Crohn's disease-like pathogenesis and lethality: a critical role of STAT3 in innate immunity. Proceedings of the National Academy of Sciences of the United States of America. 2003;100(4):1879-84.
117. Mantel C, Messina-Graham S, Moh A, Cooper S, Hangoc G, Fu XY, et al. Mouse hematopoietic cell-targeted STAT3 deletion: stem/progenitor cell defects, mitochondrial dysfunction, ROS overproduction, and a rapid aging-like phenotype. Blood. 2012;120(13):2589-99.
118. Abdulghani J, Gu L, Dagvadorj A, Lutz J, Leiby B, Bonuccelli G, et al. Stat3 promotes metastatic progression of prostate cancer. Am J Pathol. 2008;172(6):1717-28.
119. Avalle L, Pensa S, Regis G, Novelli F, Poli V. STAT1 and STAT3 in tumorigenesis: A matter of balance. Jak-Stat. 2012;1(2):65-72.
120. Molavi O, Mahmud A, Hamdy S, Hung RW, Lai R, Samuel J, et al. Development of a poly(d,l-lactic-co-glycolic acid) nanoparticle formulation of STAT3 inhibitor JSI-124: implication for cancer immunotherapy. Mol Pharm. 2010;7(2):364-74.
121. Bromberg JF, Wrzeszczynska MH, Devgan G, Zhao Y, Pestell RG, Albanese C, et al. Stat3 as an oncogene. Cell. 1999;98(3):295-303.
122. Nichols WW, Murphy DG, Cristofalo VJ, Toji LH, Greene AE, Dwight SA. Characterization of a new human diploid cell strain, IMR-90. Science. 1977;196(4285):60-3.
123. Soule HD, Maloney TM, Wolman SR, Peterson WD Jr, Brenz R, McGrath CM, et al. Isolation and characterization of a spontaneously immortalized human breast epithelial cell line, MCF-10. Cancer Res. 1990;50(18):6075-86.
124. Hirano T, Ishihara K, Hibi M. Roles of STAT3 in mediating the cell growth, differentiation and survival signals relayed through the IL-6 family of cytokine receptors. Oncogene. 2000;19(21):2548-56.
125. Hodge DR, Hurt EM, Farrar WL. The role of IL-6 and STAT3 in inflammation and cancer. European journal of cancer. 2005;41(16):2502-12.
126. Allen JC. Sample Size Calculation for Two Independent Groups: A Useful Rule of Thumb. Proceedings of Singapore Healthcare. 2011;20(2):138-40.

127. Libermann TA, Zerbini LF. Targeting transcription factors for cancer gene therapy. Current gene therapy. 2006;6(1):17-33.
128. Brennan P, Donev R, Hewamana S. Targeting transcription factors for therapeutic benefit. Molecular biosystems. 2008;4(9):909-19.
129. Frank DA. Targeting transcription factors for cancer therapy. IDrugs. 2009;12(1):29-33.
130. Overington JP, Al-Lazikani B, Hopkins AL. "How many drug targets are there?". Nature reviews. 2006;5(12):993–6.
131. Pawson T. SH2 and SH3 domains in signal transduction. Advances in cancer research. 1994;64:87-110.
132. Cohen GB, Ren R, Baltimore D. Modular binding domains in signal transduction proteins. Cell. 1995;80(2):237-48.

Curriculum Vitae
Wei Huang

EDUCATION

2008 - 2014	Indiana University, United States	Ph.D.	Pharmacology
2006 - 2008	Peking University, China	M.S.	Pharmacology
2002 - 2006	Peking University, China	B.S.	Pharmacy

ACADEMIC EXPERIENCES

2008 - 2014 Doctoral Research: Department of Pharmacology and Toxicology, School of Medicine, Indiana University, United States
Thesis: Small molecule compounds targeting DNA binding domain of STAT3 for inhibition of tumor growth and metastasis
Advisor: Dr. Jian-Ting Zhang

2006 - 2008 Master's Research: Department of Molecular and Cellular Pharmacology, School of Pharmaceutical Sciences, Peking University, China
Thesis: SLXM-2, a derivative of cyclophosphamide: mechanism of growth inhibition on hepatocarcinoma 22 cells
Advisor: Dr. Jing-Rong Cui

2002 - 2006 Bachelor's Research: School of Pharmaceutical Sciences, Peking University, China
Project: Effect of norcantharidin's derivative Nd3 on proliferation of human ovarian cancer cell line SKOV3 and its possible mechanisms
Advisor: Dr. Jing-Rong Cui

ACADEMIC ACTIVITIES

7/2013	Molecular Therapeutics of Cancer Meeting Boulder, CO, United States
3/2012	American Association for Cancer Research Annual Meeting Chicago, IL, United States
10/2011	Drug Delivery and Cancer Workshop West Lafayette, IN, United States
5/2011	13th Annual Midwest DNA Repair Symposium Toledo, OH, United States
11/2007	China-France 2nd Annual Symposium on Cancer Research Beijing, China
9/2007	World Congress of Pharmacy and Pharmaceutical Sciences Beijing, China

AWARDS

7/2013	Paradise Travel Award, Indiana University
7/2006	Advanced Individual of Social Practice in Summer Semester, Peking University

7/2004 Advanced Individual of Social Practice in Summer Semester, Peking University

PUBLICATIONS

- **Huang W**, Liu JY, Dong ZZ, Wang F, Zhang JT. Targeting DNA-binding domain of STAT3 for inhibition of cancer cell proliferation, migration and invasion. Reviewed.
- **Huang W**, Liu JY, Dong ZZ, Wang F, He YT, Hangoc G, Fu XY, Broxmeyer H, Zhang ZY, Zhang JT. Development of inS3-54 analogues targeting DNA-binding domain of STAT3 and structure-activity relationship analysis. In preparation.
- Neher TM, **Huang W**, Zhang JT and Turchi JJ. Disruption of Protein-DNA Interactions: An Opportunity for Cancer Chemotherapy, *DNA Repair and Human Health*, Sonya Vengrova (Ed.), 2011, ISBN: 978-953-307-612-6, InTech.
- Zhang N, Guo W, Wang L, **Huang W**, Xu B, Ge ZM, Li M, Li RT, Cui JR. Effect of TM208 on QGY-7703 xenograft tumor growth. *Anti-cancer Drugs*, 2008, 19(6): 593-598.
- Pang LP*, **Huang W*** (* Both authors have contributed equally to the work.), Sun Q, Guo W, Li RT, Cui JR. SLXM-2, a derivative of cyclophosphamide: mechanism of growth inhibition on hepatocarcinoma 22 cells. *Anti-cancer Drugs*, 2008, 19(2): 167-174.
- Cao JH, Xu B, Li M, Wu DZ, **Huang W**, Cui JR. Effect of norcantharidin's derivative Nd3 on proliferation of human ovarian cancer cell line SKOV3 and its possible mechanisms. *Chinese Journal of Cancer*, 2007, 26(4): 361-366.